Aus dem Veterinärwissenschaftlichen Department

der Tierärztlichen Fakultät

der Ludwig-Maximilians-Universität München

Arbeit angefertigt unter der Leitung von

Univ.-Prof. Dr. E. Wolf

Generation of a tailored pig model of Duchenne muscular dystrophy

Inaugural-Dissertation

zur Erlangung der tiermedizinischen Doktorwürde

der Tierärztlichen Fakultät

der Ludwig-Maximilians-Universität München

von

Katinka Burkhardt

aus

Ulm

München 2012

Gedruckt mit der Genehmigung der Tierärztlichen Fakultät

der Ludwig-Maximilians-Universität München

Dekan:	Univ.-Prof. Dr. Braun
Berichterstatter:	Univ.-Prof. Dr. Wolf
Korreferent:	Priv.-Doz. Dr. Wess
	Univ.-Prof. Dr. Matiasek
	Priv.-Doz. Dr. Fischer
	Univ.-Prof. Dr. Meyer-Lindenberg

Tag der Promotion: 11. Februar 2012

Meinen Eltern

und

Barb

TABLE OF CONTENTS

INDEX OF ABBREVIATIONS

AAV	adeno-associated viral vector
BAC	bacterial artificial chromosome
BMD	Becker muscular dystrophy
bGH	bovine growth hormone
CFTR	cystic fibrosis transmembrane conductance regulator
CiA	chloroform isoamylalcohol
CK	serum creatine kinase
CKCS-MD	Cavalier King Charles Spaniels-muscular dystrophy
$CXMD_J$	Beagle-based canine X-linked muscular dystrophy in Japan
DGC	dystrophin-glycoprotein complex
DMD	Duchenne muscular dystrophy
DMEM	Dulbecco modified Eagle medium
DMSO	dimethylsulfoxid
DSB	double strand break
DTT	dithiothreitol
EDTA	ethylenediaminetetraacetic acid
ENU	*N*-ethyl-nitrosourea
ESC	embryonic stem cell
ET	embryo transfer
EtOH	ethanol
FCS	fetal calf serum
G418	Geneticin
GGTA1	alpha-1,3-galactosyltrasnferase
GRMD	Golden Retriever muscular dystrophy

HCl	hydrochloric acid
HFMD	hypertrophic feline muscular dystrophy
HOAc	acetic acid (glacial)
HPRT	hypoxanthine phosphoribosyltransferase 1
IPTG	isopropyl-beta-D-thiogalactopyranoside
IR	nonhomologous or illegitimate recombination
KCl	potassium chloride
KH_2PO_4	di-potassiumhydrogenphosphate
KOAc	potassium acetate
loxP	Cre recombinase recognition sites
$MgCl_2$	magnesium chloride
NaCl	sodium chloride
$Na_2HPO_4+2H_2O$	sodiumdihydrogenphophate-1-hydrate
NaOH	sodium hydroxide
NHEJ	nonhomologous end joining
nNOS	neuronal nitric oxide synthase
ntc	non template control
2OMe	2’-omethyl-phosphorothioates
pA	polyadenylation site
PAC	P1 artificial chromosome
PBS	phosphate-buffered saline without calcium and magnesium
PCiA	phenol-chloroform-isoamylalcohol
PEG	polyethylenglycol
PGK	phosphoglycerate kinase
PMO	phosphorodiamidate morpholino oligomer

PNS	positive-negative selection
pPMO	peptide linked phosphorodiamidate morpholino oligomer
rAAV	recombinant adeno-associated viral vector
RNase A	ribonuclease A
SCNT	somatic cell nuclear transfer
SDS	sodiumdodecylsulfate
SNP	single nucleotide polymorphism
TALE	transcription activator-like effector
TALEN	transcription activator-like effector nuclease
Tris	tris-(hydroxymethyl)-aminomethan
UNG	uracil-DNA glycosylase
$V_{V(MF/M)}$	volume density of muscle fibers in muscle
X-Gal	5-bromo-4-chlor-3-indoxyl-β-D-galactopyranosid
YAC	yeast artificial chromosome
ZFN	zinc finger nuclease

I. INTRODUCTION

Duchenne muscular dystrophy (DMD), a severe muscular wasting disease, is one of the most frequent lethal heritable disorders, affecting one in 3500 males (EMERY, 1991). It is caused by a great variation of mutations in the *DMD* gene, positioned on the X-chromosome (MONACO et al., 1986; KOENIG et al., 1987), which lead to a loss of function of the protein dystrophin (HOFFMAN et al., 1987). Dystrophin is located at the membrane of muscle cells and, as a part of the dystrophin-glycoprotein complex (DGC), links actin filaments of the cytoskeleton to the extracellular matrix (ERVASTI, 2007). The loss leads to instability of the muscle membrane and eventually to muscle cell degeneration, although the precise pathological mechanisms are still unknown (DECONINCK & DAN, 2007). DMD is characterized by generalized progressive muscle weakness, which manifests at an average age of two to four years. The affected boys show an impaired motoric development, are wheelchair-bound by the age of 12 years and die in their 2nd to 4th decade of life due to respiratory and cardiac failure (BLAKE et al., 2002). Up to this date no effective/curative treatment is available, however, several promising therapeutical approaches are currently under investigation (GOYENVALLE et al., 2011; PICHAVANT et al., 2011), including treatments in early clinical trials (VAN DEUTEKOM et al., 2007; KINALI et al., 2009; CIRAK et al., 2011; GOEMANS et al., 2011). Animal models are needed to transfer promising new treatment strategies from basic research to clinical application, analyze and improve their efficiency, evaluate their (side-) effects on the organism and thereby develop a successful therapy (AIGNER et al., 2010). Already existing mammalian DMD animal models comprise various mouse models, dog models and a dystrophin deficient cat model (NAKAMURA & TAKEDA, 2011). Yet the existing animal models have different genotypical or phenotypical characteristics limiting their applications in biomedical research (WILLMANN et al., 2009). The pig is a well-established animal model in biomedical research with several advantageous characteristics and diverse pig models have already been generated for different human diseases (LUNNEY, 2007; AIGNER et al., 2010). The establishment of nuclear transfer with genetically modified somatic cells (MCCREATH et al., 2000) enables the generation of tailored porcine animal models. For the introduction of a defined genetic modification bacterial artificial chromosomes (BACs) have successfully been used in mouse embryonic stem cells (TESTA et al., 2003;

VALENZUELA et al., 2003; YANG & SEED, 2003) and also in human embryonic stem cells (SONG et al., 2010). Efficient modification (ZHANG et al., 1998; COPELAND et al., 2001) and screening protocols (VALENZUELA et al., 2003; YANG & SEED, 2003) make them convenient tools for gene targeting experiments.

The aim of this study was to generate a tailored porcine DMD animal model, by introducing a defined mutation into the *DMD* gene of primary porcine kidney cells using a modified bacterial artificial chromosome as targeting vector, followed by somatic cell nuclear transfer.

II. OVERVIEW OF LITERATURE

1 X-linked muscular dystrophies

The X-linked muscular dystrophies, Duchenne Muscular Dystrophy (DMD) and Becker Muscular Dystrophy (BMD), are characterized by progressive muscular weakness with differing severity. They are recessive monogenetic disorders of the dystrophin encoding *DMD* gene localized on the X-chromosome and are caused by a great variety of different mutations. X-linked muscular dystrophies affect mainly male persons, women are just rarely affected. DMD has an incidence of about 300×10^{-6}, whereas the incidence of BMD is 45×10^{-6} (EMERY, 1991).

Edward Meryon described DMD clinically and histologically for the first time in 1851 at a meeting of the Royal Medical and Chirurgical Society (MERYON, 1851) and published his findings in the following year (MERYON, 1852). A few years later Guillaume Duchenne described the same disease and since then it has been called Duchenne muscular dystrophy (DUCHENNE, 1868).

1.1 Clinical features

Between the X-linked muscular dystrophies, DMD and BMD, the degree of clinical manifestation is continuous. The phenotypes vary greatly (MONACO et al., 1988). However, in the case of DMD and in severe cases of BMD the course of the disease is lethal, leading to a premature death of the affected persons in their twenties (EMERY, 1993).

The children seem normal at birth, but may already have increased serum creatine kinase (CK) levels (EMERY, 1977). First symptoms, caused by a progressive symmetrical weakness of the proximal lower limps, are apparent with about 2 – 5 years. The boys start walking delayed, have difficulties in climbing stairs and gait problems, like waddling, unsteadiness and walking on tiptoes. Later on calf hypertrophy, a lordotic posture and a positive Gower's sign (Figure II.1) can be observed (GOWERS, 1879d, 1879c, 1879b, 1879a).

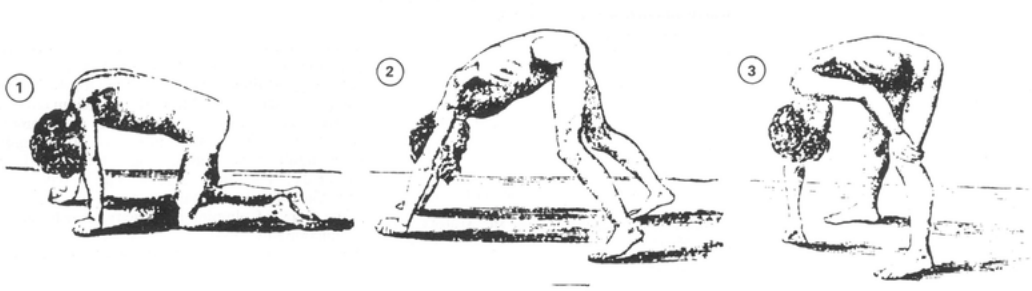

Figure II.1 Gower's sign

Gower's sign describes the typical way affected boys get up from a sitting to a standing position. They heave themselves up on their legs and straighten up by using their hands to walk up their legs; (GOWERS, 1879b).

By the age of 12 years progression of muscle weakness and joint contractures eventually lead to the dependence on a wheelchair. Arms are affected later on in the course of the disease. The overall muscle weakness induces a kyphoscoliosis. A pseudo-hypertrophy of different muscles can be observed in some patients (EMERY, 1993). Subsequent degeneration of respiratory and cardiac muscles most frequently causes the early death of the patients (BLAKE et al., 2002).

In patients affected with BMD the course of the disease is normally far milder than that in patients with DMD (reviewed in BRADLEY et al., 1978). Yet the phenotype varies greatly from a severe Duchenne-like to almost asymptomatic (BEGGS et al., 1991). Generally symptoms start delayed with around 12 years but it is possible that there are no apparent symptoms until much later. The progression of the disease is less rapid and also varies greatly. Furthermore, the life expectancy is much higher (EMERY, 1993). The criteria set by Jennekens facilitate the diagnosis by clinical manifestation (JENNEKENS et al., 1991).

All patients affected by a mutation in the *DMD* gene, even some female carriers, have an elevated serum CK concentration (VERMA et al., 2010). This can be used as a screening method or for diagnostics. In some cases of DMD as well as BMD, a cognitive and verbal impairment can be observed (HINTON et al., 2000; MEHLER, 2000) and there are also several cases in which solely the cardiac muscle is affected (FERLINI et al., 1999).

The histological picture of muscle with a dystrophinopathy shows grouped

degenerating or already necrotic fibers. In earlier stages there are signs of regeneration, such as centrally located nuclei, basophilic fibers and muscle fibers, which differ greatly in size (BELL & CONEN, 1968). Inflammatory cells like macrophages and CD4+ lymphocytes can be observed (MCDOUALL et al., 1990). Later on when the regenerating ability subsides there is an increase of fatty tissue and fibrous connective tissue (BLAKE et al., 2002).

1.2 *DMD* gene

DMD and BMD are caused by different mutations in the *DMD* gene. It has been shown that the diseases are allelic on this locus (KINGSTON et al., 1983a; KINGSTON et al., 1983b). The *DMD* gene has been localized to Xp21 on the X-chromosome (KUNKEL et al., 1985; RAY et al., 1985; MONACO et al., 1986; KOENIG et al., 1987).

1.2.1 Genetic structure

The *DMD* gene is composed of about 2.5 million base pairs and hence is the largest gene in the human genome. It comprises 79 exons and 7 different promoters with unique first exons (ROBERTS et al., 1993). Three independent promoters control the transcription of three different mRNAs sharing the same 78 exons, except for the first exon. The three promoters are named after the region of their predominant expression, brain, muscle and Purkinje promoter. The transcript of the brain promoter is mainly found in cortical neurons and the hippocampus. The product of muscle promoter is expressed in skeletal muscle cells, in cardiac muscle cells and in small amounts in glial cells of the brain and the Purkinje promoter is expressed in Purkinje cells and in skeletal muscle (BLAKE et al., 2002).

Besides the three long isoforms (Dp427) transcribed from the above mentioned promoters, there are four shorter isoforms originating from four different promoters located upstream of their first exon in intronic region. The promoter of isoform Dp260 (260 kDa) splices into exon 30. Dp260 is expressed in the retina together with the full-length brain and muscle isoforms (PILLERS et al., 1993; D'SOUZA et al., 1995). The Dp140 isoform (140 kDa), having exon 45 as second exon, was found in brain, retina and kidney (LIDOV et al., 1995; DURBEEJ et al., 1997). Exon 56 is second exon for the isoform Dp116 (116 kDa), which is located in adult peripheral nerves (BYERS et al., 1993). The shortest isoform Dp71 (71 kDa) is transcribed from a promoter, which uses exon 63 as first exon. Dp71 can be found in several tissues except skeletal muscle

(LEDERFEIN et al., 1992; AHN & KUNKEL, 1993). Besides the seven isoforms originating in different promoters there are several other isoforms caused by alternative splicing (FEENER et al., 1989; AUSTIN et al., 1995)

1.2.2 Mutations in the *DMD* gene

There is a great diversity in location and size of the mutations in the *DMD* gene. This is caused by a high new mutation frequency of one third of all mutations, based on the Haldane rule (MOSER, 1984; HALDANE, 2004).

The diversity of phenotypes can be ascribed to the mutational variance. Monaco stated 1988 the reading frame rule and explaining thereby the correlation between mutation and phenotype (MONACO et al., 1988). Mutations leading to a reading frame shift and thus generally exposing the transcript to nonsense mediated mRNA decay (KERR et al., 2001; MAQUAT, 2004) cause the loss of the dystrophin protein and lead to a DMD phenotype, whereas mutations, which leave the reading frame intact, produce a shorter but at least partially functional protein and give rise to a BMD phenotype. The knowledge of the exon structure in combination with the reading-frame rule can be used to predict the phenotype of a given mutation (KOENIG et al., 1989). The reading frame rule applies to 90% of all DMD and BMD patients, but there are exceptions to this rule (AARTSMA-RUS et al., 2006). Some patients with an in-frame mutation still show a DMD phenotype when essential parts of the protein are missing or when the resulting protein is unstable. It is also possible that the mutation affects the splicing process of the RNA and produces an out-of-frame product (GUALANDI et al., 2003). Deletions of more than 35 exons in the rod domain cause DMD, whereas deletions with less exons results in a protein which appears to be partly functional (AARTSMA-RUS et al., 2006). The complete loss of the actin-binding domain and parts of the central rod domain results also in a DMD phenotype (VAINZOF et al., 1993; ARIKAWA-HIRASAWA et al., 1995). A deleted cysteine-rich domain is always associated with DMD (BIES et al., 1992). Other patients show a Becker phenotype although the mutation changes the reading frame. The expression of a functional dystrophin in most of these cases is thought to be the result of exon skipping by alternative splicing. Deletions of exons do have different break points in the intronic sequence and might affect regulatory elements of the splicing machinery. It is also possible that factors regulating the splicing procedure have different expression levels, accounting for differences in patients with exactly the same mutation (reviewed in

MUNTONI et al., 2003 and AARTSMA-RUS et al., 2006).

The frequency of intragenic deletion of exons in the *DMD* gene varies between 60% and 72%, depending on which database was used. The deletion can affect one or more exons. Duplication of one or more exons can be found in 7% of the patients. The remaining portion consists of smaller deletions, insertions, point mutations and intronic mutations (MUNTONI et al., 2003; AARTSMA-RUS et al., 2006; TUFFERY-GIRAUD et al., 2009).

There are two mutational hotspots in the *DMD* gene (KOENIG et al., 1987; DEN DUNNEN et al., 1989). The first minor hotspot region extends from exon 2 to 20. The second and major region spans from exon 47 to 53, containing most deletions. Duplications are frequently found in the 5' hotspot region (LIECHTI-GALLATI et al., 1989; BEGGS et al., 1990). The reasons for this accumulation of large mutation in these regions are still unknown. However, it has been discovered that they correspond to major meiotic recombination hot spots (OUDET et al., 1992). Characterization of the deletion breakpoints showed that most of them can be found in just a few introns in the 3' region whereas they are evenly distributed in the 5' region (TUFFERY-GIRAUD et al., 2009). Nonhomologous or illegimate recombination (IR) with nonhomologous end joining (NHEJ) is discussed to be involved in the generation of new mutations. But sequence analysis of the deletion breakpoints did not verify this theory (SIRONI et al., 2003).

Point mutations seem to be evenly distributed. They can introduce premature stop codons, nonsense codons, cause a frame-shift or affect splice sites (reviewed in ROBERTS et al., 1994).

1.3 Dystrophin protein

The protein dystrophin is the product of the *DMD* gene (HOFFMAN et al., 1987). It has a molecular weight of 427 kDa and belongs to the β-spectrin/α-actinin protein family (KOENIG et al., 1988). It is located at the sarcolemma of the muscle cells and links γ-actin filaments of the cytoskeleton of muscle cells to the extracellular matrix (Figure II.2). Being part of the dystrophin-glycoprotein complex (DGC), it is associated with the costameric proteins, which connect the Z disk of myofibrils over the membrane to laminin-2 in the extracellular matrix. Besides dystrophin the DGC includes α- and β-dystroglycans, α-dystrobrevin, syntrophin, sarcoglycans (α, β, γ, δ),

and sarcospan (ERVASTI, 2007).

Dystrophin can be organized into four domains: the NH_2-terminus, the central rod domain, the cysteine-rich domain and the COOH-terminal domain (reviewed in AHN & KUNKEL, 1993).

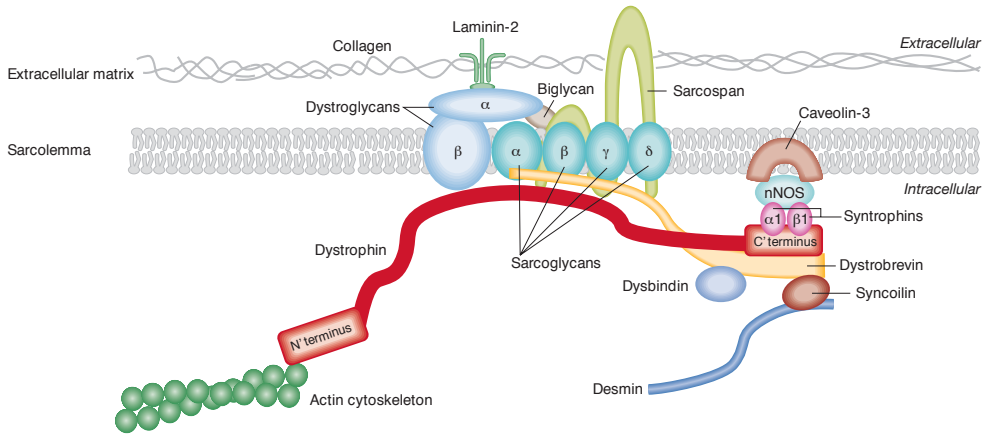

Figure II.2 Dystrophin and its interactions with the other proteins of the dystrophin-glycoprotein complex

nNOS: nitric oxide synthase; from (NOWAK & DAVIES, 2004).

The amino terminal domain has sequential and functional homologies to α-actinin and β-spectrin (KOENIG et al., 1988). The central rod domain is composed of 24 triple helical coiled-coil spectrin-like repeats, interspersed by four proline-rich hinge regions. The cysteine-rich domain consists of the two EF hand-like modules, the WW domain and the ZZ domain (KOENIG et al., 1988; BORK & SUDOL, 1994; PONTING et al., 1996). The WW domain is described as proline-rich protein binding domain, which can be found in other proteins involved in signaling and regulatory mechanisms (BORK & SUDOL, 1994). The two EF-hand motives show homologies to the calcium binding EF-hand motifs of α-actinin (KOENIG et al., 1988). The last part of the cysteine-rich region is the ZZ-domain. Like Zn^{2+} binding Zinc-Fingers this domain contains several cysteine residues (PONTING et al., 1996). The carboxy-terminal domain of dystrophin includes coiled-coil motives, which are protein interaction domains (BLAKE et al., 1995).

Interactions of dystrophin are depicted in Figure II.2. The NH_2-terminus and the central rod domain of dystrophin bind γ-actin (RYBAKOVA et al., 1996). The central

rod domain is thought to give flexibility to the protein (KOENIG & KUNKEL, 1990). β-dystroglycan is attached to dystrophin at the cysteine-rich domain and to some extent at the COOH-terminus. It is a transmembrane protein and binds to the extracellular α-dystroglycan, which is connected with laminin-2. The dystroglycans are also linked to sarcoglycans and sarcospan, thereby strengthening other molecule interaction in the DGC. The C-terminal domain is also the binding site of dystrobrevin and the syntrophins, which interact with several different signaling molecules, including the neuronal nitric oxide synthase (nNOS) (reviewed in ERVASTI, 2007).

1.4 Pathomechanism

There are several different approaches to explain the pathomechanism of muscular dystrophy (reviewed in BLAKE et al., 2002 and DECONINCK & DAN, 2007). However, the entire process is still unclear. One aspect might be that the loss of dystrophin leads to lesions in the cell membrane causing an increased fragility. This theory is supported by electron-microscopic findings, called delta lesions, and the detection of cytosolic molecules in the blood of DMD patients (MOKRI & ENGEL, 1975). Additionally extracellular proteins could be identified in the cytoplasm of the *mdx* mouse, a DMD animal model (CLARKE et al., 1993; STRAUB et al., 1997). Another aspect of the pathomechanism is the elevated intracellular calcium concentration in DMD muscle cells (EMERY & BURT, 1980). An increased influx through mechanosensitive voltage-independent calcium channels might explain the higher level of calcium (VANDEBROUCK et al., 2002). Calcium ions activate proteases i.e. caplains, which hydrolyze proteins and thereby damage the cell. Since the role of the DGC in cell signaling pathways is not yet fully understood, there might be other processes involved in muscle damage, for example the possible impaired function of the enzyme nitric oxide synthase or changed gene expression patterns (RANDO, 2001; DECONINCK & DAN, 2007).

1.5 Therapeutical approaches for DMD

Up to this date there is no effective therapy for DMD. Treatments for DMD patients at the moment are aimed at the amelioration of symptoms. Glucocorticoids, such as prednisone and deflazocort, are administered as they have positive effects on muscles (MANZUR et al., 2008). Furthermore, physical medicine and rehabilitation are important parts of the patient's management (VERMA et al., 2010). However, there are several different new therapeutical approaches studied right now, which comprise

various pharmacological strategies, gene replacement and exon skipping (reviewed in GOYENVALLE et al., 2011 and PICHAVANT et al., 2011).

Pharmaceutical approaches include the upregulation of the expression of the protein utrophin and read-through strategies for nonsense mutations. Utrophin is an orthologous protein of dystrophin, normally expressed during embryogenesis and later on at neuromuscular and myotendinous junctions (KHURANA et al., 1991; TINSLEY et al., 1992). There are great structural and functional similarities relevant for therapeutical application between utrophin and dystrophin (reviewed in PERKINS & DAVIES, 2002), giving rise to several different approaches to regulate transcription of utrophin (GOYENVALLE et al., 2011). Read-through strategies are just relevant for DMD patients with a mutation causing a stop codon. Some drugs, such as Gentamicin and Ataluren, introduce an amino acid at a premature stop codon, causing the translation to carry on (PICHAVANT et al., 2011).

Rather than repairing the defect in the *DMD* gene, the aim of gene replacement is to introduce another functional copy of the *DMD* gene in muscle. Viral vectors, such as lentiviral, adenoviral and adeno-associated viral vectors (AAV), are currently used as a method of gene delivery. Physical approaches such as hydrodynamic pressure or electroporation are also available. Lentiviral vectors transduce proliferating and terminally differentiated muscle cells (LI et al., 2005). However, their transduction rate *in vivo* is low and they may cause insertional mutagenesis (MACKENZIE et al., 2005; BEARD et al., 2007). Initial experiments with adenoviral vectors were promising, but in non-human primates and in humans they initiated major adverse immunological effects (RAPER et al., 2003; BRUNETTI-PIERRI et al., 2004). Mainly recombinant AAV (rAAV) vectors are used in clinical trials. Several different serotypes are described, but just rAAV1, 6, 7, 8 and 9 are interesting for muscular application (SCHULTZ & CHAMBERLAIN, 2008). The limited carrying capacity of viral vectors requires modifications of the *DMD* gene to reduce its size. On the basis of BMD patients with great deletions in the *DMD* gene mini- and micro-dystrophin cDNA genes were constructed with deletions in the rod domain and the C-terminal (HARPER et al., 2002).

Mutations causing DMD generally disrupt the reading frame, whereas mutations, which leave the reading frame intact, give rise to a BMD phenotype. Antisense-induced exon-skipping strategies try to convert an out of frame deletion into an in

frame deletion by skipping one or more exons and induce a BMD phenotype, with a shortened but functional dystrophin (AARTSMA-RUS et al., 2009). Table II.1 indicates the mutations listed in the Leiden DMD database, which can be treated with skipping of certain exons and the percentage of the affected patients within the database (VAN DEUTEKOM & VAN OMMEN, 2003).

Table II.1 Overview of theoretic therapeutic exon skipping for certain DMD mutations

Skippable exon	Therapeutic for DMD deletions (exons)	Percentage of deletions in LDMD database
2	3–7, 3–19, 3–21	2.9
8	3–7, 4–7, 5–7, 6–7	4.5
17	12–16, 18–33, 18–41, 18–44	1.8
43	44, 44–47, 44–49, 44–51	3.7
44	14–43, 19–43, 30–43, 35–43, 36–43, 40–43, 42–43, 45, 45–54	7.8
45	12–44, 18–44, 44, 46–47, 46–48, 46–49, 46–51, 46–53, 46–55	11.2
46	21–45, 45, 47–54, 47–56	5.6
50	51, 51–53, 51–55	5.2
51	45–50, 47–50, 48–50, 49–50, 50, 52, 52–63	17.5
52	51, 53, 53–55	4.0
53	10–52, 45–52, 46–52, 47–52, 48–52, 49–52, 50–52, 52	7.5
55	45–54, 48–54	1.8
Total	12 AONs	73.5

from: (VAN DEUTEKOM & VAN OMMEN, 2003)

Synthetic single-stranded DNA or RNA molecules with a length of about 25 bp bind to specific splice motifs of the pre-mRNA and thereby causing the desired exon to be left out in the mature mRNA. 2'-Omethyl-phosphorothioates (2OMe) and phosphorodiamidate morpholino oligomers (PMO) differ from each other in chemical modifications of the oligonucleotides to enhance their pharmaceutical properties (reviewed in NAKAMURA & TAKEDA, 2009). Improvement of the cellular uptake of PMOs is expected by fusing different molecules to PMOs, for example an arginine-rich peptide (pPMO). However, pPMOs show a toxic effect in kidneys (AMANTANA et al., 2007; MOULTON & MOULTON, 2010). Clinical trials on the basis of skipping exon 51 have been conducted and had promising results (VAN DEUTEKOM et al., 2007; KINALI et al., 2009; CIRAK et al., 2011; GOEMANS et al., 2011). Improvements in body-wide distribution with effective levels and an overall enhancement of the exon skipping efficiency is still essential (WOOD, 2010). Immunological reactions against the vectors or even against the newly build dystrophin are aspects, which have to be considered in further developments

(MENDELL et al., 2010; MOORE & FLOTTE, 2010).

2 DMD animal models

Available options for treatment of DMD are still insufficient. Animal models are needed to transfer promising new treatment strategies from basic research to clinical application and analyze their potential and efficiency as well as the adverse effects (AIGNER et al., 2010). There are certain requirements an animal model should comply with. The genetic basis for the muscular dystrophy in animals should resemble the human situation. Furthermore, should the model's phenotype approximate the human phenotype and variation in phenotype between individual animals should be minor, also over generations, to ensure comparability of experiments. The animal model should be well characterized, easy and inexpensive to maintain and easy to handle (WILLMANN et al., 2009).

2.1 Murine DMD models

Various different DMD mouse models have been established. Several of the mouse models display mutations in the *Dmd* gene, however, there are also mouse models, which have additionally other genes affected. The *mdx* mouse has a spontaneous mutation occurring in the *Dmd* gene, whereas the other mouse models have mutations introduced by targeting or derived from *N*-ethyl-nitrosourea (ENU) chemical mutagenesis treatment.

The *mdx* mouse was the first discovered DMD mouse model. It has a point mutation in exon 23 of the *Dmd* gene, which occurred naturally in the C57BL/10 strain, leading to a premature stop codon (BULFIELD et al., 1984). The observed pathology in affected mice is less severe than that in human DMD patients and they have just a slightly reduced lifespan. From 2 to 8 weeks of age their muscle pathology is most pronounced, with elevated serum CK levels and showing marked degeneration and regeneration, with necrotic muscle fibers and newly generated fibers with centrally located nuclei and differing sizes. From 8 weeks on the pathological changes decrease to a lower level (MCGEACHIE et al., 1993) and the muscle weakness just becomes obvious in old age (LEFAUCHEUR et al., 1995). Muscle fibrosis in *mdx* mice is less striking than that in DMD patients, except for the diaphragm (MULLER et al., 2001). The heart muscle is also affected, partially resembling the human DMD heart phenotype (QUINLAN et al., 2004). Skeletal muscle pathology can be worsened by

increased exercise (WILLMANN et al., 2009). There are several different approaches to explain the mild phenotype of the *mdx* mice. First of all, mice seem to have a higher regenerative capacity compared to human. They also might compensate the loss of dystrophin with the homologous protein utrophin (DURBEEJ & CAMPBELL, 2002).

Four additional DMD mouse models (*mdx*^{2Cv}, *mdx*^{3Cv}, *mdx*^{4Cv} and *mdx*^{5Cv}) were created by treating mice with the chemical mutagen ENU (CHAPMAN et al., 1989). *mdx*^{2Cv} and *mdx*^{3Cv} mice both have a point mutation in the splice acceptor sequence in intron 42 and in intron 65 respectively. A point mutation in exon 53 in *mdx*^{4Cv} leads to a premature stop codon and *mdx*^{5Cv} mice display a new splice donor caused by a point mutation in exon 10 (IM et al., 1996; COX et al., 1993). Although they show varying mutations in the *Dmd* gene, affecting the expression of different dystrophin isoforms, their phenotype mainly resembles that of the *mdx* mouse with slight differences, (reviewed in WILLMANN et al., 2009).

A complete deletion of the *Dmd* gene has been achieved using the Cre-*loxP* recombination system. Although the resulting DMD-*null* mice do not express any dystrophin isoforms, their phenotype does not differ considerably from the *mdx* phenotype. However, changes in behavior were reported in DMD-*null* mice (KUDOH et al., 2005).

In order to create a DMD mouse model, which also affects shorter dystrophin isoforms, exon 52 knockout mice were generated by targeted mutagenesis, imitating a human mutation leading to a DMD phenotype. In *mdx52* mice expression of dystrophin isoforms Dp140, Dp260 and Dp427 is disrupted, whereas the expression of isoforms Dp71 and Dp116 is not affected. The *mdx52* mice do not show any obvious signs of muscular weakness up to 1 year of age. Yet the limb muscles of affected animals display a hypertrophy similar to that in DMD patients. Degeneration and regeneration of muscle fibers can be observed, but there is no apparent fibrosis or fat infiltration. The diaphragm is markedly affected (ARAKI et al., 1997). The loss of Dp260, which is located in the retina, may cause an abnormal electroretinogram (KAMEYA et al., 1997). But the loss of Dp140, located in the brain, does not give rise to pathological changes in the brain and the behavior seemed normal. The pathology of the *mdx52* is similar to that of the *mdx* mice, except for the hypertrophy of the limb muscles and the abnormal electroretinogram (ARAKI et al., 1997).

Besides the mouse models, which affect just the *Dmd* gene, there are several other

mouse models displaying an additional mutation in another gene, like the *utrophin*, *MyoD, α-dystrobrevin, α7β1intergrin* and *parvalbumin* gene. These mouse models were established to aggravate the phenotype and to obtain information about functional importance of the deleted genes (WILLMANN et al., 2009).

2.2 Canine DMD models

X-linked muscular dystrophy caused by spontaneous mutations in the *DMD* gene has been discovered in divers dog breeds, amongst others the Golden Retriever (COOPER et al., 1988), the German Short-Haired Pointer (SCHATZBERG et al., 1999) and the Cavalier King Charles Spaniel (WALMSLEY et al., 2010). The mutation of the Golden Retriever Muscular Dystrophy (GRMD) has been characterized (SHARP et al., 1992) and introduced into Beagles, giving rise to the Beagle-based Canine X-linked Muscular Dystrophy in Japan ($CXMD_J$) (SHIMATSU et al., 2003).

The two most widely used canine models are based on a naturally occurring mutation found in Golden Retriever. This point mutation is localized in the canine *DMD* gene at the acceptor splice site in intron 6, resulting in the skipping of exon 7 and in consequence in a premature stop in exon 8 (SHARP et al., 1992). The characteristics of GRMD are similar to those of DMD, however, the phenotypes are very variable (AMBROSIO et al., 2009). Generally the muscle weakness is progressive and the muscles show extensive degeneration and necrosis from birth onwards. Impairment of motoric abilities can be observed. Later on muscle fibrosis and joint contractures give rise to skeletal deformations and hypertrophy of tongue, pharynx and oesophagus muscles, which cause problems like regurgitation and dysphagia. GRMD dogs also develop a cardiomyopathy and the serum CK concentration is always increased (COOPER et al., 1988; VALENTINE et al., 1988).

The beagle DMD model ($CXMD_J$) and the GRMD dogs resemble each other in their phenotype, although the manifestation of the symptoms is milder in $CXMD_J$ and the dogs are easier to handle because of their smaller size (WILLMANN et al., 2009).

Recently Cavalier King Charles Spaniels with muscular dystrophy were discovered (CKCS-MD). A missense mutation in the 5' donor splice site of exon 50 results in the deletion of this exon. The phenotype of the 3 dystrophic dogs, described in this study, seems to resemble that of the GRMD and $CXMD_J$ dog models (WALMSLEY et al., 2010).

2.3 Feline DMD models

Dystrophinopathy in cats has been described as hypertrophic feline muscular dystrophy (HFMD) (VOS et al., 1986; CARPENTER et al., 1989; GASCHEN et al., 1992). The deletion of the muscle and Purkinje promoters results in the loss of dystrophin in skeletal and heart muscle (WINAND et al., 1994). The main characteristic of the disease is the marked muscle hypertrophy of the skeletal muscles and especially the tongue muscles. This leads to a stiff, bunny-hopping gait, decreased exercise tolerance, increased salivation and regurgitation (SHELTON & ENGVALL, 2005). Histology shows degenerating and regenerating fibers and calcification spots, but it does not show any fibrosis. The serum CK concentration is increased and HFMD cats additionally display a dilated cardiomyopathy (GASCHEN et al., 1999). Affected cats eventually die due to a compression of the esophagus by the hypertrophic diaphragm or because of renal failure, caused by a decreased water intake due to an enlargement of the tongue (GASCHEN et al., 1992).

2.4 Other DMD models

Dystrophin orthologous have been described in several different non-mammalian animals, like zebrafish, *C. elegans*, *Drosophila* and the sea urchin. Zebrafish have also orthologs of most DGC proteins with similar localization at the membrane. Dystrophin deficiency in fish causes a bent morphology and reduced activity (GUYON et al., 2003). *C. elegans* express a dystrophin homologue *dys-1*. Mutations in this gene lead to hyperactivity, hypercontraction and increased sensitivity to acetylcholine and its inhibitor (BESSOU et al., 1998).

2.5 DMD models for therapeutical approaches

A DMD animal model for therapeutical approaches has to comply with several different requirements as mentioned above. Using mouse models in DMD research has various reasons. They are very well characterized, easy and inexpensive to maintain, easy to handle and have a consistent genetic background and phenotype (GROUNDS et al., 2008). A major drawback of murine DMD models is their relatively mild phenotype compared to human and past failures of therapies, which worked in mice but did not work in humans (COLLINS & MORGAN, 2003). Additionally does the *DMD-null* mouse model not display a mutation found in human and a complete knockout of the *Dmd* gene reduces the number of treatment approaches, which can be tested with this model. Double knockout mice are not

suitable for therapy testing due to the lack of concordance between their double mutations and the human mutations, although their phenotype may have a higher resemblance to the human phenotype. The GRMD, the $CXMD_J$ and the CKCS-MD dog models seem to be appropriate DMD models, because they have a very similar phenotype to human DMD patients and a similar size. However, the severity varies greatly between individuals, what makes comparison of experiments difficult. High expenses for maintaining colonies are another disadvantage of using dogs as models for DMD in pre-clinical testing (WILLMANN et al., 2009). Dystrophic cats are not often used as DMD models, because their phenotype varies greatly from human DMD patients and the expenses to maintain colonies are high. Large numbers of the non-mammalian animal models, the potential for genetic manipulation, high reproducibility of experiments and easy breeding and maintenance make them suitable for the usage in high-throughput initial studies, although their musculature and their phenotype do not resemble the phenotype of human DMD patients (COLLINS & MORGAN, 2003).

Several different studies for therapeutical applications have been conducted with the existing models (NAKAMURA & TAKEDA, 2011). One has to bear the limitations of each animal model in mind when evaluating the results. The *mdx* mouse has been used for exon skipping experiments with 2OM antisense oligonucleotides (LU et al., 2003), PMO (FLETCHER et al., 2006; WELLS, 2006), pPMO (JEARAWIRIYAPAISARN et al., 2008) and also with recombinant AAVs as vectors for exon-skipping experiments (GOYENVALLE et al., 2004) and for gene replacement experiments (GREGOREVIC et al., 2004; WANG et al., 2005; BISH et al., 2008). *Mdx52* mice can also be used for exon-skipping therapy trials. There are several human DMD patients, which would benefit from this approach. Skipping exon 51 in these models is supposed to restore the reading frame. Recently PMO were used to skip exon 51 successfully (AOKI et al., 2010). Gene therapy experiments with adenoviral vectors and AAV vectors with mini-dystrophins (HOWELL et al., 1997; HOWELL et al., 1998; KORNEGAY et al., 2010) and chimeric RNA/DNA oligonucleotide for exon-skipping were tested in the GRMD dog (BARTLETT et al., 2000). 2OMe, PMO or pPMO have been compared in cultured GRMD muscle cells (MCCLOREY et al., 2006). In CKCS-MD muscle cell cultures skipping of exon 51 restored the reading frame and protein expression (WALMSLEY et al., 2010). In $CXMD_J$ dog model experiments with multiexon skipping via PMOs and experiments

to evaluate efficiency of rAAVs have been conducted (YUASA et al., 2007; OHSHIMA et al., 2009; YOKOTA et al., 2009).

3 Genetic engineering of large animal models

Genetic diseases are caused by mutations, which lead to an alteration of function. In the case of DMD mutations of the *DMD* gene lead to the loss of the dystrophin function. Up to this date there is no curative/effective treatment available for DMD. Animal models with a corresponding functional deficiency are needed for further research and particular for developing a successful therapy. Yet existing animal models are of limited relevance, because they do not meet the requirements of a satisfactory DMD model. Therefore, a more suitable model is required. In order to create an animal model with a corresponding loss of function a site directed mutagenesis of the desired gene, in this case of the *DMD* locus, is necessary. This can either be achieved by homologous recombination, by designer nucleases like zinc finger nucleases (ZFN) or by combination of both. With the exception of mouse, and more recently rats, no germ line competent embryonic stem cells (ESCs) are available. Thus alternative technologies are inevitable for the generation of site-directed mutations in other species. To date somatic cell nuclear transfer (SCNT) of genetically modified cells is the preferred method establishing a model with defined targeted mutations (reviewed in AIGNER et al., 2010).

3.1 Large animal models/pig models

Several similarities between humans and pigs make the pig a suitable model for humans in various fields of medical research. They have got a similar size, anatomy, physiology, metabolism and pathology (reviewed in LUNNEY, 2007). Reproductive characteristics like an early sexual maturity, a short generation interval, large litter size, no seasonal break in breeding and also standardized housing conditions (REHBINDER et al., 1998) are advantageous (reviewed in AIGNER et al., 2010).

The pig genome is almost completely sequenced. Data are permanently updated on the Ensembl website (http://www.ensembl.org/Sus_scofa/Info/Index). Bioinformatics analyses on the pig genome are only rudimentary available. But comparison of representative exonic, intronic, 3'UTR, 5'UTR, intergenic regions and miRNAs of human, pig and mouse revealed a greater phylogenetic similarity between human and pig than between human and mouse (WERNERSSON et al., 2005). The cDNA

analysis of human, mouse and pig proteins supports this thesis (JORGENSEN et al., 2005).

Pigs, even without genomic alterations, have proven to be adequate models in various diseases (LUNNEY, 2007). Genetically modified porcine models were established for neurodegenerative diseases, cardiovascular diseases (reviewed by AIGNER et al., 2010), cystic fibrosis (ROGERS et al., 2008) or diabetes mellitus (RENNER et al., 2010). Pigs do also play a major role in xenotransplantation (KLYMIUK et al., 2010).

3.2 Nuclear transfer

SCNT of genetically modified primary cells overcomes the lack of porcine ESCs. In SCNT nuclei of donor cells obtained from various tissues are transferred in enucleated oocytes or zygotes (reviewed in WOLF et al., 1998). This technology has various favorable characteristics. Donor cells can be pre-selected and screened regarding gender or transgene integration qualities, the resulting organisms are genetically identical and they are not a mosaic (AIGNER et al., 2010). Even so comparison of SCNT efficiency is difficult due to differences in experimental protocols, embryo selection and data presentation, it is generally below 5% (CAMPBELL et al., 2005). The low efficiency is ascribed to incorrect epigenetic reprogramming (SHI et al., 2003), causing abnormalities of placenta, embryos, fetuses and offspring (ZHAO et al., 2010). Abnormalities in pigs include contracted tendons and enlarged tongues (PRATHER et al., 2004).

For the first time successful application of somatic cells in nuclear transfer was reported in sheep (WILMUT et al., 1997). Since then various transgenic animal models have been established in various animal species, such as sheep, goats and cattle (MCCREATH et al., 2000; DENNING et al., 2001; KUROIWA et al., 2004; SENDAI et al., 2006; YU et al., 2006; RICHT et al., 2007; KUROIWA et al., 2009; ZHU et al., 2009). It was later on also established in pigs, using fetal fibroblasts, cultured adult granulosa cells and fetal cells (BETTHAUSER et al., 2000; ONISHI et al., 2000; POLEJAEVA et al., 2000). Targeted genes of the porcine genome comprise the alpha-1,3-galactosyltrasnferase (*GGTA1*) (LAI et al., 2002), cystic fibrosis transmembrane conductance regulator (*CFTR*) (ROGERS et al., 2008), the kappa light chain constant region (RAMSOONDAR et al., 2011) and the heavy chain joining region (MENDICINO et al., 2011).

3.3 Introduction of DNA into primary cells

For the site-directed genetic modification of the primary cells used as donor cells in SCNT DNA or RNA has to be introduced into the cells. This can be achieved either by viral or non-viral methods. Non-viral methods can be divided in to chemical or physical methods.

Viral gene transfer presents one possibility to insert a transgene into the genome of cells. Known viral systems used for gene transfer are prototypic retroviruses, lentiviruses and AAVs. However, only AAVs, single stranded parvoviruses with several serotypes and differing tissue tropisms, have been described to perform site-directed mutagenesis (RUSSELL & HIRATA, 1998) and one tailored pig model was established (ROGERS et al., 2008). Other viral gene transfer systems, like lentiviruses (PFEIFER, 2004), can be used successfully for producing transgenic animals (HOFMANN et al., 2003). They transport the transgenes directly into the nucleus enabling transgenesis of dividing and non-dividing cells, but the integration of the transgenes occurs randomly, which may cause unwanted side effects. The genetic material of retroviruses undergoes extensive silencing when inserted into the host genome impairing the expression (FOLLENZI et al., 2000; HOFMANN et al., 2006). It has to be taken under consideration that the packing capability of viral vectors is limited to < 10 kb at most (ROBL et al., 2007), AAV vectors even just being able to carry 4.5 kb of foreign material (HENDRIE & RUSSELL, 2005).

Chemical introduction of nucleic acids is achieved by lipofection, calcium phosphate precipitation, cationic polymers or molecular conjugates. Physical methods include biolistic bombardment technique, microinjection and electroporation (COLOSIMO et al., 2000). The nucleofection technology is a further development of electroporation and presents a combination of chemical and physical methods. Lipofection, electroporation and nucleofection are the most commonly used non-viral transfection methods for primary cells today. Lipofection is based on the delivery of DNA or RNA via encapsulation in cationic liposomes (FELGNER et al., 1987). These artificial particles either fuse with the cell membrane or enter the cell via endocytosis. Lipofection can reach a relatively high efficiency, however, reaction conditions, such as DNA and liposome ratio, have to be optimized for each experiment. Several different formulas for lipofection are available (RECILLAS-TARGA, 2006). Electroporation delivers the genetic material into the cell by electric pulses, which lead to the permeabilisation of the cell membrane for DNA molecules (NEUMANN et

al., 1982). Due to an increased cell death after electroporation, the parameters, like pulse length and strength, have to be optimized for differing cell types and also for different DNA molecules. Nucleofection combines electroporation with cell type specific solutions in order to transport the genetic material directly into the nucleus in contrast to other methods, which transfer DNA or RNA just into the cytoplasm (HAMM et al., 2002). For each cell type specific nucleofection solutions and electroporation programs have been established in order to increase efficiency and minimize cell death (MAURISSE et al., 2010). Targeting efficiency, cell toxicity and number of random integration events differ greatly between all these methods, also depending on which cell type and transfection conditions are used. Several studies have been conducted to determine the most efficient method. Earlier studies comparing lipofection and other chemical methods, with electroporation showed that electroporation seems to be the most efficient method (YANEZ & PORTER, 1999; VASQUEZ et al., 2001). More recent studies, which compare nucleofection with lipofection and electroporation for several different cell types generally revealed a higher targeting efficiency of nucleofection. Though cytotoxicity also seems to be higher with nucleofection compared to lipofection (JACOBSEN et al., 2006; CAO et al., 2010; MAURISSE et al., 2010; MO et al., 2010). However, one study comparing lipofection with nucleofection states that nucleofection is less efficient, but also less cytotoxic (SKRZYSZOWSKA et al., 2008).

3.4 Site directed mutagenesis of primary cells

Today site-specific genome modification of primary cells can either be achieved by homologous recombination (HR), by designer nucleases like ZFN or by combination of both. The first gene targeting was accomplished in erythroleukemia cells at the human the β–globin locus (SMITHIES et al., 1985). Gene targeting via homologous recombination makes use of the cell's own repair mechanisms for double strand breaks (DSB). DSB occur naturally in all cell types and are either repaired by nonhomologous end joining (NHEJ) or by HR (HABER, 2000). In HR a homologous DNA molecule is used to repair the DNA strand carrying the DSB. The mechanism of homologous recombination may be accomplished by three different pathways, all of them beginning with the resection of the 5'end of the DSB. Processes of HR and NHEJ are reviewed by HABER, 2000 and PARDO et al., 2009. When introducing a DNA fragment, which is homologous to a specific sequence, it is assumed that the DNA fragment locates to and recombines with its homologous region in the cell's

genome mediated by the available DNA repair enzymes (SORRELL & KOLB, 2005). However, the foreign molecules are also inserted randomly, which may be caused by NHEJ (VASQUEZ et al., 2001). Generally HR is a rare event and occurs in about 1 per 10^5 or 10^6 treated cells, 3-4 × 10^4 times less frequent than NHEJ in mouse ESCs and even less frequent in primary somatic cells (DOETSCHMAN et al., 1987; SEDIVY & SHARP, 1989; HASTY et al., 1991; SEDIVY & DUTRIAUX, 1999). Also did comparison of targeting efficiency of an active and a non-expressed gene show that an expressed gene can be more easily targeted (KUROIWA et al., 2004).

3.4.1 Vectors for gene targeting

Gene targeting can be achieved either by introduction of any mutation at a defined site or by the integration of a defined mutation. The first one is often done when a DSB occurs, which can be artificially caused by ZFN. The DSB is repaired by NHEJ and may result in mutations leading to a loss of function of the targeted gene (PORTEUS & CARROLL, 2005). Defined mutations require vectors carrying the designed modification as well as sequences upstream and downstream of the modification cassette, which are homologous to the target locus and thus facilitate HR between the genome and the vector. The length of homology between the DNA sequence of vector and genome target locus is said to play a major role in efficiency: a longer homology leads to an increase in frequency (DENG & CAPECCHI, 1992; SCHEERER & ADAIR, 1994). Large vectors such as yeast artificial chromosomes (YACs), P1 artificial chromosomes (PACs) or bacterial artificial chromosomes (BACs) thus increase the rate of HR. It may not be necessary that the sequence of the DNA molecule is isogenic for targeting in all cell types (SEDIVY et al., 1999), although it was shown to be beneficial for targeting frequency in mouse ESCs (TE RIELE et al., 1992).

AAVs provide, in addition to the efficient transfer of exogenous DNA into the nucleus of the target cell an additional benefit: they have a relatively high targeting efficiency. A successful targeting of the *CFTR* gene has been achieved in the pig using AAVs as targeting vector with targeting efficiencies from 0.07 to 10.93%. Although these numbers include targeted cell clones, which were not examined for randomly integrated constructs (ROGERS et al., 2008). The exact mechanism of integration is still discussed (HENDRIE & RUSSELL, 2005; SCHULTZ & CHAMBERLAIN, 2008), but it is known that an increase in length of homologous sequences, in virus

dose, in time after infection and a centrally positioned transgene in the viral genome elevates the targeting frequency. Limited packing ability of foreign DNA of 5 kb may restrict the applications of AAV vectors (HIRATA & RUSSELL, 2000; VASILEVA et al., 2006).

3.4.2 Positive selection

The efficiency of introduction of foreign DNA into the cell and, even more, the efficiency of integration of the foreign DNA into the genome are rare processes. In order to distinguish cells with stably integrated transgene from negative cells a selection strategy is needed. The easiest way is to insert a gene for antibiotic resistance as a positive selection cassette into the vector with all necessary elements for transcription, such as a promoter and a terminating polyadenylation signal. The promoter has to be active in the transfected cells, thus ubiquitous promoters such as the one of the phosphoglycerate kinase (*PGK*) gene are preferred to provide transcription of the selection gene in any transfected cell type (CHEAH & BEHRINGER, 2001). Frequently used positive selection markers are genes providing resistance to neomycin, blasticidin, puromycin or hygromycin (VAN DER WEYDEN et al., 2002). The selection cassette should generally be flanked by recognition sequences for site-specific recombinases, to provide a possibility to remove the selection cassette if necessary, as it may affect gene expression in and around the targeted locus (FIERING et al., 1995; PHAM et al., 1996). Recognition sites for Cre, FLPe or ϕC31 have been used regularly (SORRELL & KOLB, 2005).

3.4.3 Negative selection

Cells with integrated transgene are selected positively without differentiating between random or site directed insertion. However, a lot of cell clones have to be screened for positive integration in order to find a clone, which has undergone HR, as there are far more random integration events than HR events. To increase the number of cell clones with targeted mutation several different methods can be used. For positive-negative selection (PNS) a negative selection cassette, such as thymidine kinase or diphtheria toxin A, is placed in addition to the positive selection cassette outside of one or both of the homologous sequence of the linearized transgene (NAGY et al., 2003). In the case of HR the cassette is lost, otherwise the cell succumbs to the negative selection. PNS yields 2-10 fold enrichment for targeted clones compared to positive selection resistance alone. The low enrichment values may be caused by damage of the

sequence of the negative selection cassette (SORRELL & KOLB, 2005). Mario R. Capecchi, Sir Martin J. Evans and Oliver Smithies were awarded the Nobel Prize in 2007 for their discoveries of principles for gene targeting in mice including the PNS.

3.4.4 Gene trapping

Besides the less efficient selection cassette approaches, one can achieve a positive clone enrichment of up to 5000-10000 fold by using a promoter-trap selection method (HANSON & SEDIVY, 1995). In the promoter-trap selection the expression of a promoter-less resistance gene is depended on the targeted integration of the transgene as it is expressed under the gene's own promoter (JASIN & BERG, 1988; SEDIVY & SHARP, 1989). It has to be kept in mind, that this selection strategy is only applicable for active genes. A similar strategy is the polyadenylation-trap selection, which is based on the absence of a polyadenylation signal for the resistance gene, making it also suitable for targeting of silent genes (THOMAS & CAPECCHI, 1987; DONEHOWER et al., 1992).

Further approaches to optimize gene targeting frequencies include the attempt to shift the ratio between HR and NHEJ in order to increase HR compared to NHEJ by interfering with the expression of genes considered to play a role in these processes. Vasquez et al. give an overview of possible genes (VASQUEZ et al., 2001). Triplex forming oligonucleotides can also be used to stimulate HR. They are short nucleotide sequences binding sequence specific with a high affinity to purine-rich sequences in the major grove of the DNA double helix and form a triplex structure with the DNA, which induces repair mechanisms (reviewed in SEIDMAN & GLAZER, 2003).

3.4.5 BAC vectors

Besides enrichment by selection, there are several other attempts to increase targeting frequency, such as an increase in length of homologous arms. Like mentioned above this can be achieved by using alternative vectors like YACs, PACs and BACs. Compared to YACs, BAC and PAC vectors have been proven to be advantageous (COPELAND et al., 2001), thereof BACs being more commonly used. They are fertility-(F-) factor-based plasmid vectors, replicating in low copy numbers (HOSODA et al., 1990). BACs can generally contain genomic DNA inserts of about 200 kb, but can accommodate far larger inserts (SHIZUYA et al., 1992). The length of the genomic inserts compared to conventional targeting vectors (generally up to 20 kb) makes them suitable for various applications besides gene targeting. Genome

sequencing approaches, such as the porcine genome are based on BAC libraries, providing a map of the pig genome and making BAC sequences accessible for various gene loci (CHEN et al., 2007; HUMPHRAY et al., 2007). BACs have been applied in several other fields of research in the mouse, like identification of mutation or characterization of regulatory sequences and functions of genes *in vivo*. Sequences adjacent to genes of interest on BACs may include genomic regulatory segments. Therefore, genes can be expressed under their own regulatory elements independent of their integration site, yet dependent on copy number and endogenous gene expression (CHANDLER et al., 2007). BACs are stable and easy to handle (GIRALDO & MONTOLIU, 2001), however, genetic modifications were difficult to achieve and screening by ordinary methods such as PCR and Southern blot is not possible due to the long homologous arms (VALENZUELA et al., 2003). Establishment of phage based recombination in *E. coli* made the modification of BAC sequences feasible and thus enabled the application of BACs in gene targeting experiments. There are two commonly used methods: ET cloning and recombineering (COPELAND et al., 2001; ZHANG et al., 1998). ET cloning uses the RecET system derived from the prophage Rac. Recombination is induced by addition of L-arabinose. Recombineering is accomplished by Red recombinase derived from bacteriophage λ, induced by heat shock. The development of screening methods for positively targeted cell clones by large vectors like the real-time PCR based "loss-of-native-allele" assay and applying the FISH assay made screening in BAC targeting experiments viable (VALENZUELA et al., 2003; YANG & SEED, 2003; GOMEZ-RODRIGUEZ et al., 2008). For the first time site-directed mutagenesis was successfully accomplished in murine ESCs (TESTA et al., 2003; VALENZUELA et al., 2003; YANG & SEED, 2003) and later on also in human ESCs (SONG et al., 2010). Effective targeting efficacies of up to 28% could be observed (YANG & SEED, 2003).

3.4.6 Designer nucleases

Another approach to increase targeting frequencies is to induce artificial DSB at the desired locus for site-directed mutagenesis in the genome via designer nucleases and thus induce homologous recombination. Initially *SceI*, a homing endonuclease, was used to induce DSB and HR frequencies were greatly increased (ROUET et al., 1994; CHOULIKA et al., 1995). Yet *SceI* requires the introduction of its specific recognition sequence to the target locus before it can be applied, which makes it unsuitable for gene targeting experiments. Zinc finger nucleases (ZFNs) are artificial molecules

where the nonsequence-specific DNA cleavage domain of the FokI type II restriction endonuclease is fused to a sequence-specific zinc finger DNA binding domain (reviewed by PORTEUS & CARROLL, 2005). ZFNs can be designed to target specific sequences and create DSB at desired loci. By offering a homologous donor substrate, rates for HR could be increased at the target loci in human cells and site directed mutagenesis could be achieved (URNOV et al., 2005). However, due to unspecific activity, ZFNs can generate random DSB in the cells' genome and have a cytotoxic effect. Quite recently a novel designer nuclease (TALEN) has been established based on transcription activator-like effector (TALE) proteins isolated from plant pathogens *Xanthomonas* (CHRISTIAN et al., 2010). They are said to have a high nuclease activity combined with a lower cytotoxicity, compared to ZFNs (MUSSOLINO et al., 2011).

III. ANIMALS, MATERIAL AND METHODS

1 Animals

For the production of the DMD pigs, landrace mix gilts were used as embryo recipients. Furthermore, the produced DMD pigs were characterized and age, as well as weight matched pigs, were used as controls. All pigs were housed in planar stables with straw covered floor. The DMD piglets were fed with an artificial feeding system with commercial milk powder (Normi Porcinorm PIGI, Norlac) and after weaning with commercial food mixed with water. Control piglets were raised by their mothers and fed with commercial pig food after weaning. All animal experiments were carried out according to the German Animal Welfare Act (55.2-1-54-2531-86-10).

2 Material

2.1 Apparatuses

Abi Prism 7000 Sequence detection system	Applied Biosystems, USA
AccuJet® pro Pipetman	Brand Wertheim
Agarose gel electrophoresis chamber	OWL Inc., USA
Zeiss Axiovert 200 M fluorescence microscope	Carl Zeiss, Oberkochen
Centrifuges 5415 D, 5417 R, 5810R	Eppendorf, Hamburg
Centrifuge Biofuge pico	Heraeus, Osterode
Centrifuge Labofuge M	Heraeus, Osterode
Centrifuge Rotanda 96	Hettich, Tuttlingen
Chyo scales	YMC Co., Japan
E.coli pulser electroporation device	BioRad, Munich
Eppendorf HH Mastercycler Gradient	Eppendorf, Hamburg
GeneAmp® PCR System 9700	Applied Biosystems, USA
GeneQuant Pro spectrophotometer	Amersham, UK
Gel documentation system	BioRad, Munich
GFL 3031 shaker	Hilab, Düsseldorf
Glass pipettes	Hirschmann, Eberstadt

Incubators	Memmert, Schwabach
	Heraeus, Osterode
Microscope DM IL	Leica, Wetzlar
MS1 minishaker	IKA Labortechnik, Staufen
Finnpipette® Multichannel pipet (300 µl)	Thermo Fisher Scientific, USA
Nucleofector™ II	Lonza, Cologne
Neubauer counting chamber	Assistent, Sondheim
Microprocessor pH meter	WTW, Weilheim
Pipettes	Gilson Inc., USA
	Eppendorf, Hamburg
Power Pac 300 gel electrophoresis unit	BioRad, Munich
REAX2 Automatic swivel unit	Hilab, Düsseldorf
RH Basic heating plate with magnetic stirrer	IKA Labortechnik, Staufen
Severin 900 microwave	Severin, Sundern
SS35 50 ml centrifuge tubes	Eppendorf, Hamburg
Steril benches Laminair® HB2448K, HB2472	Heraeus, Osterode
Thermomixer 5436	Eppendorf, Hamburg
Thermostat Plus	Eppendorf, Hamburg
Vidoeplan image analysis system	Zeiss-Kontron, Munich
Water bath sub14	Grant, UK
WB6 water bath	Firmengruppe Preiss-Daimler, Medingen

2.2 Consumables

ABgene® 96-well PCR plates	Thermo Scientific, Ulm
Centrifuge tubes (15 ml, 50 ml)	Falcon®, Becton Dickinson, Heidelberg
6-well, 96-well F-bottom culture dishes Cellstar®	Greiner bio-one, USA
Cultupe sterile culture tubes	Simport, Canada
Culture dishes	Roth, Karlsruhe
Cryotubes 1 ml	Nunc™, Denmark

Cryotubes 2 ml	Almeco, Denmark
Microamp™ optical 96-well reaction plate	Applied Biosystems, USA
Microamp™ optical adhesive film	Applied Biosystems, USA
Parafilm®M	American Can Company, USA
PCR reaction tubes (0.2 ml)	Braun, Wertheim
Pipette tips	Eppendorf, Hamburg
Pipette tips with filter	Axygen Inc., USA
QIAtip 500	Qiagen, Hilden
SafeGrip® Latex gloves	SLG, Munich
Safe-Lock reaction tubes (1.5 ml, 2 ml)	Eppendorf, Hamburg
Serological pipettes Cellstar®	Greiner bio-one, USA
Steritop GP 0,22 µm Express®plus membrane	Millipore, USA
Sterivex GP 0,22 µm	Millipore, USA
Tissue culture dishes (6 cm, 10 cm)	Sarstedt, Nümbrecht

2.3 Chemicals

All chemicals were used in p.a.-quality, if not stated otherwise.

Acetic acid (glacial) (HOAc)	Merck, Darmstadt
Agar-agar	Roth, Karlsruhe
Agarose Universal	Bio&SELL, Nürnberg
Agarose UltraPure™	Invitrogen, Karlsruhe
Amphothericin B	PAA, Austria
Ampicillin	Roth, Karlsruhe
Betain	Sigma-Aldrich, Steinheim
Blasticidin, bla	PAA, Austria
Bromophenolblue	Roth, Karlsruhe
β-Mercaptoethanol	Sigma-Aldrich, Steinheim
Chloramphenicol	Sigma-Aldrich, Steinheim
Chloroform	Merck, Darmstadt
Dimethylsulfoxid (DMSO)	Sigma-Aldrich, Steinheim

Doxycycline	Sigma-Aldrich, Steinheim
Dithiothreitol (DTT)	Biomol, Hamburg
Ethylenediaminetetraacetic acid (EDTA)	Roth, Karlsruhe
Ethanol (EtOH)	Roth, Karlsruhe
Ethidiumbromide	Merck, Darmstadt
Geneticin (G418)	Invitrogen, Karlsruhe
Glucose	Roth, Karlsruhe
Glycerol	Roth, Karlsruhe
Hydrochloric acid, 37% (HCl)	Roth, Karlsruhe
Isopropyl-beta-D-thiogalactopyranoside (IPTG)	Thermo Fisher Scientific, USA
Isoamylalcohol (CiA)	Roth, Karlsruhe
Kanamycin	Roth, Karlsruhe
Magnesium chloride ($MgCl_2$)	Merck, Darmstadt
Mineral oil	Roth, Karlsruhe
Polyethylenglycol (PEG) 8000	Roth, Karlsruhe
Peptone/Tryptone	Roth, Karlsruhe
Phenol	Roth, Karlsruhe
Potassium acetate (KOAc)	Roth, Karlsruhe
Potassium chloride (KCl)	Sigma-Aldrich, Steinheim
di-Potassiumhydrogenphosphate (KH_2PO_4)	Roth, Karlsruhe
2-Propanol	Roth, Karlsruhe
Sodiumdodecylsulfate (SDS), ultrapure	Roth, Karlsruhe
Sodium chloride (NaCl)	Roth, Karlsruhe
Sodiumdihydrogenphophate-1-hydrate ($Na_2HPO_4+2H_2O$)	Merck, Darmstadt
Sodium hydroxide (NaOH)	Roth, Karlsruhe
Sodium pyruvate	Invitrogen, Karlsruhe
D(+)-Sucrose	Roth, Karlsruhe
Tris-(hydroxymethyl)-aminomethan (Tris)	Roth, Karlsruhe
TRIzol® Reagent	Invitrogen, Karlsruhe

Yeast extract	Roth, Karlsruhe
5-Brom-4-chlor-3-indoxyl-β-Dgalactopyranosid (X-Gal)	Roth, Karlsruhe

2.4 Enzymes, kits and other reagents

2.4.1 Enzymes

DNase I and buffer (10 ×)	Thermo Fisher Scientific, USA
Herculase®II and buffer (5 ×)	Agilent, Böblingen
Taq Polymerase and buffer (10 ×)	Agrobiogen, Hilgertshausen
Proteinase K	Roth, Karlsruhe
Restriction enzymes and buffer	Thermo Fisher Scientific, USA
RevertAidTM H-Minus M-MuLV Reverse Transcriptase and buffer (5 ×)	Thermo Fisher Scientific, USA
RiboLock™ RNase inhibitor and buffer (5 ×)	Thermo Fisher Scientific, USA
Ribonuclease A (RNase A)	Roche, Mannheim
T4 DNA Ligase and buffer (10 ×)	Thermo Fisher Scientific, USA
Uracil-DNA Glycosylase (UNG)	Thermo Fisher Scientific, USA

2.4.2 Kits

CloneJET™ PCR Cloning Kit	Thermo Fisher Scientific, USA
E.Z.N.A™ Endo-free Plasmid Maxi Kit	Omega, USA
Fermentas Midi Prep DNA	Thermo Fisher Scientific, USA
Amaxa™ Basic Nucleofector™ Kit for Primary Mammalian Fibroblasts	Lonza, Cologne
Qiaex® II Gel Extraction Kit	Qiagen, Hilden
Qiagen Endofree Plasmid Kit	Qiagen, Hilden
Absolutely RNA Nanoprep Kit	Agilent Technologies, USA

2.4.3 Other reagents

Arabinose	Thermo Fisher Scientific, USA
BigDye® terminator v3.1	Applied Biosystems, USA
6 × DNA loading dye	Thermo Fisher Scientific, USA

DNA molecular weight standards:

Gene Ruler^{TM} 1 kb DNA Ladder	Thermo Fisher Scientific, USA
pUC Mix Marker, 8	Thermo Fisher Scientific, USA
dNTPs (dATP, dCTP, dGTP, dTTP)	Thermo Fisher Scientific, USA
Oligo(dT)$_{18}$ Primer	Thermo Fisher Scientific, USA
Omega ETR Reagent	Omega, USA
SYBR® Green PCR Mastermix	Applied Biosystems, USA

2.5 Reagents for cell culture

CollagenR	Serva, Heidelberg
Difco^{TM} Trypsin 250	BD, USA
Dulbecco Modified Eagle Medium (DMEM)	Invitrogen, Karlsruhe
Fetal calf serum (FCS)	Invitrogen, Karlsruhe
L-Glutamine (200 mM)	PAA, Austria
L-Glutamine + Penicillin/Streptomycin (100 ×)	PAA, Austria
Non-essential amino acids (100 ×)	Invitrogen, Karlsruhe

2.6 Buffers, media and solutions

Solvent was, if not stated otherwise, in a Millipore machine deionized water called aqua bidest. Media and Solutions used in cell culture were filtered sterile before use and stored on 4°C. FCS was inactivated by heating up to 56 °C for 30 minutes, filtered sterile and stored at −20 °C.

Chloroform-isoamylalcohol (CiA)

96 ml chloroform

4 ml isoamylalcohol

Stored at 4 °C protected from light.

Culture medium for porcine kidney cells

DMEM with

10% or 15% (v/v) FCS

1% (v/v) Non-essential amino acids (100 ×)

1% (v/v) Sodium pyruvate (100 ×)

1% (v/v) L-Glutamine (200 mM) + Penicillin/Streptomycin (100 ×)

0.1 mM β-Mercaptoethanol

Cryo medium

10% (v/v) DMSO

90% (v/v) FCS

DNA loading buffer (10 ×)

10% glycerol in aqua bidest.

1 spatula tip of bromophenolblue

Add 0.5 M NaOH until colour turns blue

Stored at 4 °C.

DNA molecular weight standards

100 µl pUC8 Mix Marker 8 or 1 kb DNA ladder standard

100 µl 6 × loading dye

400 µl aqua bidest

Stored at -20 °C

dNTPs

2 mM or 10 mM respectively dATP, dCTP, dGTP, dTTP

Stored at -20 °C.

LB medium

5 g yeast extract

10 g tryptone/peptone

2.5 g NaCl

Ad 1000 ml aqua bidest

pH 7.0 (adjust with 5 M NaOH)

Autoclave

Stored at room temperature.

LB-agar plates

5 g yeast extract

10 g tryptone/peptone

5 g NaCl

pH 7.0 (adjust with 5 M NaOH)

15 g agar-agar

Autoclave

Cool down to 60 °C

Add 1 ml respective antibiotic (ampicillin 50 mg/ml, chloramphenicol 12.5 mg/ml, kanamycin 25 mg/ml)

Pour into culture dishes

Stored at 4 °C.

Lysisbuffer for DNA isolation (High salt precipitation)

100 µl PK buffer (1 ×)

10 µl SDS (10%)

4.4 µl DTT (1M)

Lysisbuffer for DNA isolation (PCiA extraction)

160 mM Saccharose

80 mM EDTA pH 8.0

100 mM Tris/HCl pH 8.0

0.5% (w/v) SDS

Phosphate-buffered saline without Calcium and Magnesium (PBS)

8 g NaCl

0.2 g KCl

0.2 g KH_2PO_4

2.14 g $Na_2HPO_4+7H_2O$

Ad 1000 ml aqua bidest

pH 7.2-7.4

Stored at room temperature.

Phenol-chloroform-isoamylalcohol (PCiA)

25 ml phenol

25 ml CiA

Stored at 4 °C, protected from light.

PEG-$MgCl_2$

40% (w/v) PEG 8000

30 mM $MgCl_2$

Stored at room temperature.

PK buffer (10 ×)

200 mM Tris

1 M NaCl

40 mM EDTA

Stored at room temperature.

Plasmid A

50 mM glucose

25 mM Tris/HCl pH 8.0

10 mM EDTA/NaOH pH 8.0

Stored at room temperature.

Plasmid B

0.1 M NaOH

0.5% (w/v) SDS

Prepared freshly before each use.

Plasmid C

3 M KOAc

pH 4.8 with 9 M HOAc

Autoclave

Stored at room temperature.

Proteinase K 20 mg/ml

Stored at 4 °C

RNaseA 20 mg/ml

Stored at −20 °C

Selection medium with G418 100 mg/ml

Culture medium with

1.2 mg/ml G418

Sequencing buffer (5 ×)

17.5 ml 1 M Tris/HCl (pH 9.0)

125 µl 1 M $MgCl_2$

Ad 50 ml aqua bidest

Stored at -20 °C.

Starvation medium

DMEM with

0.5% (v/v) FCS

1% (v/v) Non-essential amino acids (100 ×)

1% (v/v) Sodium pyruvate (100 ×)

1% (v/v) L-Glutamine (200 mM) + Penicillin/Streptomycin (100 ×)

STE

10 mM Tris/HCl pH 8.0

100 mM NaCl

1 mM EDTA/NaOH pH 8.0

Stored at room temperature.

Stop Medium

10% (v/v) FCS

90% (v/v) DMEM

T-buffer

10 mM Tris

Adjust to pH 8.0 with HCl

Stored at room temperature.

TAE (50 ×)

242 g Tris

100 ml 0.5 M EDTA (pH 8.0)

57 ml AcOH

Ad 1000 ml aqua bidest

Stored at room temperature and diluted to respective concentration prior to use.

Trypsin/EDTA

PBS without calcium and magnesium with

0.5% (w/v) Trypsin

0.04% (w/v) EDTA

2.7 Oligonucleotides

Oligonucleotides were either designed by hand or with the primer 3 software. They were manufactured by Thermo Fisher Scientific, USA.

DMD3BNf	5'-ATGGATCCGCGGCCGCAAACTGGAACCACAAGAC-3'
DMD3KPr	5'-ATGGTACCTTAATTAATCTGCTCTCTGGTCACTC-3'
DMD5BNPr	5'-TGGATCCTCGCGACTGCAGCCTTAGAAG CAGTCTCCTTC-3'
DMD5SPf	5'-ATGAGCTCTTAATTAAGGTGTTCTCTCCTCTATG-3'
DMDexBr	5'-GTAGATCTAAGTACCACTGCATACAGGAG-3'
DMDexSf	5'-GAGTCGACCCATCTACCACATTTCACCTC-3'
DMDsc1f	5'-CTGGTATGAGCACCAGATTG-3'
DMDkosc2r	5'-GGACAGGTCGGTCTTGACAA-3'
DMDwtsc1r	5'-ATAGGTCTCAAGGTACTGTG-3'
DMD-int51-MSf1	5'-CAGTTAGGAACTGCTGGTAG-3'
DMD-int-MSr1	5'-TGTCAGTCATTGAGCTAGTCAC-3'
DMDFLPeTest3fw	5'-AATCTGCTCTCTGGTCACTC-3'
DMDFLPeTest5rv	5'-TCTATGGATGGCTCAGTGGA-3'
FLPeSf	5'- ATGTCGACCACCATGAGCCAATTTGA-3'
FLPeXr	5'-CATCTAGATATCACAGATCTTCTTCAG-3'
FLPf1	5'-AAGCATCTGGGAGATCACTG-3'
FLPf2	5'-GGAACTCTGAACCAGTCCTA-3'
FLPr1	5'-CAGTGATCTCCCAGATGCTT-3'
FLPr2	5'GTATATGTGCCTACTAACGC-3'
EM7r	5-TGCTCCATGGTTTAGTTCCTCACCTTG-3
M13	5'-GGAAACAGCTATGACCATG-3'
T7	5'-GTAATACGACTCACTATAGG-3'
pJETforward	5'-CGACTCACTATAGGGAGAGCGGC-3'
pJETreverse	5'-AAGAACATCGATTTTCCATGGCAG-3'
neokanf	5'-GACAATAGCAGGCATGCTG-3'
neokanR	5'-GTGGATGTGGAATGTGTGC-3'

neof	5'-TGATTCCCACTTTGTGGTTC-3'
blaf	5'-CCATGGCCAAGCCTTTGTC-3'
bla241r	5'-TTCCGATCGCGACGATACAAGTCAG-3'
bla343r	5'-GTGAGGAAGAGTTCTTGCAGCTC-3'
rTAf	5'-AGAAGCTTGGTGTAGAGCAG-3'
rTAr	5'-CGTCTAAGTGGAGCTCGTC-3'
TAREf1	5'-CTCGTTTAGTGAACCGTCAGATC-3'
TAREf2	5'-GTATGTCGAGGTAGGCGTGTAC-3'
CAGf	5'-CTCTGCTAACCATGTTCATG-3'
CAG1377f	5'-GGTAATCGTGCGAGAGG-3'
CAGex1f	5'-CTGACTGACCGCGTTACT-3'
27G20f2	5'-GATACAAGGATGTGGTAGTCTAG-3'
9G11f2	5'-CATCTATCCGGACAAAGCTCTAC-3'
BACr1	5'-GTACTGATTCAGTCAGGGTTTCTG-3'
BACr2	5'-CAGAGTTCACACACTGGAGAC-3'
qPCRDMD11fw	5'-TGCACAATGCTGGAGAACCTCA-3'
qPCRDMD12rv	5'-GTTCTGGCTTCTTGATTGCTGG-3'
qPCRDMD5fw	5'-CAGCAGCAGTCAAAGGGCATA-3'
qPCRDMD9rv	5'-AGGCAAGTCTGGGAAGCATCA-3'
GGTA3423fw	5'-TCATCAGTGGATTCACCCCAA-3'
GGTA3640rev	5'-CACCACGGGAATGCCTTC-3'
HPRT834i2fw	5'-TGTCTGCGACCCACACCA-3'
HPRT987i2rev	5'-GCATGCATCAGTAAGGAACTGG-3'
PACT954f	5'-CGCTCGTGGTCGACAACG-3'
PACT1919r	5'-CTGGATGGCCACGTACATG-3'
Cs3f	5'-AACGTTAACGCGAACCCAGCTAG-3'
Cs3r	5'-CCTCTTTCCTGGGCAGGTGTCCTTC-3'
Ad-SB53	5'-TCGACGTTCGATGACCAGTGGTCCAGC-3'
Ad-SB35	5'-TTAAGCTGGACCACTGGTCATCGAACG-3'
AdK53E	5'-ATGATCTAGGTACCACGACGC-3'

AdK35E	5'-AATTGCGTCGTGGTACCTAGATCATGTAC-3'
AdA53LN	5'-CGCGCCATAACTTCGTATAATGTATGCTATACGA AGTTAT-3'
AdA35LN	5'-CTAGATAACTTCGTATAGCATACATTATACGAAG TTATGG-3'
FRT53	5'-CGAGAAGTTCCTATACTTTCTAGAGAATAGGAAC TTCGAATTCAGGTCCTTAAGCTCCAGTCGACGGATC CTACTGGCGCGCCTACTATCAATTGGAAGTTCCTAT ACTTTCTAGAGAATAGGAACTTCGC-3'
FRT35	5'-GGCCGCGAAGTTCCTATTCTCTAGAAAGTATAGG AACTTCCAATTGATAGTAGGCGCGCCAGTAGGATCC GTCGACTGGAGCTTAAGGACCTGAATTCGAAGTTCC TATTCTCTAGAAAGTATAGGAACTTCTCG-3'

2.8 BACs and plasmids

BACs:	BACPAC, CHORI, USA
CH242-9G11	
CH242-27G20	
CH242-520G21	
CH242-284A18	
pBluescript II SK (−)	Thermo Fisher Scientific, USA
pGEM®-T Easy Vector (5ng/µl)	Promega, USA

2.9 Bacterial strains

SW106	NCI Frederick, USA
DH10B	New England Biolabs, USA
TOP10	Invitrogen, Karlsruhe

2.10 Software

Abi Prism 7000	Applied Biosystems, USA
BioEdit Sequence Alignment Editor	Ibis bioscience, USA
Double Digest™	Thermo Fisher Scientific, USA

FinchTV Version 1.3.1	Geospiza Inc., USA
Macromedia Freehand MX	Adobe, USA
NEBcutter V2.0	New England Biolabs, USA
OligoAnalyzer 3.1	IDT Inc., USA
Primer 3	Whitehead Institute for Biomedical Research, USA

3 Methods

3.1 Molecular genetic protocols

During the establishment of a DMD pig model several molecular genetic standard protocols were applied regularly. These protocols are listed below. Aberrations or modifications are specified at the appropriate step in the procedures.

3.1.1 PCR

3.1.1.1 End-point PCR

PCR reactions were performed in 0.2 ml reaction tubes and prepared at room temperature. Standard composition of PCR reaction mix for Taq-Polymerase and Herculase II with an end volume of 25 µl was:

Taq-Polymerase	Herculase II	
2.5 µl	5 µl	10 × PCR buffer
2.5 µl	-	$MgCl_2$ (15 mM)
2.5 µl	2.5 µl	dNTPs (2 mM)
0.5 µl	0.5 µl	Primer forward (10 µM)
0.5 µl	0.5 µl	Primer reverse (10 µM)
0.2 µl	0.2 µl	Taq-Polymerase (5 U/µl)
1 µl	1 µl	DNA
15.3 µl	15.3 µl	Aqua bidest

Standard cycler protocol was:

4 min	95 °C	Denaturation
30 sec	95 °C	Denaturation
30 sec	X °C	Annealing
Y min	72 °C	Elongation
Go to step 2 34 ×		
10 min	72 °C	Elongation
15 min	4 °C	Termination

Depending on the reaction sequence specific primers were used. Primer pair specific approximate values for X were calculated by the 4 + 2 rule (2 °C for each A and T, 4 °C for each G and C, value − 5). Depending on the amplicon length Y is calculated with 2 kb/min.

3.1.1.2 qPCR

The standard curve was prepared beforehand from DNA of Niere m cells, which was isolated via PCiA extraction (3.1.7.1). The values for copy numbers of the standard curve were assigned to 10000, 7500, 5000, 2500, 500, 250, 50 and 25, assuming that 100 ng of DNA equates 15000 DNA copies. For each standard curve a calibrator was prepared from the same initial DNA. DNA for qPCR screening was isolated by high salt precipitation (3.1.7.1). Samples, standard curve and reaction components were warmed to room temperature, except for UNG, which was stored at − 20°C. The reaction was pipetted on ice and carried out in Microamp™ optical 96-well reaction plates. For each set of samples three plates were prepared, one primer pair on one plate. All samples were run as doublets, except for the calibrator, which was run in triplets and the non template control (ntc), as a single sample. The position of the samples was identical on each plate. The reaction mix was composed as follows:

	GGTA	HPRT	DMD
SYBR green	6.25 µl	6.25 µl	6.25 µl
UNG	0.075 µl	0.075 µl	0.075 µl
Primer forward (5 µM)	0.75 µl	0.25 µl	0.5 µl
Primer reverse (5µM)	0.75 µl	0.25 µl	0.5 µl
Template	2.5 µl	2.5 µl	2.5 µl
Aqua bidest	2.175 µl	3.175 µl	2.675 µl

The layout of the plates stayed always the same. The standard curve samples were

located on the left and the three calibrator samples and the non template control (ntc) were placed on the right bottom. After filling, plates were closed with a Microamp™ optical adhesive film and either run immediately or stored at − 20°C.

Reaction took place in an ABI Prism 7000 Sequence detection system with following cycler protocol:

2 min	50 °C	UNG activation
10 min	95 °C	Polymerase activation
15 sec	95 °C	Denaturation
1.30 min	63 °C	Annealing and elongation
Repeat steps 3 and 4 39 ×		

After the last cycle, the plates were again heated from 60 °C to 95 °C in order to obtain a dissociation curve of the PCR products.

3.1.2 Agarose gel electrophoresis

DNA fragments were separated according to their size via agarose gel electrophoresis. Agarose gels were prepared by heating 1× TAE buffer with 0.7% or 2% agarose respectively in a microwave until agarose was completely melted. After cooling down to approximately 60 °C ethidiumbromide (0.5 µg/ml) was added, the gel was poured into a gel electrophoresis chamber with an appropriate comb. After curing the chamber was filled with 1×TAE. DNA loading buffer (1/10 volume) was added to the DNA samples. The samples and a molecular weight standard were loaded into the gel slots and an electric current was applied. Bands were visualized by UV-light and pictures were taken (BioRad). The DNA fragments were characterized by comparison with the molecular weight standard.

If fragments were to be further processed, agarose UltraPure™ was used and fragments were cut out of the gel under UV light control. Otherwise Universal agarose was used for gel preparation.

3.1.3 Elution

After agarose gel electrophoresis DNA fragments were excised and eluted out of the agarose gel for subsequent processing with the Qiaex® II Gel Extraction Kit according to the manufacture's protocol.

In order to determine the concentration of the eluate, 3 µl were mixed with 15 µl aqua

bidest and 2 µl DNA loading buffer and loaded onto a 0.7% agarose gel, together with a molecular weight standard. For concentration determination band intensity was compared to the molecular weight standard.

3.1.4 Restriction digest

Plasmids and BACs were digested with restriction enzymes (generally 10 IU/µl) either for subsequent ligation or for analysis. Restriction enzyme recognition sites could be identified using NEBcutter V2.0. Appropriate suggestions for reaction conditions for desired enzyme combinations were obtained from DoubleDigest™. For analysis approximately 1 µg of DNA was digested, for subsequent ligation at least 2 µg of DNA were digested. Generally 1 unit of restriction enzyme was used per 10 µl reaction mix. Restriction digests were incubated overnight at 37 °C.

If the digest was only used for qualitative analysis, the samples were loaded onto an agarose gel directly. If the DNA fragments were afterwards used for ligation, they were extracted with PCiA and purified before gel separation. The reaction volume was adjusted to 150 µl with aqua bidest and 100 µl PCiA was added. The mixture was shaken for 1 min and subsequently centrifuged for 3 min at 16100 × g. The aqueous supernatant was transferred into a new 1.5 ml reaction tube. 15 µl 3 M NaOAc and 400 µl EtOH 100% (cooled to −20 °C) were added. Samples were placed at −80 °C for 30 - 60 min. Afterwards they were centrifuged for 30 min at 18100 × g, the supernatant was removed and the DNA pellet was air dried for 6 min. It was then resolved in 20 µl T-buffer.

After PCiA purification the samples were loaded onto an ultra-pure Agarose gel with an appropriate concentration and the desired band was cut out and eluted.

The BAC targeting vector was linearized prior to nucleofection with SfiI in following reaction mix:

X µl	Targeting vector (20 µg)
2 µl	SfiI (10 IU/µl)
6 µl	Buffer Green
Ad 60 µl	Aqua bidest

The reaction mix was incubated at 50 °C overnight and was covered with mineral oil. On the next day the DNA in the reaction mix was purified with PCiA and solved in 25 µl T-buffer.

3.1.5 Ligation

Eluted DNA fragments, either PCR products or fragments of digestion, were ligated into a respective vector with the T4 DNA Ligase. After determination of the concentration (see 3.1.3) of vector and fragment, they were added in equal amounts to the reaction mix. 20 µl of the reaction mix were composed as follows:

X µl	Vector DNA (100 ng)
Y µl	Insert DNA (PCR product or restriction digest fragment)
1 µl	T4 DNA ligase
2 µl	10× Ligation buffer
Ad 20 µl	Aqua bidest

Y: Amount of insert DNA is dependent on the vector DNA; it was stoichiometric equally added into the reaction mix

The reaction was left at room temperature for at least 4 h and was subsequently terminated by heating the samples at 65 °C for 15 min.

3.1.6 Heat shock transformation

In order to multiply plasmids in high copy numbers with rare mutational events, they were brought into competent *E.coli*, strain TOP10 via heat shock transformation. Heat shock competent cells were thawed up on ice and DNA added: 9 µl of plasmid DNA, which has been ligated prior to transformation or 1 µl of undiluted isolated plasmid DNA and 1 µl of 1/1000 diluted isolated plasmid DNA and mixed carefully. Samples were placed on ice for 20 min and subsequently heated at 42 °C for 45 sec. They were then placed on ice for 2 min. Afterwards 1 ml LB medium was added followed by incubated at 37 °C for 45 min. Eventually samples were centrifuged for 5 min at 2300 × g and the pellet was resuspended in 100 - 200 µl of the supernatant and plated on LB agar plates with appropriate selection medium (ampicillin 50 µg/ml, kanamycin 25 µg/ml and chloramphenicol 12.5 µg/ml). If pGEM®-T Easy Vector was used LB agar plates were treated before use with 40 µl IPTG (100 mM) and X-Gal (20 mg/ml in Dimethylformamide) for differentiation of positive and negative plasmid colonies. The agar plates were incubated at 37 °C overnight. After counting colonies, plates were wrapped airproof in Parafilm®M and stored at 4 °C until further processing.

3.1.7 DNA isolation

Different protocols were used for DNA isolation according to the type of sample the DNA was isolated from or the purpose for which the DNA was isolated. After

isolation DNA concentration was measured with the GeneQuant Pro spectrometer at a wavelength of 260 nm by adding 5 µl DNA to 95 µl aqua bidest (1:20 dilution). Samples were stored at 4 °C if used frequently. Otherwise they were stored at −20 °C.

3.1.7.1 Isolation of genomic DNA

Two different protocols were used for DNA isolation from tissue samples or cell pellets. High salt precipitation was applied when DNA was used in qPCR. For other applications DNA was isolated via PCiA extraction. For the PCiA extraction the tissue samples were cut into small pieces (about 1 g, 5 × 5 × 5 mm^3) and 400 µl lysis buffer for DNA isolation and 20 - 30 µl ProteinaseK were added. The samples were mixed and incubated at 60 °C overnight. When the tissue pieces were completely digested, the samples were centrifuged at 16100 × g for 5 - 6.5 min and the supernatant was transferred into a new reaction tube. First 400 µl of 4.5 M NaCl were added, then 600 µl PCiA and the samples were shaken for 1-2 min by hand or for 10 min on an automatic shivel. Afterwards they were centrifuged for 5 - 6.5 min at 16100 × g and the supernatant was transferred to a new reaction tube. The steps of adding PCiA, shaking, centrifugation and transfer into a new tube were repeated twice. Then 2-propanol (2/3 volume of supernatant) was added and the DNA precipitated. The DNA pellet was transferred twice into a new reaction tube with 600 µl 70% EtOH and was then left in the second tube overnight at 4 °C. The 70% EtOH was removed and the DNA pellet was air dried for 6 min and resolved in 55 µl T-buffer. DNA was then left overnight at 4 °C or at 50 °C for 10 min before concentration was measured.

DNA from single wells of 96-well cell culture plates was isolated using the high salt precipitation protocol. 114.4 µl of the lysisbuffer for DNA isolation by high salt precipitation were added to the cell pellet and the samples were incubated at 60 °C for 60 min. 2 µl ProteinaseK were added, followed by incubation at 60 °C. After 60 min 30 µl NaCl (4.5 M) were added, samples placed on ice immediately and subsequently centrifuged at 16100 × g for 20 min. The supernatant was transferred into a new reaction tube, 103 µl of 2-propanol was added and the reaction tubes were shaken carefully. They were then centrifuged at 16100 × g for 20 min, supernatant was removed and 500 µl 70% EtOH was added. DNA pellets in 70% EtOH were stored at 4 °C overnight. The next day the samples were shaken carefully and centrifuged at 16100 × g for 20 min. The supernatant was removed and the DNA pellets were air dried for 6 min. They were then resolved in 35 µl T-buffer and left at 55 °C for at least

1 h.

3.1.7.2 Isolation of plasmid and BAC DNA

Plasmid and BAC DNA used for analysis was isolated with a plasmid preparation protocol. If high quantities were needed a midi prep was done with a tripled volume.

For multiplication single colonies of bacterial strains carrying the desired plasmids or BACs were inoculated in 5 ml LB medium with the appropriate antibiotic (ampicillin 50 µg/ml, kanamycin 25 µg/ml and chloramphenicol 12.5 µg/ml) and unless indicated otherwise grown with shaking at 37 °C overnight. From the overnight cultures glycerol stocks were made by mixing 900 µl 60% glycerol with 300 µl overnight culture. They were stored at −80°C.

If the overnight cultures were used for PCR screening 10 µl were mixed with 20 µl T-buffer and heated at 95 °C for 10 min. Afterwards the reaction mix was cooled down to 4 °C and centrifuged at 2300 × g for 5 min. 1 µl from the supernatant was used as template in the PCR.

For the preparation of larger scales of plasmids or BACs, overnight cultures were centrifuged at 1300 × g for 10 min and the supernatant discarded. Pellets were resuspended in 750 µl STE buffer and transferred into a new reaction tube. Samples were again centrifuged at 4500 × g and the supernatant discarded. Pellets were resuspended in 200 µl Plasmid A and 400 µl of Plasmid B. was added. The samples were mixed gently by turning 7 times and placed on crushed ice for 5 min. 300 µl of Plasmid C was added, the samples again gently mixed and placed on ice for 3 min. After cooling they were centrifuged for 10 min at 16100 × g. The supernatants were transferred into new reaction tubes, 4 µl RNaseA added and were left at 37°C for 45 min. Afterwards 300 µl PCiA was added and samples shaken for 1 min, centrifuged for 2.5 min at 16100 × g. After transfer of the aqueous phase to a new reaction tube, 650 µl of 2-Propanol was added. The precipitated DNA was pelleted by centrifugation at 16100 × g for 10 min. The supernatant was discarded, 700 µl 70% EtOH added and the DNA pellets was left in 70% EtOH either overnight or for a few hours. Afterwards the samples were centrifuged at 16100 × g for 2.5 min and the 70% EtOH discarded. The DNA pellet was air dried for 6 min and resolved in 55 µl T-buffer.

3.1.7.3 Endotoxin free isolation of DNA

Plasmid DNA was isolated endotoxin free using the E.Z.N.A.™ Endo-free Plasmid Maxi Kit following the manufacturer's protocol.

For the endotoxin free isolation of BAC DNA a protocol, established by Katrin Krähe in our lab, with the combination of the Endofree Plasmid kit (Qiagen), the ETR Reagent (Omega Biotech) and QIAtip 500 columns (Qiagen), was applied. Bacterial strains carrying the desired BAC were inoculated in 3 ml of LB medium with chloramphenicol (12.5 µg/ml) and left at 32 °C (SW106) or 37 °C (DH10B) respectively for 5 h. In the evening the pre-culture was inoculated in 200 ml LB medium with chloramphenicol (12.5 µg/ml) overnight culture and left shaking at 32°C or 37°C respectively. In the morning the overnight culture was centrifuged at 4600 × g for 15 min at 4 °C. The supernatant was decanted; the pellet resuspended in 10 ml P1 solution (+RNase). 10 ml of solution P2 were added and the samples left at room temperature for 5 min. Then 10 ml of solution P3 (pre-cooled on ice) were added and samples left on crushed ice for 15 min. They were then centrifuged for 40 min at 17000 × g at 4 °C and the supernatant transferred into a new 50 ml falcon tube. Approximately 3 ml (1/10 of the volume) Omega ETR Reagent was added, the reaction mix turned 7 times and placed on crushed ice for 10 min. It was then split onto two 15 ml Falcon tubes and incubated at 42 °C for 15 min. The samples were again centrifuged at 5000 × g for 10 min at room temperature and the supernatant was transferred to a new 50 ml Falcon tube. Half of the volume of the supernatant 100% EtOH was added and the samples were incubated for 2 min at room temperature. In the mean time QIAtip 500 columns were equilibrated with 10 ml QBT solution. The samples were transferred onto a QIAtip 500 column and let run through. After the column was washed twice with 30 ml QC solution, the DNA was eluted with 15 ml QF solution into a 50 ml Falcon tube. 10.5 ml 2-Propanol were added, the samples divided onto two 15 ml Falcon tubes and centrifuged at 13900 × g for 40 min at 4 °C. The supernatant was discarded and the DNA pellet washed with 5 ml 70% EtOH ideally overnight at 4 °C. The pellets were resolved in 25 µl T-buffer.

3.1.8 Recombineering and Cre mediated recombination

For recombineering (COPELAND et al., 2001) and Cre mediated recombination SW106 *E.coli* strains were used (LIU et al., 2003). Apart from that BACs were kept in DH10B *E.coli* strains and plasmids in TOP10 *E.coli* strains. The SW106 strain carries

a fragment of a λ prophage, which contains the genes *exo*, *bet* and *gam* transcribed from the λPL promoter. The promoter is under the control of the repressor cI857. At 32 °C the expression is repressed and at 42°C transcription from the *exo*, *bet* and *gam* genes recombination proteins is activated. SW106 cells were therefore never exposed to temperatures exceeding 32 °C, except when activation of the recombination proteins was desired. The exo protein is a 5'-3' exonuclease, which produces single stranded overhangs at linear DNA fragments. The bet protein stabilizes the single stranded overhangs and plays an assisting role in the recombination process. The gam protein protects the introduced linear DNA fragments from degradation through the *E.coli* RecBCD protein. Introduction of linear DNA fragments with a homology to DNA molecules in the SW106 cells in the presence of the recombination proteins leads to recombination between the homologous sequences of the DNA molecules.

SW106 cells are also capable of arabinose induced Cre mediated recombination as they contain a *Cre* gene under the control of an arabinose inducible promoter. Similar to the above described procedure a given plasmid or BAC is modified after its introduction in SW106 cells, activation of the *Cre* gene and electroporation of a linear modification fragment. In contrast to the λ prophage mediated recombination, which allows recombination between any homologous sequence, Cre recombinase exclusively mediates recombination between palindromic loxP sites.

For their respective application they were prepared beforehand with following protocols (according to Recombineering protocols http://web.ncifcrf.gov/research/brb/protocol.aspx).

3.1.8.1 Preparation of electro-competent cells

Cultures of SW106 or DH10B cells were grown in LB medium without antibiotic, as they do not contain a resistance gene. If they contained a plasmid or BAC, either ampicillin (50 µg/ml) or chloramphenicol (50 µg/ml) respectively was added. A 5 ml overnight culture of the desired bacterial strain was inoculated and transferred the next day into a larger volume of LB medium (1 ml overnight culture per 100 ml). They were grown until they reached a certain OD value. For the preparation of conventional competent cells they were grown at 32 °C until they reached an OD_{600} of 0.6 – 0.8. Competent cells for recombineering were grown until 0.4 – 0.5 at 32 °C and then transferred to a 42 °C waterbath where they were kept for 15 min under continuous shaking. Competent cells for Cre mediated recombination were grown at 32 °C until

0.3 – 0.4. Then arabinose (100 mg/ml) was added and the cells shaken at 32 °C for one additional hour. After these individual procedures for conventional, arabinose induced as well as heat induced cells, the same washing procedure was used, during which cells were kept at 4 °C. The cell suspension was cooled down with occasional shaking for 10 min. Cells were then harvested by centrifugation for 10 min at 1700 × g at 4 °C. The supernatant was carefully removed and the cell pellet resuspended in 50 ml ice-cold aqua bidest. Cells were again pelleted by centrifugation for 10 min at 1700 × g on 4 °C. The supernatant was removed and cells resuspended in 20 ml ice-cold aqua bidest. Cells were again pelleted by centrifugation for 10 min at 1700 × g at 4 °C and the supernatant removed. The cell pellets were resuspended in 5 ml ice-cold 10% glycerol and again centrifuged for 10 min at 1700 × g at 4 °C. The supernatant was removed and the cells resuspended in 1 ml ice-cold 10% glycerol. Aliquots of 50-80 µl were made and stored at −80 °C or used directly.

3.1.8.2 Electroporation

Aliquots of respective SW106 or DH10B competent cells were used for electroporation with the BioRad E.coli pulser electroporation device. The DNA was mixed with aliquot of electro-competent cells, transferred to precooled cuvettes and pulsed at 1.75 kV. 1 ml LB medium was added to the cuvette, mixed with the cells and then transferred to a 1.5 ml reaction tube. Cells were incubated at 32 °C for 45 min in LB medium to introduce a plasmid or BAC into DH10B or SW106. If modifications either by λ prophage or Cre recombinase were desired, electroporated cells were kept for 2 h at 32 °C without antibiotic treatment. After the recovery and modification phase, cells were centrifuged at 2300 × g for 5 min, most the supernatant was removed, except for 100-200 µl and the cells resuspended in the remaining supernatant. Subsequently the cells were plated on LB agar plates with the appropriate antibiotic.

3.1.9 Sequencing

DNA sequencing was accomplished by capillary sequencing at the Helmholtz Center Munich. Plasmids were purified for sequencing by PEG precipitation. 20 µl aqua bidest and 20 µl PEG-$MgCl_2$ were mixed with 20 µl plasmid. The mix was then equilibrated 10 min at room temperature, centrifuged 20 min at 16100 × g and the supernatant discarded. The DNA pellet was washed with 100 µl 70% EtOH overnight. Afterwards samples were centrifuged for 2 min at 16100 × g, the supernatant was

discarded and the DNA pellet air died for 6 min and resolved in 20 µl T-buffer. Afterwards DNA concentration was determined (see 3.1.7). In order to obtain best sequencing results DNA amount in nanogram used in sequencing reaction was calculated by following formula:

DNA amount (ng) = the length of sequence, which is to be sequenced / 100 × 1.5

DNA samples were diluted with aqua bidest to the desired concentration. For fragments ligated into a pGEM vector, pGEM specific primers T7 and M13 were used as standard primers and pJETforward and pJETreverse for plasmids with a PJET vector backbone. Additionally DNA fragment specific primers were used.

Sequencing reaction mix was prepared in 0.2 ml reaction tubes at room temperature with a final volume of 10 ml. Reaction composition:

4 µl	5 × sequencing buffer
1 µl	BigDye (keep on ice)
1 µl	Primer (10 µM)
2 µl	Template
2 µl	Aqua bidest

Cycler protocol for sequencing:

1 min	95 °C	denaturation
5 sec	95 °C	denaturation
10 sec	50 °C	annealing
4 min	60 °C	elongation
Repeat steps 2 to 4 39 ×		

The samples were purified via EtOH precipitation after the sequencing PCR reaction. First 2.5 µl 125 mM EDTA, followed by 30 µl 100% EtOH (cooled to −20 °C), were added. The samples transferred to new 1.5 ml reaction tube, incubated on ice for 15 min and centrifuge for 30 min at 16100 × g at 4 °C. The supernatant was discarded and the pellet washed in 50 µl 70% EtOH. The samples were again centrifuged for 2.5 min on 16100 × g, the supernatant was discarded and the pellet was air dried for 6 min. Afterwards the pellet was resolved in 30 µl aqua bidest and transferred to a sequencing plate (ABgene® 96-well PCR plates). Sequencing plates were stored at −20 °C before transferring them to the Helmholtz Center Munich. Sequencing results were analyzed with the software FinchTV Version 1.3.1 and sequences copied to

BioEdit for alignments and further comparison.

3.2 Cell culture

A primary cell line "Niere m" established by Dr. Annegret Wünsch was used for transfection experiments. Cells were isolated from the kidney of a 3 months old male Landrace pig. Minced tissue was digested with Collagenase II. The Niere m is a mixed cell population of cells with fibroblast-like and epithelial-like morphology. The karyotype, nuclear transfer capability and targeting suitability of this cell line were tested by Dr. Annegret Wünsch, Dr. Mayuko Kurome and Katrin Krähe.

All experiments were carried out under sterile conditions at a sterile bench. Media and solutions were pre-warmed to 37 °C and culture dishes were used at room temperature. Culture dishes were coated with CollagenR (0.2 mg/ml), diluted with aqua bidest. Cells were incubated at 37 °C, 5% CO_2 and 95% humidity.

3.2.1 Cell culture, passaging and cryopreservation

Frozen Niere m cells (passage 1 or 2), stored in liquid nitrogen, were thawed by transferring the cells into 10 ml stop medium. After centrifugation at 180 × g for 5 min the supernatant was discarded. The remaining cell pellet was resuspended in an appropriate amount of culture medium containing 10% FCS and transferred onto 10 cm culture dishes (approximately 1×10^6 cells per dish). When the cells reached 90% confluence they were passaged as follows. They were washed twice with PBS (equal amount as culture medium) and detached from the culture dish surface by incubation with 1.5 ml Trypsin/EDTA 0.5% for approximately 3 min until the cells got a round shape and became detached. The reaction was stopped with 10 ml stop medium and cells were transferred into an appropriate Falcon tube. A Neubauer Hemocytometer was filled with the stop medium containing the cells and the amount of cells was calculated. The appropriate volume containing 1×10^6 cells was transferred to a new reaction falcon and centrifuged at 180 × g for 5 min. The supernatant was removed and the cell pellet was resuspended with 10 ml culture medium containing 10% FCS and transferred to a 10 cm culture dish. For each transfection experiment two 10 cm culture dishes were prepared with 1×10^6 cells. The remaining cells were frozen in 1 ml pre-cooled FCS containing 10% DMSO, placed at -80 °C and later on transferred for storage in liquid nitrogen.

3.2.2 Transfection

For the transfection of the cells the Amaxa Nucleofector™ Technology from Lonza was applied. This technology combines electrical pulses and cell type specific solutions in order to transfer the foreign DNA directly into the nucleus (HAMM et al., 2002). Nucleofection solution, cuvette and plastic pipette were components of the Amaxa™ Basic Nucleofector™ Kit for Primary Mammalian Fibroblasts, Lonza.

Cells were grown to a confluence of 60 – 80%, harvested and counted as described above (3.2.1). 5×10^5 or 1×10^6 cells were resuspended in 100 µl nucleofector solution, 5 µg of the modified targeting vector DNA was added and the reaction mix was transferred into a nucleofection cuvette and pulsed with the preset program U12. After nucleofection the cells were transferred with a plastic pipette into a 6-well culture dish in 3 ml culture medium containing 15% FCS . After 24 h the cells were evaluated culture medium was exchanged and 48 h after nucleofection the selection was started, except for nucleofection experiment 100831, in which selection was started after 24 h. Figure III.1 gives a schematic overview of the nucleofection experiments.

3.2.3 Selection

It was necessary to produce cell clones originating from a single cell in order to screen for the correct genetic modification. The targeting construct carries a neomycin resistance cassette. Therefore, the selection medium contained 1.2 mg/ml geneticin (G418), which has been determined by Dr. Annegret Wünsch to be the optimal concentration for the Niere m cell line to eliminate cells without integrated construct within one week. Transfected cells as well as untreated Niere m cells were harvested and counted as described above (see 3.2.1). For optimal growth 2000 cells were seeded out into one 96-well. Thereby transfected cells were co-seeded with untreated cells in the ratios 1:4, 1:3 or 1:1. Medium was exchanged every 48 h and after 7 days the 96-well plates were screened for G418 resistant clones. Only wells containing single colonies were considered for further processing. When the cell clones reached a confluence of 70% they were washed twice with 200 µl PBS, treated with 30 µl trypsin/EDTA 0.5% for 3 min and resuspended with 170 µl selection culture medium. In the initial experiments where the targeting efficiency by homologous recombination was determined, each cell clone was just transferred into a new well of a 96-well plate to promote proliferation. In subsequent experiments the cell clones were splitted into

two wells (96-well plate), since one well was needed for screening and the other had to be cryopreserved, for potential SCNT (Figure III.1). For screening the cell clones were trypsinized as soon as they reached 100% confluence, resuspended with 100 µl stop medium and centrifuged at 330 × g for 10 min. The supernatant was removed, the cell pellets were placed on crushed ice and then transferred to −80 °C for storage until DNA was isolated via high salt precipitation (see 3.1.7.1). The cells for potential SCNT were trypsinized when they reached a confluence of 80%. The reaction was stopped using directly 200 µl cryo medium. The cell solution was transferred to 1.5 ml reaction tubes, placed on ice and transferred within 30 min to −80 °C for storage.

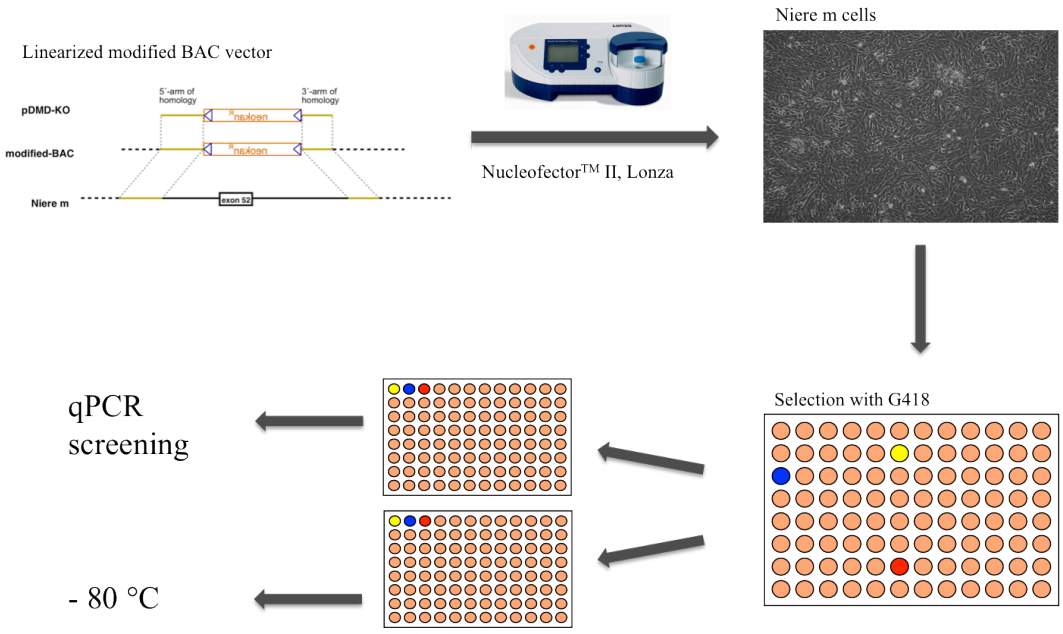

Figure III.1 Schematic overview of the nucleofection experiments

The linearized modified BAC vector, carrying a resistance cassette in exchange for the exon 52 of the *DMD* gene was transfected into Niere m cells; cells with integrated vector were selected with G418, harvested, screening for correctly targeted cell clones and a backup portion was stored on – 80 °C for subsequent SCNT and ET.

3.3 Nuclear transfer and embryo transfer

Frozen portions of cell clones that were found to have undergone homologous recombination, were thawed by adding 1 ml stop medium and subsequent centrifugation for 5 min at 180 × g. The supernatant was discarded, the cell pellet resuspended in 300 µl culture medium with 20% FCS and splitted on three wells on a 96-well culture plate. 48 h prior to SCNT cells were treated with starvation medium.

SCNT was carried out by Dr. Mayuko Kurome, Dr. Barbara Kessler, Dr. Valeri Zakhartchenko and Tuna Gungör according to the protocol described by KUROME et al., (2006). The obtained embryos were transferred to estrus synchronized gilts (ET) (BESENFELDER et al., 1997). After 3 weeks gilts were controlled by ultrasonic examination for the first time for conception and afterwards in regular intervals for preservation of the pregnancy.

3.4 Characterization of the DMD pigs

3.4.1 Quantitative stereological and morphometric analysis

Determination of the muscle fiber proportion to the whole muscle volume of the musculus biceps femoris and the muscle fiber diameter (minimal Feret's diameter) was conducted with twelve digital images (image size: 340 x 268 µm) of anti-dysferlin immunostained cross sections of the musculus biceps femoris of three newborn *DMD* knockout piglets and three age matched controls. Images were taken with a Zeiss Axiovert 200 M fluorescence microscope (40x objective).

The muscle fiber proportion to the whole muscle volume or the volume density of muscle fibers ($V_{V(MF/M)}$) was determined by point counting in a randomly positioned rectangular test field with 40 evenly distributed points per test field (area of test field: 57.8×10^3 µm^2). The test field was superimposed over the images to be counted (12 images per animal). The ($V_{V(MF/M)}$) was calculated as the quotient of the cross section profile area of muscle fibers (points hitting muscle fibers) and the corresponding area of muscle sections (points counted per animal; 12×40).

For quantification of the muscle fiber size the minimal Feret's diameter (minimum distance of parallel tangents at opposing particle borders) was determined (BRIGUET et al., 2004). A randomly positioned unbiased counting frame (GUNDERSEN, 1977) (counting frame area: 10.4×10^3 µm^2) was superimposed over each of the twelve images per animal and the muscle fiber cross section profile were measured using a Videoplan image analysis system (Zeiss-Kontron, Munich).

3.4.2 Gait and movement analysis

Evaluation of gait and movement were carried out in comparison with weight matched controls. The *DMD* knockout pig was conditioned to follow persons offering it sweets as incentive. The control animals were trained to get accustomed to handling by daily apple feeding and playing.

For gait analysis a 15 meters long and 80 cm wide run was staked off with a fence along a wall. The ground was covered with grass. The *DMD* knockout pig followed a person through the run and the control animals were chased through with differing speed. The animals were filmed for comparison.

Furthermore, the ability to climb a 25 cm step was tested. Therefore, the DMD pig was compared with a control animal.

IV. RESULTS

1 *DMD* gene constitutive targeting vector

For the establishment of a porcine DMD model with a loss of function of the protein dystrophin it was decided to delete exon 52 of the *DMD* gene, leading to a frame shift of the transcript. BAC vectors were chosen as targeting vector as it is assumed that an increased length of the homologous sequence leads to a higher targeting efficiency.

For a constitutive knockout the DMD exon 52 and its flanking intronic regions were replaced by a neomycin/kanamycin (neokan) resistance cassette flanked by Cre recombinase recognition sites (loxP) as depicted in Figure IV.1. The targeting construct replaced approximately 5.2 kb (134150 – 139440) of wild-type sequence including the exon 52 with the neokan resistance cassette.

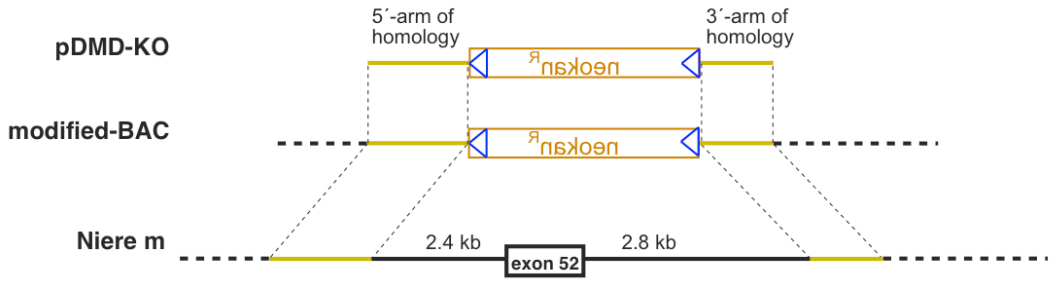

Figure IV.1 Targeting by homologous recombination of exon 52 of the *DMD* gene in Niere m cells

For the targeting of exon 52 of the *DMD* gene a BAC vector, carrying exon 52 and adjacent sequences, was modified by replacing the exon 52 with a neokan resistance cassette flanked by loxP sites (blue triangles). The resistance cassette was introduced into the BAC vector by recombineering between the two homologous arms 5' and 3'. The modified BAC vector was used for targeting of the desired locus in Niere m cells by homologous recombination.

1.1 Allelic differences of BAC vectors

Amongst others BACs CH242-9G11 and CH242-27G20 were found to cover the genomic region comprising the exon 52 of the *DMD* gene. Their sequences were deposited in a pre-annotated status at the ensemble.org database. Alignment in BioEdit software of the sequences of BACs CH242-9G11 and CH242-27G20 showed an overlap of 27 kb. Besides several single nucleotide polymorphisms (SNP), two

major differences were found. An 8450 bp insert was found approximately 6660 bp upstream of exon 52 on CH242-9G11, but was missing in CH242-27G20. BLAST search of this insert identified it to be a L1 Transposon. Additionally a microsatellite was found 5540 bp upstream of exon 52 with differing length between the two BACs. As both BACs were obtained from a single Duroc female (http://www.ensemble.org/Sus_scrofa/Info/Index) the comparison of the sequences in the overlapping region indicates that the diversity of the pig population is high, even in so-called "defined" breeds. Although BAC vectors show long homologous regions that avoid decreased recombination efficiency due to SNPs, larger differences might influence the recombination process. Therefore, the genomic region around exon 52 on the single X-chromosome of the Niere m cell line and on the genomic DNA from other individuals of different pig breeds was examined for both, the transposon integration and the microsatellite.

The allelic character concerning the L1 Transposon of the Niere m cell line as well as several different pig breeds was examined by a screening PCR with common reverse primers and forward primers, specific for the integrated as well as for the non-integrated transposon (Figure IV.2).

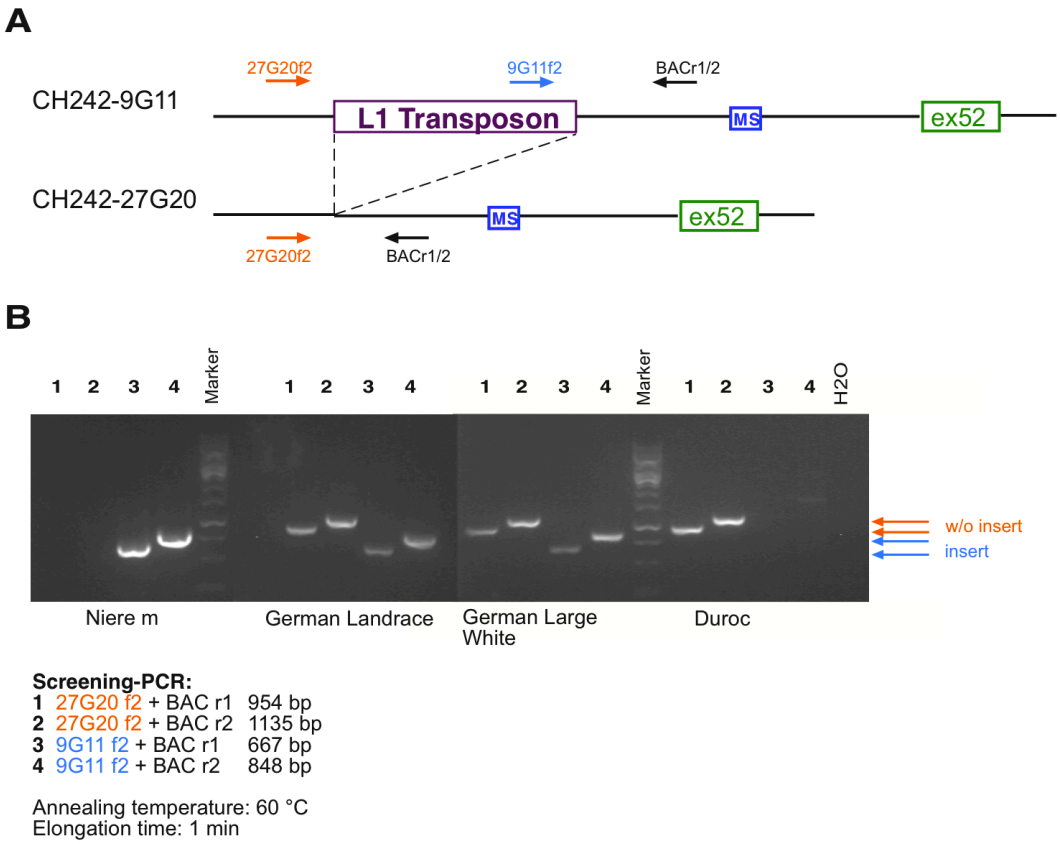

Figure IV.2 Screening PCR for L1 Transposon of genomic DNA of Niere m cells and several different pig breeds

(A) Position of the L1 Transposon and microsatellite on the BAC sequences with primers for the screening the L1 Transposon are indicated as arrows; **(B)** Screening PCR for L1 Transposon; amplicons with differing length are generated; **(A/B)** abbreviations: MS: microsatellite; ex52: *DMD* exon 52; w/o: without.

Screening for the transposon integration revealed that the male cell line Niere m contained the insert, contrary to the genomic DNA from a Duroc female animal, which lacked the insert on both alleles. The female animals of the German Landrace breed as well as German Large White breed showed a heterozygous genotype.

The region containing the microsatellite was sequenced from Niere m and several other different pigs from different breeds for further comparison. The obtained sequences are shown in Figure IV.3.

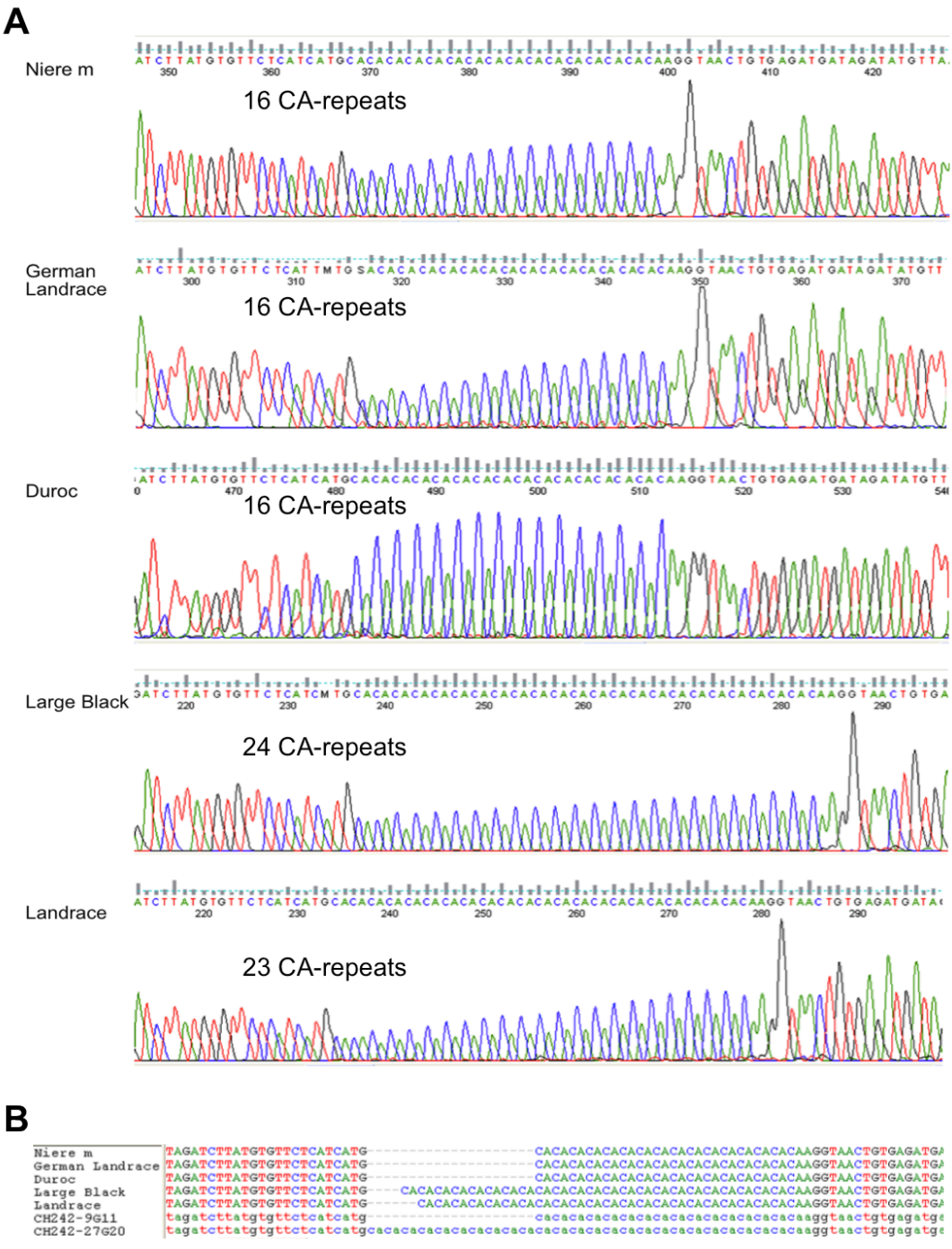

Figure IV.3 Sequencing results of the region containing the microsatellite of Niere m and several other animals of different breeds

(A) Sequencing results of the microsatellite of the Niere m cell line and various animals of different breeds; **(B)** Sequencing results aligned to sequences of CH242-9G11 and CH242-27G20; **(A/B)** Fragments containing the microsatellite were obtained by PCR with the primer pair DMD-int51-MSf1 and DMD-int51-MSr1, an annealing temperature of 58°C and 1 min elongation time; sequencing was done with T7, M13 as well as DMD-in51-MSf1 and DMD-int51-MSr1 primers.

Sequencing results showed varying length of the microsatellites in the different animals analyzed. However, CH242-9G11 and Niere m have the same number of CA-repeats.

Altogether the data indicate a broad diversity of the examined polymorphisms in the pig population. Niere m and CH242-9G11 show the same genotype for the L1 Transposon as well as the microsatellite. As major genetic modifications may have an influence on the targeting efficiency, the BAC CH242-9G11 was chosen for the targeting experiments. The SNPs between CH242-9G11 and Niere m were not further examined.

1.2 Construction of the *DMD* gene targeting vector

1.2.1 Assembly of the plasmid based modification vector

The usage of a modified BAC vector as a targeting vector requires assembling of plasmid based modification vector that is introduced into a BAC via recombination. The modification vector was assembled from the 5'-homologous arm, 3'-homologous arm and the floxed neokan resistance cassette in a pBSK vector as indicated in Figure IV.1.

The 5'-homologous arm and 3'-homologous arm, were amplified from intronic sequences from BACs, carrying the porcine exon 52 sequence (CH242-9G11, -520G21, -27G20). PCR's annealing temperature was 60 °C and elongation time 1.30 min for both primer pairs. DMD5SPf and DMD5PNBr gave rise to the 5'-homologous arm amplicon of 582 bp and DMD3BNf and DMD3PKr to the 3'-homologous arm of 407 bp. The homologous arms were ligated into pGEM®-T-easy Vector and sequenced. The SacI/BamHI digested 5'-homologous arm and the BamHI/KpnI digested 3'-homologous arm were ligated simultaneously into a SacI/KpnI linearized pBSK vector and sequenced.

The neokan resistance cassette with a murine 3-phosphoglycerate kinase promoter (mPGK), a T7 promoter, a bovine growth hormone (bGH) polyadenylation site (pA) and with two flanking lox-sites was obtained by restriction digest with NsiI and BamHI and cloned into the PstI/BamHI linearized pBSK vector containing both homologous arms and sequenced for verification.

The sequence of the final construct corresponded to the sequence, assembled *in silico*.

However, several nucleotide variations could be identified in the homologous arms, which could not be found on either BAC sequence (CH242-9G11 or CH242-27G20). On the 5'-homologous arm an "a" was exchanged with a "g" at 134077 bp of the CH242-9G11 sequence. On the 3'-homologous arm a "t" was exchanged with a "c" twice, once at 134014 bp and at 134077 bp. The respective positions were identical in CH242-27G20 and CH242-9G11, indicating that the polymorphisms were caused by PCR amplification.

1.2.2 BAC modification

BAC CH242-9G11 was chosen for targeting experiments as it shows equal allelic characteristics in the major polymorphic sites described above as the cell line Niere m used in targeting experiments. In order to modify the BAC it was transferred into a recombineering capable SW106 *E.coli* strain. One colony was obtained from electroporation and screened for the uptake of CH242-9G11 via PCR with sequence specific primers, for the homologous arms and the exon 52 (Figure IV.4).

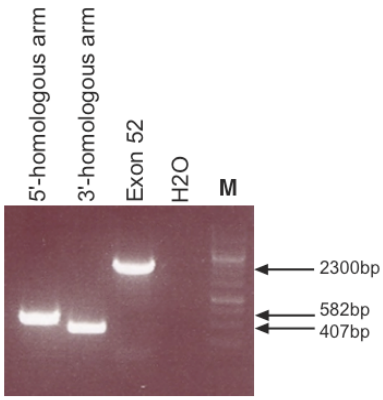

Figure IV.4 Screening PCR for the integration of CH242-9G11 in SW106 cells

Screening PCR with CH242-9G11 sequence specific primer pairs DMD5SPf and DMD5PNr, DMD3BNf and DMD3PKr and DMDexSf and DMDexBr, an annealing temperature of 60 °C and elongation time of 1.30 min; M: Marker

The modification vector was excised with the restriction enzymes PacI and PvuI, purified and electroporated into competent cells of the heat induced SW106 *E.coli* strain carrying the BAC CH242-9G11. After selection on kanamycin 163 colonies were obtained, 27 colonies were picked for overnight cultures and screened for the

correct modification of the BAC by PCR (Figure IV.5 A). In 5 colonies the BAC has undergone homologous recombination and was correctly modified (Figure IV.5 B).

DNA from two positively screened bacterial clones was chosen for electroporation of the modified BAC into DH10B bacterial cells. 274 colonies were obtained and 24 picked for overnight cultures. 8 of the 24 DH10B colonies were screened for the modified BAC by PCR, 7 out of 8 clones reflected the screening result of the BACs in the SW106 cells (Figure IV.5 C).

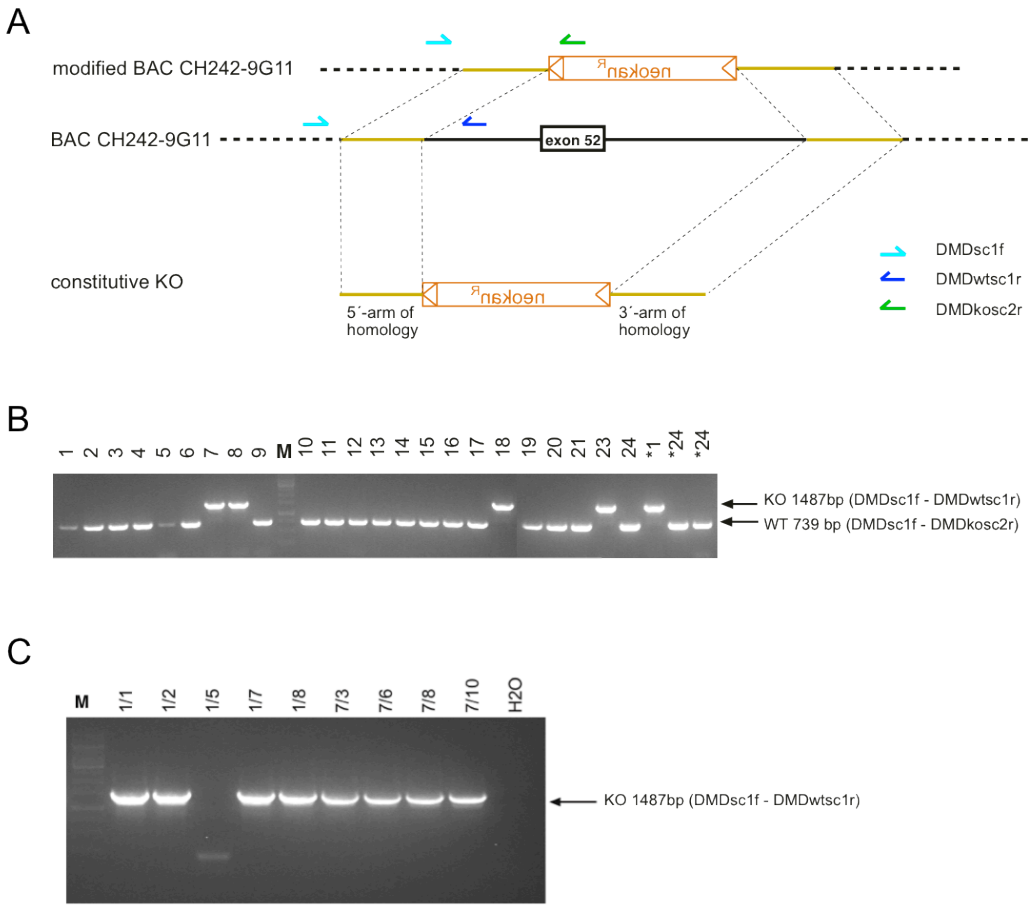

Figure IV.5 Screening PCR for the integration of the modified BAC CH242-9G11 in SW 106 and DH10B cells

(A) Primer positioning of DMDsc1f and DMDwtsc1r/DMDkosc2r on the wild-type BAC and the modified BAC represented schematically; **(B)** Screening of colonies obtained after recombineering with both reverse primers in SW106 cells; **(C)** Screening of colonies obtained after electroporation of the modified BAC into DH10B cells, they were only screened with the KO primer pair (DMDsc1f and DMDkosc2r); **(B/C)** PCR was run with an annealing temperature of 57 °C and an elongation time of 1 min; M: Marker; KO: modified BAC integrated; WT: wild-type BAC

Furthermore, the integrity of the modified BAC was examined by restriction digest of BACs CH242-27G20, CH242-9G11 and the modified CH242-9G11 with PvuII and XbaI respectively. The restriction pattern of CH242-27G20 and CH242-9G11 is significantly different, as they do only share an overlap of 27 kb while at least 120 kb are unique for both clones. In contrast was the restriction pattern of the unmodified and the modified CH242-9G11 quite similar, as they do only differ in a length of 6 kb while they share a common sequence of 150 kb. *In silico* digest of the pre-annotated CH242-9G11 sequence and its modified counterpart predicted that a 10553 bp band in the XbaI digest of the unmodified BAC is lost due to the exchange of exon 52 by the resistance cassette and the introduction of a XbaI recognition site, which gives rise to the additional bands of 5932 bp and 1223 bp in the modified BAC. The restriction digest of the BACs confirmed this prediction (Figure IV.6): as a restriction fragment of the vector backbone is visible at approximately 10500 bp as well, the comparison of the intensities of the bands with 10553 bp band suggested a ratio of 2:1 and indicated the loss of the 10553 bp band in the modified BAC. The identification of the fragments 5932 bp and 1223 bp was not possible because of the great number of further bands. In the PvuII digest the modification of the BAC was more distinct, as the overall pattern was identical and a single 10280 bp band in the unmodified BAC was clearly lost by the modification. The additional fragments of the modified BAC 4073 bp, 967 bp and 844 bp were not to be identified within the other bands of the restriction digest. PCR screening and restriction pattern of the modified BAC indicates that (i) the BAC was modified correctly and (ii) the BAC did not undergo aberrations during the transfection into the SW106 and the subsequent recombineering procedure.

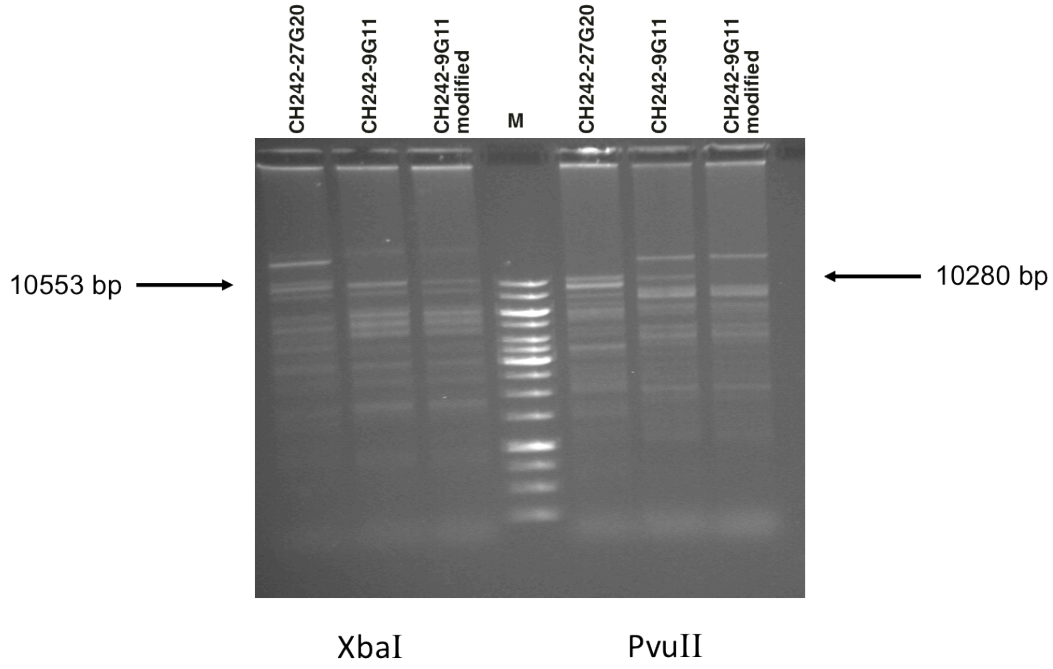

Figure IV.6 Restriction digests of the BACs CH242-27G20, CH242-9G11 and modified CH242-9G11 with XbaI and PvuII

Additional XbaI and PvuII recognition sites in the sequence of the modified CH242-9G11 BAC lead to variations in the band patterns of the respective BACs after restriction digest. Apart from that the band patterns correspond to each other; M: Marker

1.2.3 Targeting BAC preparation

Based upon the evaluation of the modified BACs, clone #1/2 was chosen and DNA was isolated endotoxin free for nucleofection experiments. Additionally DNA of the targeting vector was also isolated with the non-endotoxin free protocol midi prep and further processed in equal manner.

25 µg of CH242-9G11 with the targeting construct could be obtained from the first endotoxin free isolation (#1). After digest with SfiI linearized BAC with a concentration of 685 ng/µl were available for targeting experiments in cell culture. In a second endotoxin free isolation 40 µg DNA of the modified BAC were isolated and after restriction digest with SfiI linearized BAC with a concentration of 955 ng/µl was obtained (#2). Further 88 µg modified BAC were isolated in a non-endotoxin free manner and linearized vector with a concentration of 3698 ng/µl (Midi Prep/PCiA) was produced.

2 Targeting of the *DMD* gene in primary porcine kidney cells

2.1 Cell culture

Five nucleofection experiments were carried out with the modified and linearized BAC CH242-9G11 (Table IV.1). For experiments 100203 and 100413 the same DNA was used (endotoxin free #1), for experiments 100831A and 100912 DNA from a later preparation was used (endotoxin free #2). 100831B was carried out with DNA, which was isolated following the conventional midi prep protocol. Nucleofection was performed with Niere m cells either in passage 3 or 4. For each experiment 5.0×10^5 cells were transfected with 5 µg DNA, except for experiment 100912 in which 1.0×10^6 cells were transfected. Selection with G418 was started with differing amount of cells, ranging from 4.0×10^5 and 52.8×10^5. However, selection in experiments 100831A and B was started 24 h after nucleofection, which may have contributed to the low cell number in these experiments. Selection in experiment 100912 was started with 2.7×10^6 cells of the total 3.5×10^6 cell for reasons of feasibility. The remaining cells were cryopreserved. Furthermore, was the ratio of the co-seeded untreated cells to the transfected cells changed from 4:1 to 3:1 and 1:1 in the experiment 100912. A variable number of single cell clones, 0.1 ‰ - 0.2 ‰ of seeded transfected cells, was obtained after selection in each experiment. Except for experiment 100831B where no single cell clone was obtained. Overall 637 clones were splitted after selection, with values ranging from 0 to 275 clones. In experiments 100203 and 100413 an almost equal number of clones (162 and 156 respectively) were splitted. A total of 436 clones were harvested for DNA isolation and 322 portions of clones were harvested in passage 6 or 7 for cryopreservation, as the first experiment (100203) was carried out without generation of backup clones. Between the single experiments varying proportions from 22.7% to 42.9% of clones were lost after splitting.

Table IV.1 Transfection experiments of Niere m cells

Nucleo-fection	Passage at nucleo-fection	Typ of DNA	DNA volume 5 µg (µl)	Cells at selection start ($\times 10^5$)	Single cell clones after selection	Cell clones harvested / (%)
100203	P3	EF #1	7.3	8.6	162	114 (70.4)
100413	P3	EF #1	7.2	8.6	156	89 (57.1)
100831 A *	P4	EF #2	5.2	4	44	34 (77.3)
100831 B *	P4	PCiA	1.4	4.4	0	0
100912 #	P4	EF #2	5.2	27.2	275	199 (72.4)
Total				52.8	637	436 (68.4)

EF: endo free

* Start of selection 24 h after nucleofection

1×10^6 cells transfected and seeded in the ratios of transfected to untreated cells of 1:1 and 1:3

2.2 Screening

DNA was isolated via high salt precipitation from the 436 cell clones obtained in targeting experiments and used for screening of correct integration of the targeting construct by qPCR with the "loss-of-native-allele" assay. In correctly targeted cells the modified BAC integrates into the genome of the Niere m cells at the desired locus by homologous recombination and thereby the exon 52 of the *DMD* gene is replaced by the resistance cassette. Therefore, a primer pair (qPCRDMD11fw and qPCRDMD12rv) was designed on the targeting site specific wild-type *DMD* sequence. The primer pairs GGTA3423fw/GGTA3640rev and HPRT834i2fw/HPRT987i2rev on the sequence of the alpha(1,3)galactosyl transferase (*GGTA*) gene and the hypoxanthine phosphoribosyltransferase 1 (*HPRT*) gene respectively were established as reference amplicons by Katrin Krähe and Katrine Skou. In order to screen for correctly targeted cell clones the copy number of the amplicon of the *DMD* gene is compared to the copy number of the two reference genes. In the case of random integration of the targeting vector the *DMD* gene stays intact and leads to a copy number ratio of 1:1 (*DMD/HPRT*) or 1:2 (*DMD/GGTA*). In case of a successful targeting by homologous recombination no DMD amplicon can be detected and the ratios change to 0:1 and 0:2 respectively (Figure IV.7).

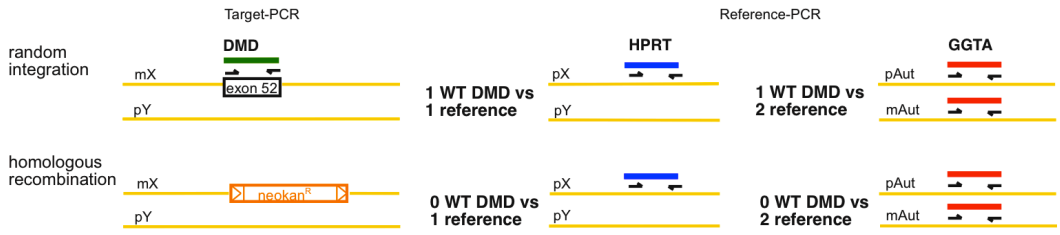

Figure IV.7 Schematic depiction of the qPCR screening method

For the screening of correctly targeted clones the copy number of the target sequence was compared to the copy number of two reference genes. *HPRT* is located on the X-chromosome, whereas *GGTA* lies on an autosomal chromosome; mX: maternal X-chromosome; pY paternal Y-chromosome; WT: wild-type; pX paternal X-chomosome; mAut: maternal autosomal chromosome; pAut: paternal autosomal chromosome.

The 436 samples were pooled into sets for the qPCR screening. Each set comprising up to 38 samples. From each set the copy numbers of the amplicons of the *DMD, GGTA* and *HPRT* primers were determined on individual plates, using the same standard curve with the same copy number values. Three calibrators on each plate were used for the calibration of the obtained copy numbers from the primer pairs for each sample. A cell clone with a calibrated copy numbers below 100 in any of the four values of the reference genes (*GGTA* and *HPRT*) was omitted from the set and was not considered in further processing. From the remaining samples the copy number ratio between the calibrated copy numbers of each primer pair were calculated: *DMD/GGTA*, *DMD/HPRT* and *GGTA/HPRT*. The mean value and standard deviation was calculated from the resulting four values for each primer pair ratio. Samples were excluded from the set when the standard deviation of any ratio was higher than 0.3. From all samples meeting the quality criteria (calibrated copy number >100, standard deviation of all ratios <0.3), those were considered positively targeted, which had a ratio of *DMD* to *GGTA* and *DMD* to *HPRT* below 0.1 and a ratio of *GGTA* to *HPRT* of 1 (see Table IV.2 and Table IV.3).

In order to evaluate the reliability of the screening for correctly targeted cell clones by the comparison of the copy number ratios, characteristic values like the median, mean value, maximal value, minimal value and the standard deviation, were determined (see Table IV.2 and Table IV.3). Values of the correctly targeted clones for the *DMD/GGTA* and *DMD/HPRT* ratios are obviously outliers compared to the values of the remaining cell clones. The maximal value of the correctly targeted cell clone is

still 65 times smaller than the lowest value of the other cell clones. Moreover does the comparison of the median and mean value show that the ratios of the *DMD* copy number to the reference gene copy number is actually 0:1 in correctly targeted cell clones and 1:1 in negative cell clones.

Table IV.2 Characteristic values of the mean values of the respective ratios of evaluated cell clones; correctly targeted cell clones are excluded

	DMD/GGTA	*DMD/HPRT*	*GGTA/HPRT*	Total
Median	1,097564	1,096151	0,942765	1,076487
Mean value	1,121972	1,096243	0,979425	1,079678
Maximal value	1,808750	1,416499	1,567319	1,808750
Minimal value	0,633267	0,544155	0,635529	0,544155
Standard deviation	0,164448	0,150268	0,187355	0,177088

Table IV.3 Characteristic values of the mean values of the respective ratios of correctly targeted cell clones

	DMD/GGTA	*DMD/HPRT*	*GGTA/HPRT*
Median	0,000698	0,000788	1,075482
Mean value	0,002344	0,002411	1,044429
Maximal value	0,007728	0,008360	1,241085
Minimal value	0,000069	0,000061	0,832771
Standard deviation	0,002891	0,003027	0,135488

436 clones were screened by qPCR and the obtained data were analyzed. The set of samples #1-7 and #12 were examined for the copy numbers of *DMD, GGTA* and *HPRT*. The set of samples #8-11, #13 and #14 were examined only for *DMD* and *GGTA*. Cell clones from the latter set of samples that revealed a ratio of *DMD/GGTA* below 0.1 were verified within an extra set of samples (#12) using *DMD, GGTA* and *HPRT* primers. Of the 436 clones tested 381 met the quality criteria whereas 33 clones had a standard deviation higher than 0.3, 20 had a copy number below 100 and 2 clones were not considered because of a pipetting error or backup contamination. Thus a total of 55 clones were excluded from the analysis.

8 clones of the 381 evaluated clones had a ratio of *DMD* copy number to both reference gene copy numbers below 0.1 and were therefore considered as positively

targeted. All of the clones were analyzed in an independent set of samples, where they were confirmed as correctly targeted. A targeting efficiency of 2.1% of the *DMD* locus was achieved. The obtained ratios of qPCR plates with correctly targeted clones are illustrated in diagrams of Figure IV.8 and Figure IV.9. For a clearer illustration the ratio of *GGTA* to *HPRT* was left out.

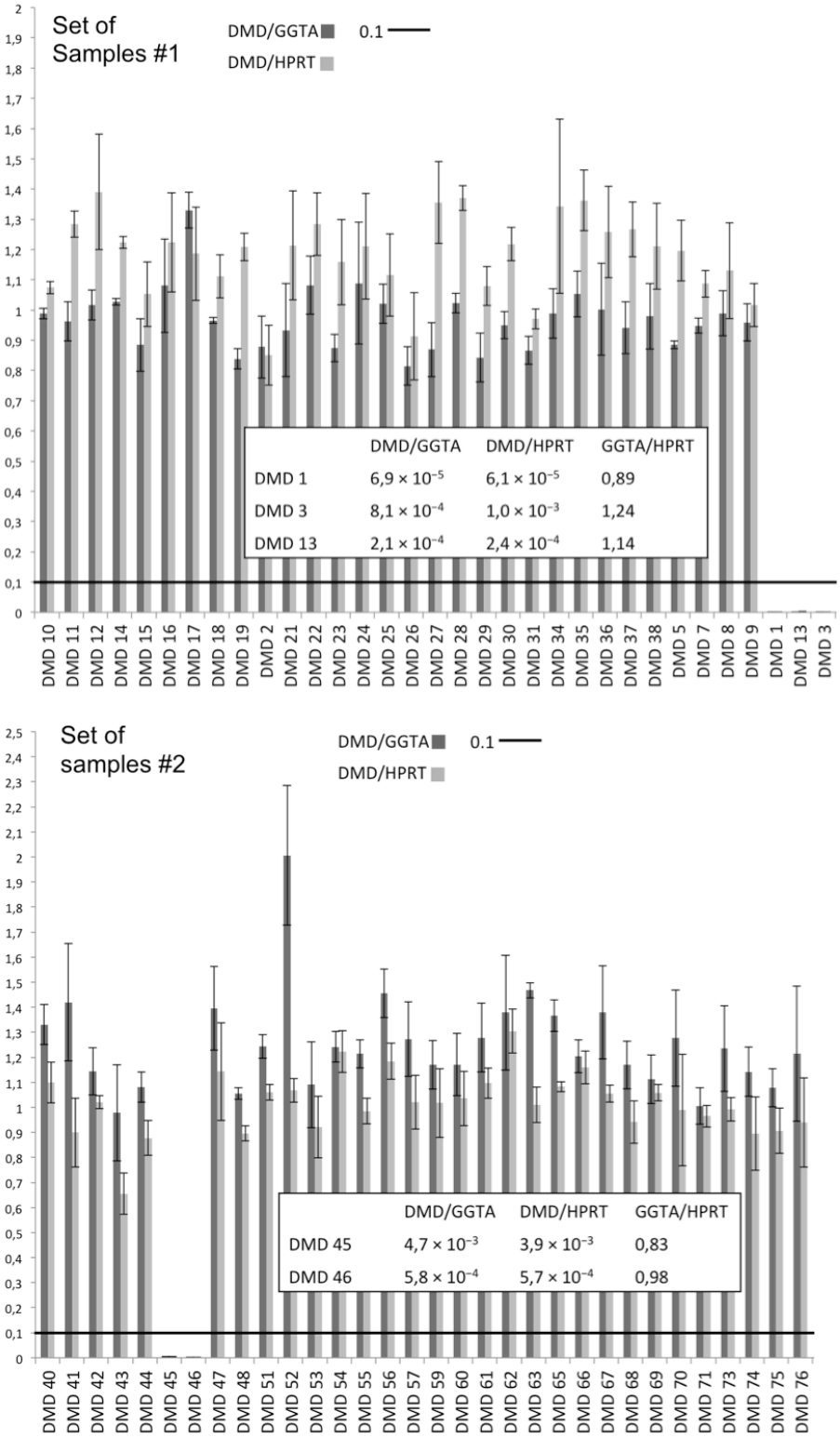

Figure IV.8 Set of samples #1 and #2 of the qPCR screening for correctly targeted cell clones

Diagrams of the mean values of the ratios DMD/GGTA and DMD/HPRT of the set of samples #1 and #2 with the correctly targeted cell clones #1, #3, #13, #45 and #46; contrary to the cell clones with random integration events the ratio of the DMD copy numbers to the reference genes of cell clones, which have undergone homologous recombination tends to zero; actual ratios of correctly targeted clones are specified.

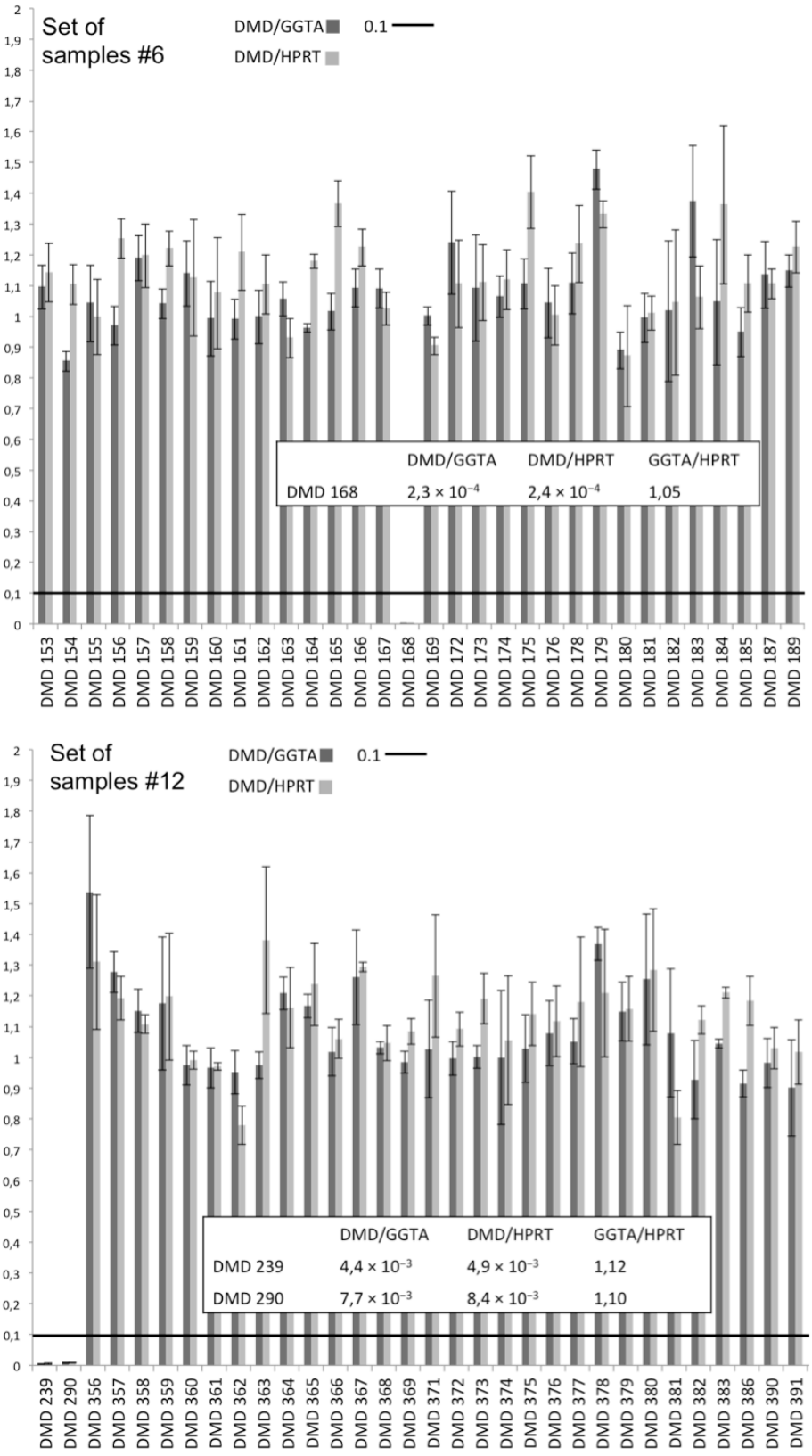

Figure IV.9 Set of samples #6 and #12 of the qPCR screening for correctly targeted cell clones

Set of samples #6 and #12 include the cell clones #168, #239 and #290, which have undergone homologous recombination; their copy number ratios of DMD/GGTA and DMD/HPRT tend to zero (white box), compared to the ratios of the other cell clones.

3 Generation and characterization of the DMD pig model

3.1 Nuclear transfer and embryo transfer

Cell clones #1, #3, #13, #45, #46, #168, #239 and #290 were considered as correctly targeted. From these cell clones #168, #239 and #290 were used for SCNT.

Overall ten SCNTs and ETs with 1085 embryos were carried out by Dr. Barbara Kessler and Dr. Mayuko Kurome to date. Table IV.4 gives an overview of all conducted experiments. Two SCNT were performed using cell clone #239, five with #168 and three with #290. From the SCNTs five pregnancies originated, of which three pregnancies, each based upon a different cell clone, were delivered to term. One pregnancy was lost in the second half of the gestation period, whereas the second one was already lost in the first half.

The pregnancy based upon cell clone #168 gave rise to two piglets (#1300 and #1301). Four piglets were born based upon cell clones #239 (#1249-1252) and #290 (#1261-1264) respectively.

Table IV.4 SCNTs and ETs with *DMD* knockout cell clones

Cells clone	Nucleo-fection experiment	NT-Embryos	US1	US2	US3	US4	Piglets (n)
#168	100413	123	+ (d 33)	+ (d 58)	- (d 93)		
#168	100413	116	+ (d 32)	- (d 57)	- (d 92)		
#168	100413	50	? (d 25)	- (d 33)	- (d 62)		
#168	100413	99	- (d 27)	- (d 58)			
#168	100413	120	+ (d 29)	+ (d 55)			2
#239	100912	140	+ (d 40)	+ (d 54)	+ (d 82)	+ (d 99)	4
#239	100912	61	- (d 25)				
#290	100912	167	- (d 22)	? (d 40)	- (d 82)		
#290	100912	102	? (d 23)	- (d 34)			
#290	100912	107	- (d 22)	+ (d 33)	+ (d 83)		4

US 1-4: ultrasonic pregnancy controls; d: days after ET; +/-/?: pregnant/not pregnant/not to be determined

3.2 Characterization of the *DMD* pig model

Delivered *DMD* knockout piglets were genotypically and phenotypically analyzed. Muscle tissue samples were taken by Prof. Dr. Maggi Walter and Dr. Barbara Kessler

from the muscles m. biceps femoris, m. triceps brachii, longissimus dorsi, diaphragm and heart muscles of dead DMD piglets and aged matched controls. Additionally the kidneys were obtained for the establishment of primary cell lines. From all *DMD* knockout piglets ear tissue samples were taken for cell isolation. Blood samples were taken from the *DMD* knockout piglets #1249, #1251, #1263, #1264 and 5 age matched controls and values of the serum creatine kinase (CK) were determined by the Pig Clinic LMU, Munich.

Besides the evaluation of genetic modification of the genome of the cloned piglets by PCR, they were also examined by immunoblot, histological and immunohistochemistry analysis by Prof. Dr. Maggie Walter and Dr. Benedikt Schoser from the Friedrich Baur Institut, Munich. Dead piglets were sent to the Institute for Veterinary Pathology of the LMU, Munich, for pathological examination by Dr. Andreas Blutke, Dr. Nadja Herbach, Dr. Daniela Emrich and Prof. Dr. Rüdiger Wanke. Andrea Klanner, Alexander Graf, Dr. Stefan Krebs and Dr. Helmut Blum, LAFUGA, Munich performed a whole transcriptome analysis. Cells were isolated and primary cell cultures established by Anne Richter.

3.2.1 qPCR

DNA for qPCR screening was isolated from kidney cells or ear fibroblasts respectively. qPCR was performed as described for cell clones from targeting experiments, yet two samples of each piglet were tested instead of one sample. The ratios of the copy number of the amplicons of exon 52 to the copy number of the reference genes tended to zero for all *DMD* knockout pigs (Figure IV.10). DNA from already negatively tested cell clones was used as wild-type controls.

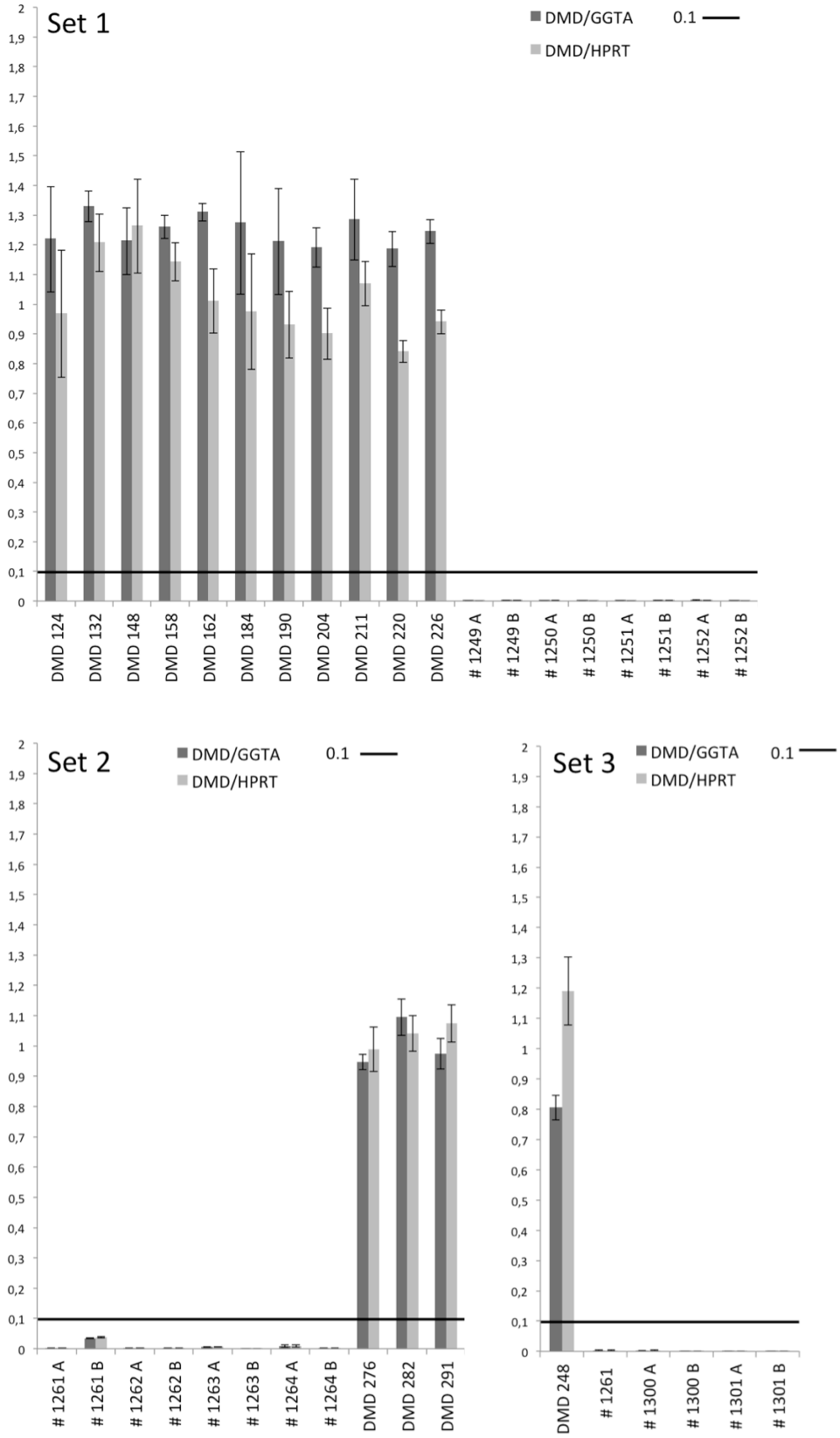

Figure IV.10 Sets 1-3 of the qPCR screen of the delivered *DMD* knockout piglets

DNA from delivered *DMD* knockout piglets was isolated and screened by qPCR for the loss of exon 52 of the *DMD* gene. Ratios of *DMD/GGTA* and *DMD/HPRT* are shown; DNA from formerly screened cell clones was used as wild-type controls.

3.2.2 End-point PCR

Besides qPCR screening DNA from *DMD* knockout piglets was also screened by end-point PCR for the loss of exon 52. Genomic DNA isolated from ear tissue samples via PCiA extraction protocol (#1249, #1250, #1251, #1252) and from ear fibroblasts via high salt precipitation (#1261, #1262, #1263, #1264, #1300, #1301) was used as template. No amplicons from the exon 52 could be detected in the DNA samples from *DMD* knockout pigs (Figure IV.11).

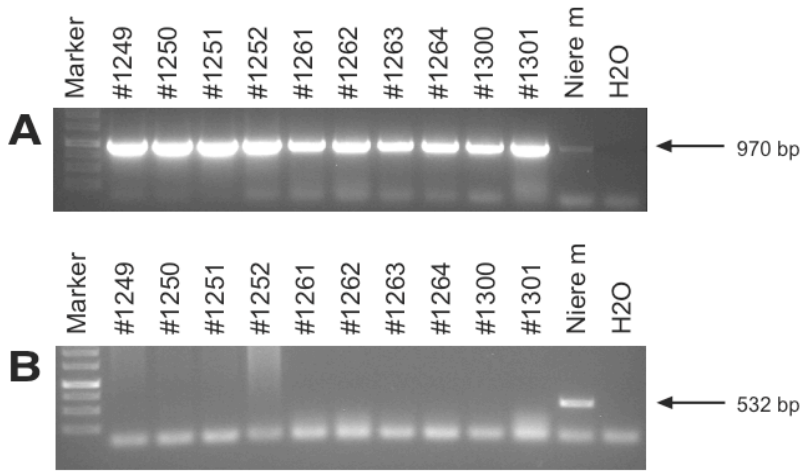

Figure IV.11 Genotyping PCR of the delivered *DMD* knockout piglets

(A) The primer pair designed on the sequence of the *β-actin* gene (PACT954f and PACT1919r) was used as reference for DNA integrity control; **(B)** Targeting site specific primers qPCRDMD5fw and qPCRDMD9rv were applied for the detection of exon 52 of the *DMD* gene; **(A/B)** Niere m DNA was used as wild-type control; Annealing temperature was 60°C and elongation time 1 min.

3.2.3 Transcriptome, immunoblot and histological analysis

After the verification of the successful deletion of exon 52 on the genomic level, the transcribed RNA of two *DMD* knockout piglets of the first litter and of two wild-type controls was examined by RNA sequencing of the exon junctions between exons 50 to 54 (Figure IV.12). In the control animals, junctions between 50/51, 51/52, 52/53 and 53/54 were readily detected, without any reads indicating alternative splicing. In the DMD piglets junctions between 50/51 and 53/54 could be detected, whereas no sequence of exon 52 was identified. However, transcripts with a junction between exons 51 and 53 were detected, that would lead to a + 1 frame shift resulting in six stop codons within exon 53 (two stop codons) and exon 54. Stop codons in exon 53 are at least 100 nucleotides upstream of the exon junction between exons 53 and 54.

The number of reads detected also differs between the wild-type piglets and the *DMD* knockout piglets. Generally more reads are detected in wild-type controls.

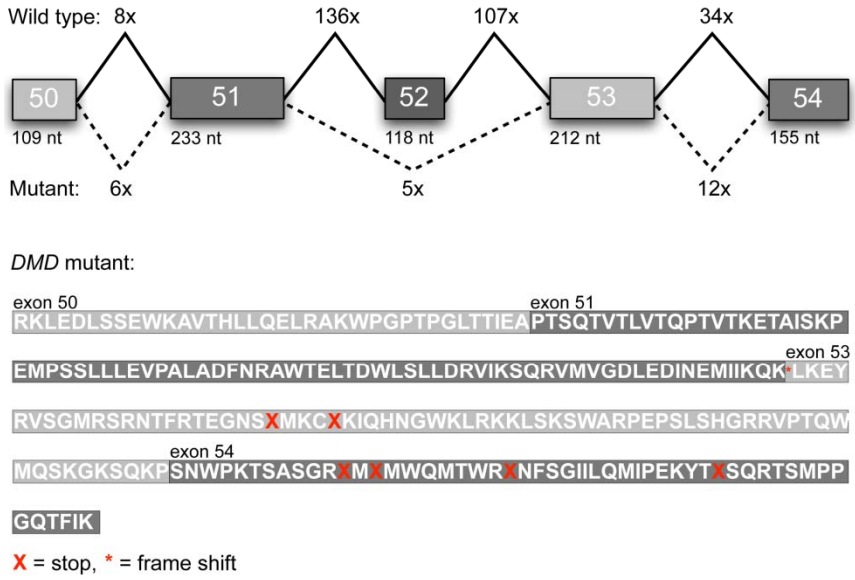

Figure IV.12 RNA sequencing of exon junctions in the transcript of the *DMD* gene

Exon junctions 50/51, 51/52, 52/53 and 53/54 of two *DMD* knockout piglets and two wild-type control animals were sequenced and the resulting stop codons depicted in the amino acid sequence (red crosses); lines between the exon boxes indicate the number of reads detected, the continuous line the reads from wild-type controls and the dotted line from *DMD* knockout piglets; kindly provided by Dr. Helmut Blum.

Furthermore, the immunoblot analysis showed the loss of the protein dystrophin in the skeletal muscles of *DMD* knockout pigs #1249 and #1250 (Figure IV.13); confirming the desired loss of function of the protein by the knockout of exon 52 of the *DMD* gene.

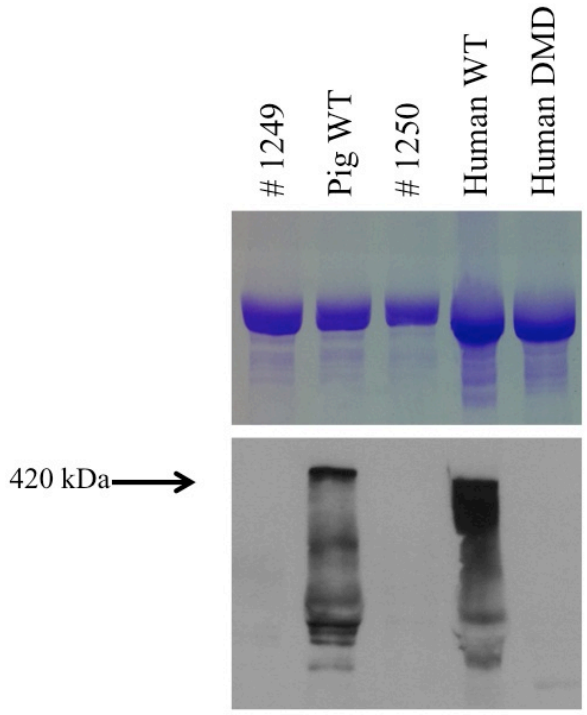

Figure IV.13 Immunoblot of *DMD* knockout piglets #1249, #1250 and a wild-type pig compared to human samples

The imunoblot demonstrates the loss of the protein dystrophin in the muscles of the DMD piglets compared to a wild-type control, mimicking the human situation. In order to show the equal loading of the gel the Coomassie-stained SDS gel is presented above; 20 µg protein were separated by 5.5% SDS-PAGE and blotted to a nitrocellulose membrane; dystrophin was labeled with monoclonal antibodies (NCL-DYS1 and NCL-DYS2, 1:150) and horseradish peroxidase-coupled polyclonal rabbit anti-mouse antibodies (PO260, 1:1000, Dako); antibodies were visualized using ECL reagent (RPN2106, GE Healthcare Amersham Bioscience); WT: wild-type; kindly provided by Prof. Dr. Maggie Walter.

Immunostaining of muscle sections of *DMD* knockout piglets and wild-type controls was performed with two monoclonal antibodies against two different epitopes of the human dystrophin protein, the central rod domain and the COOH-terminal domain, with cross-reactivity to the porcine dystrophin protein. In order to illustrate the membrane integrity, a monoclonal antibody against a further membrane protein, dysferlin, was used. Staining of wild-type control exhibited a clear dystrophin signal, whereas almost no signal could be detected in samples of the *DMD* knockout pigs (Figure IV.14). Providing a further evidence for the loss of a functional protein dystrophin. However, isolated revertant fibers could be found (not shown).

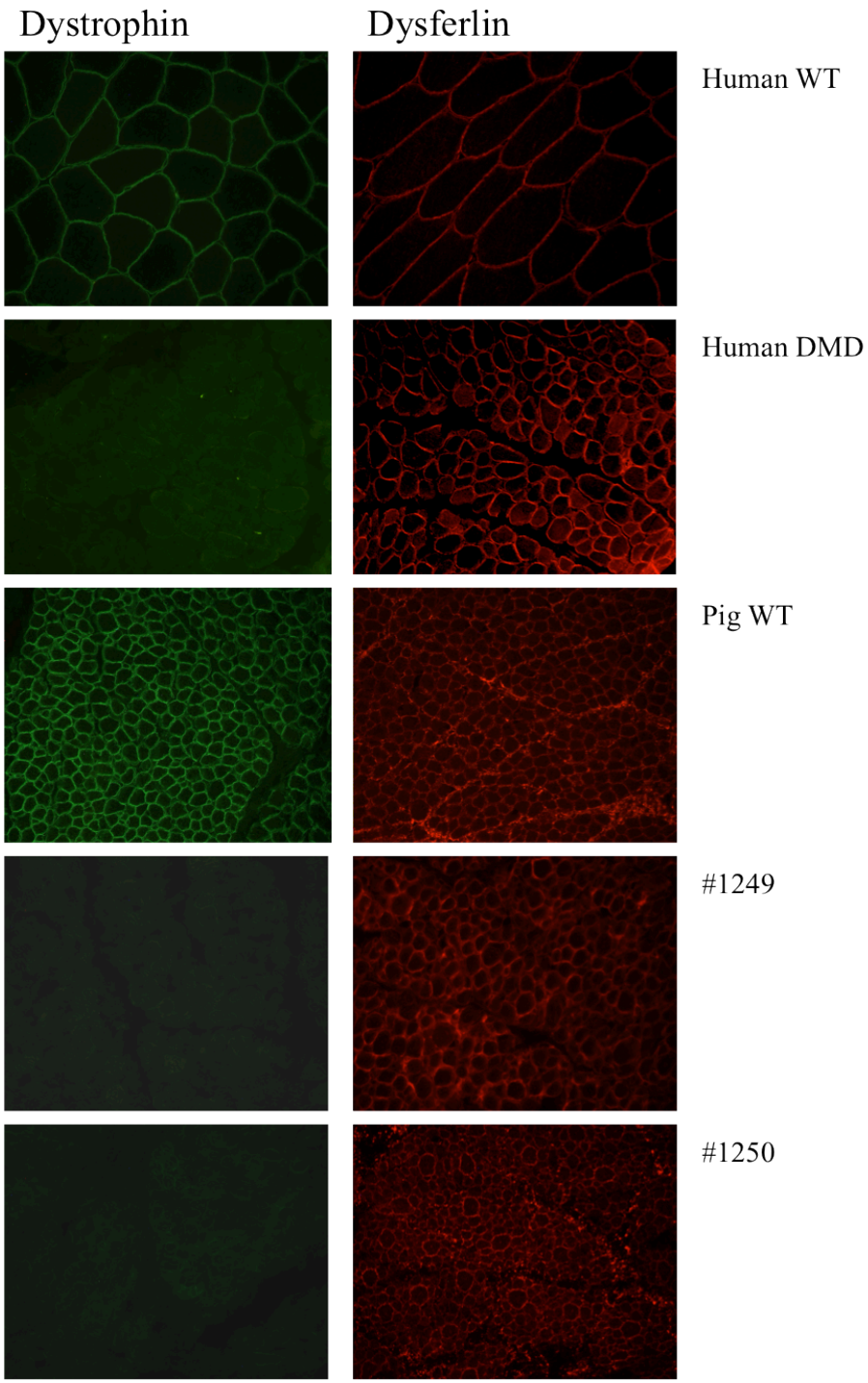

Figure IV.14 Immunofluorescence analysis of *DMD* knockout pigs

Samples are stained with primary antibodies against dystrophin (NCL-DYS1, NCL-DYS2, 1:10, Novocastra) and against dysferlin (NCL-hamlet, 1:25, Novocastra) as membrane integrity control. Compared to the wild-type control no dystrophin is detectable in the muscle sections of the *DMD* knockout piglets. This finding corresponds to the situation in human DMD patients; secondary antibodies used were anti-mouse IgH (H+L) coupled to Alexa Fluor 488 (1:300, A11029, Invitrogen-Molecular Probes) for dystrophin and biotinylated sheep anti-mouse IgG (RPN 1001V, 1:100, GE Healthcare Amersham Bioscience) and Cy3 conjugated streptavidin (016-160084, 1:000, Dianova); WT: wild-type; kindly provided by Prof. Dr. Maggie Walter

The histological analysis of the muscles from the *DMD* knockout piglets by the Institute for Veterinary Pathology of the LMU Munich and the Friedrich Baur Institute, showed atrophic, hypertrophic and hypercontracted fibers, as well as muscle fibers with a rounded shape, basophilic staining, centrally located nuclei and differing fiber diameters (Figure IV.15). Additionally focal interstitial fibrosis, mononuclear infiltration and focal calcifications were observed.

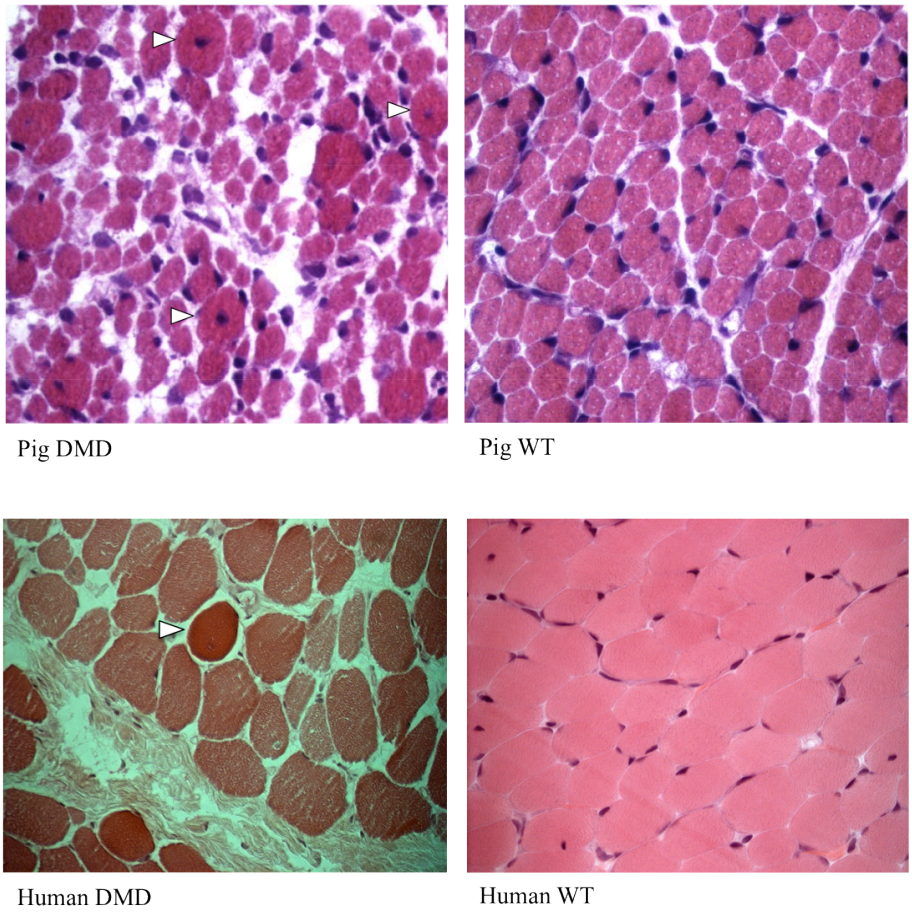

Figure IV.15 Histological examination of the muscles of 2 days old *DMD* knockout piglets

Sections of the m. biceps femoris of the *DMD* knockout pig and a control wild-type animal were stained with hematoxylin and eosin; in the muscle of the *DMD* knockout pig centrally located nuclei (white arrows), rounded muscle fibers and a great variation of fiber diameters can be observed; original magnification: 400×; WT wild-type; kindly provided by Prof. Dr. Maggie Walter.

The histology of the 3-months-old pig bore the same symptoms described for the younger piglets, but deteriorated (Figure IV.16). Additionally branching fibers,

segmental necrosis of muscle cells with histiocytic cell infiltrations and a fatty replacement of muscle tissue could be observed. The heart muscle did not show any pathological changes, except for a few degenerating single fibers.

These are signs of severe muscular dystrophy with muscle degeneration, regeneration and subsequent replacement of muscle tissue, also observed in human DMD patients.

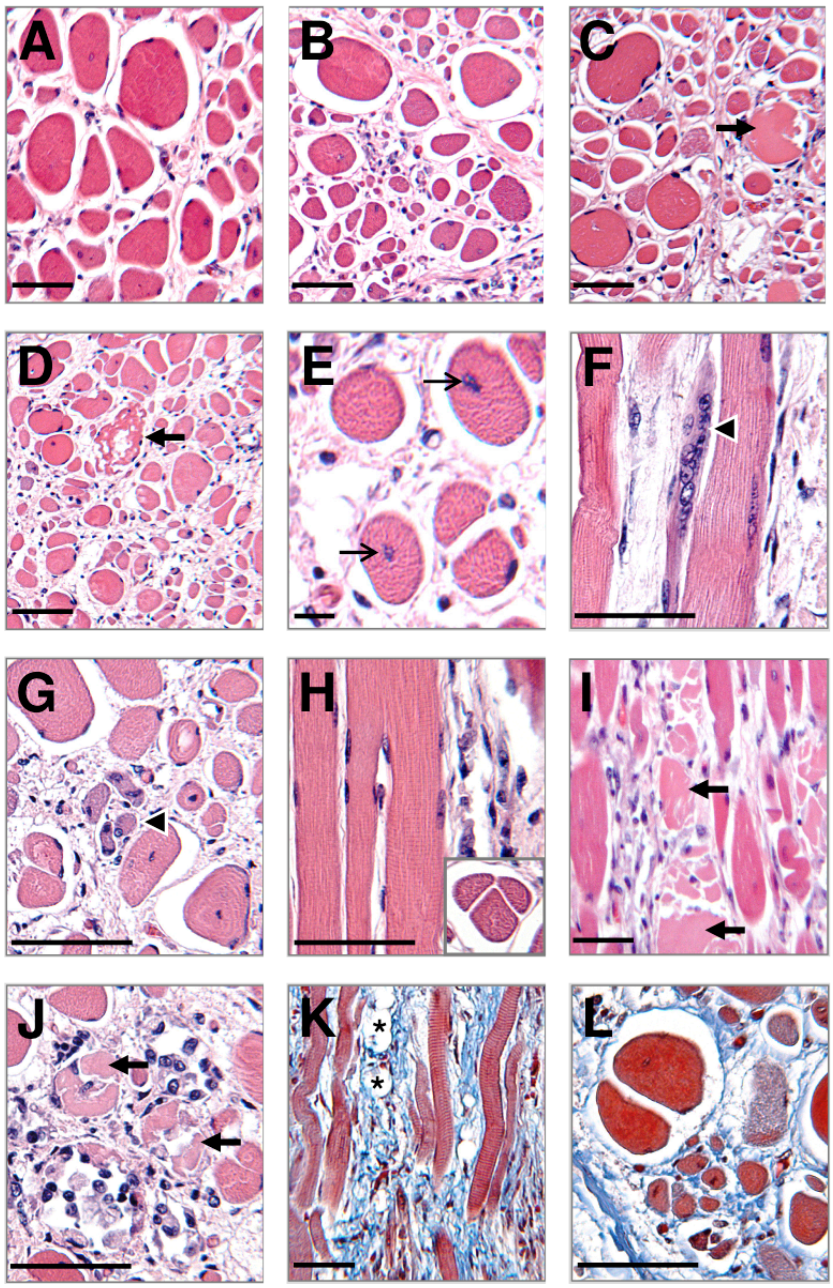

Figure IV.16 Histopathology of skeletal muscles of the three-months-old DMD pig

A-D: Cross sections of the triceps brachii (**A**), biceps femoris (**B**), longissimus dorsi (**C**) and the diaphragm (**D**) demonstrating excessive variation of fiber diameters with hypertrophic rounded fibers. **E** (biceps femoris, cross section): Centrally located nuclei (arrows). **F** (triceps brachii, longitudinal section) and **G** (diaphragm, cross section): Regenerating fibers (arrowheads). **H** (triceps brachii, longitudinal section; inset: biceps femoris, cross section): Branching/splitting of fibers. **I** (biceps femoris, longitudinal section) and **J** (diaphragm, cross section): Segmental necrosis of fibers (arrows in **I**, **J**, and in **D**) with peri- and endomysial mononuclear (histiocytic) cell infiltration. **K** (diaphragm, longitudinal section) and **L** (diaphragm, cross section): Interstitial fibrosis (blue color) and fatty replacement (asterisks in **K**) of muscle tissue. Paraffin sections. HE-staining (**A-J**), Trichrome-Masson-staining (**K**, **L**). Bars in **A-D**, **F-L**: 50 µm, bar in **E**: 10 µm; kindly provided by Dr. Andreas Blutke

Moreover the volume density of muscle fibres in the muscle ($V_{V(MF/M)}$) was calculated and the muscle fiber Feret's diameters were determined of three newborn DMD pigs and three age matched controls.

For the $V_{V(MF/M)}$ an average of 354 ± 38 muscle fiber points were counted per case. The calculated volume density of muscle fibres in the muscle (musculus biceps femoris) of DMD piglets (0.71) and wild-type control animals (0.78) do not differ significantly (Figure IV.17).

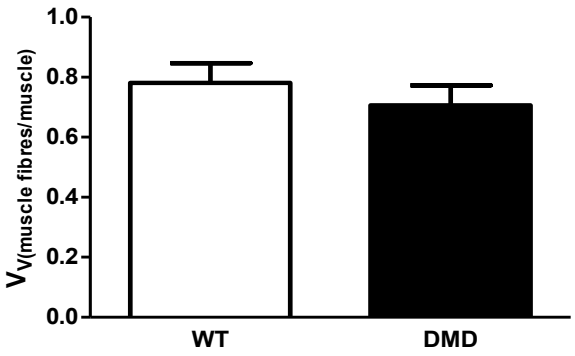

Figure IV.17 Volume density of muscle fibres in the muscle of DMD piglets and wild-type controls

$V_{V(MF/M)}$ of DMD piglets (n=3) and wild-type controls (n=3) was determined in the musculus biceps brachii; WT: wild-type, DMD: *DMD* knockout, V_V: volume density.

The minimal Feret's diameter was measured in order to confirm the fiber diameter variations seen in muscle fiber cross sections. It was determined of an average of 636 ± 74 muscle fiber cross sections per animal. The obtained data were categorized into ten diameter classes (≤ 4, 4.1-6, 6.1-8, 8.1-10, 10.1-12, 12.1-14, 14.1-16, 16.1-18, 18.1-20 and ≥ 20.1), the data were divided into the respective classes and the proportion of the class on all measured diameters was calculated. To compare wild-type and DMD muscle phenotypes, p-values were calculated using an unpaired two-sample t-test, assuming equal variances. P-values of < 0.05 were considered statistically significant (Figure IV.18).

A left shift to smaller minimal Feret's diameters of the muscle fiber cross sections of DMD piglets can be observed compared to the wild-type controls.

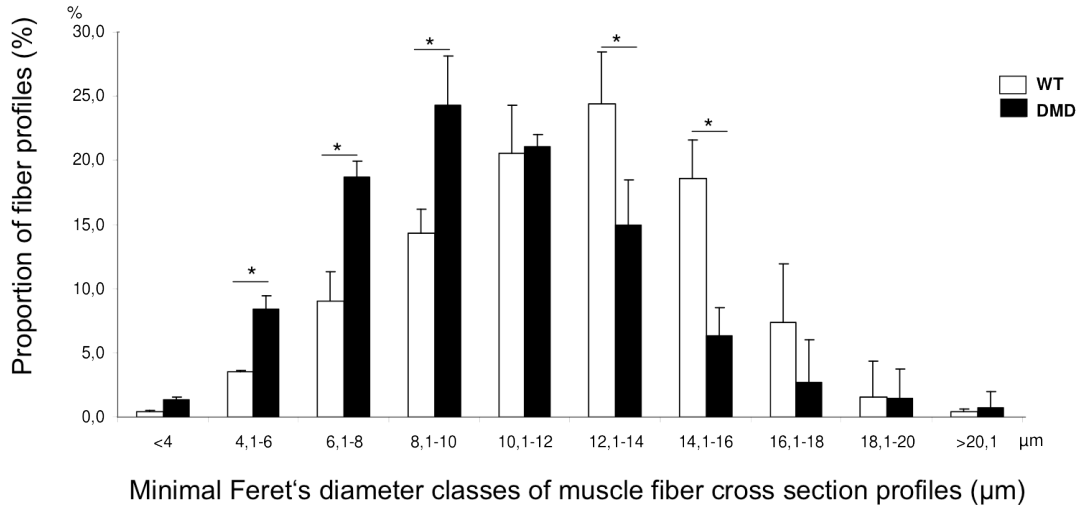

Figure IV.18 Minimal Feret's diameter of muscle fiber cross section profiles

The minimal Feret's diameter was determined of *DMD* knockout piglets (n=3) and age matched controls (n=3); obtained data was categorized into 10 classes; *: $p < 0.05$; WT: wild-type, DMD: *DMD* knockout

3.2.4 Clinical analysis

Serum CK levels from the examined *DMD* knockout piglets were grossly increased compared to age matched wild-type controls, serum CK levels being an indicator for pathological events of the musculature. Values of wild-type controls ranged from 111-401 U/l with a mean value of 209 U/l. The values of the DMD piglets were generally increased: #1263 had 1649 U/l and #1264 2117 U/l. #1249 and #1251 had the highest values with 324324 U/l and 186984 U/l respectively.

Piglets #1249 and #1251 from the first litter descending from clone #239 showed a severe phenotype congenitally. They had a highly impaired movement, not being able to move and feed on their own. When put to the sow's teats they tried to suckle even lying on their side. They were euthanized shortly after birth. Piglets #1250 and #1252 were able to move independently and feed on their own. They died within 24 h after birth, probably being crushed by their mother due to a decreased movement capability.

Piglets #1261-1264, based upon cell clone #290, were delivered by cesarean because of a birth canal obstruction. #1261 and #1262 died during birth. #1261 displayed a macroglossia, which can be attributed to clonal side effects. The remaining two piglets were raised in an artificial feeding system (Figure IV.19A). For the first few days their condition was impaired due to the anesthesia administered to the sow for the

cesarean. Afterwards they were able to move and feed on their own, however, their movement ability was impaired compared to age matched controls. After two weeks #1264 died due to diarrhea and pneumonia. #1263 was also affected by the disease, but survived after a treatment with spectinomycin. From birth onwards it showed growth retardation. Pig #1263 was measured twice a week from week six after birth to week eleven after birth (Table IV.5). Weighing was stopped in order to reduce the stress due to handling the DMD pig #1263 was exposed to, as an involvement of the heart muscle was assumed.

Table IV.5 Weight comparison of wild-type pigs and DMD pig #1263

weeks after birth	Wild-type piglets (kg)	#1263 at beginning/ end of the week (kg)
6	10.0-12.8	-/7.4
7	12.8-16.0	7.3/8.5
8	16.0-19.5	9.5/10.5
9	19.5-23.4	9.1/9.5
10	23.4-27.6	11.9/12.6
11		11.9/-

From: (KAMPHUS et al., 2004)

The pig developed a progressive enlargement of the tongue and skeletal muscles, which was apparent from the age of approximately four weeks onwards (Figure IV.19B). With increasing age breathing, feeding and moving became progressively worse. #1263 died with the age of three months, because of an obstruction of the airways by the profound circumferential growth of the adjacent tissue. In the pathological examination the profound enlargement of the tongue and skeletal muscles and additionally of the laryngeal and pharyngeal muscles was confirmed.

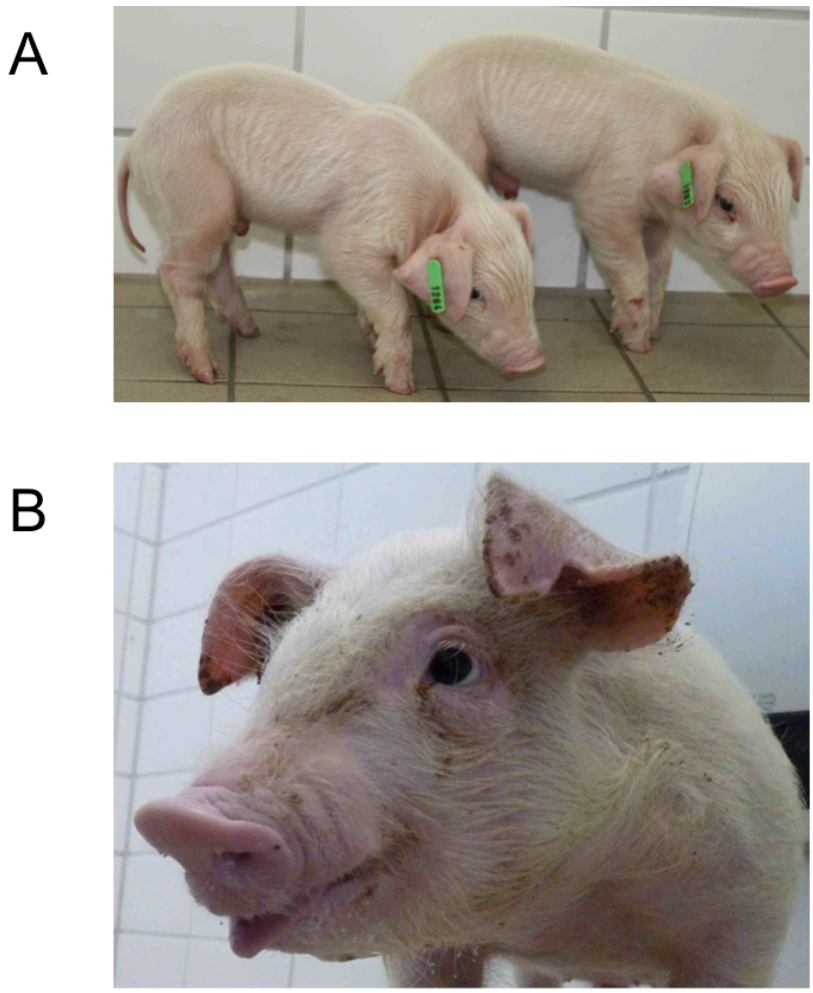

Figure IV.19 *DMD* knockout piglets #1263 and #1264

(A) *DMD* knockout piglets #1263 and #1264 10 days after birth; kindly provided by Prof. Dr. Maggie Walter; **(B)** #1263 displaying a protruding tongue with the age of eight weeks.

#1300 and #1301, descending from cell clone #168, were able to move and feed on their own after birth, although #1300 had a congenital malformation of the spinal column. #1300 died within 24 h hours after birth, death was probably caused by the congenital malformation. #1301 died within one week. Pathological examination showed enteritis and a persistent ductus arteriosus, which can be ascribed to the young age of the piglet.

Locomotion analysis was performed with #1263 and two wild-type controls. As a consequence of the growth retardation, two weight matched piglets were used as wild-type controls. At the time of the experiments, the *DMD* knockout pig was nine weeks old and weighted 12 kg. The control animals were four weeks old and weighted 11 kg.

The wild-type controls showed a typical walking gait with a four-beat rhythm, setting

the claw of the hind leg almost exactly at the same place where the front claw has been set. #1263 showed an irregular rhythm and short strides particularly of the hind legs. Trotting the wild-type pigs showed a diagonal two-beat rhythm with wide strides. Compared to an irregular trot with short strides of the *DMD* knockout pig. Running the control pigs exhibited a typical fast four-beat gallop, whereas #1263 showed a gallop with short strides, which had a hopping appearance of the hind legs. The overall movement seemed stiff and rigid compared to the wild-type controls. After several times passing the run the DMD piglet was fatigued and unwilling to carry on.

Additionally the ability to climb a step was tested. The wild-type controls jumped onto the 25 cm step repeatedly, the *DMD* knockout pig was not able to climb the step once, as illustrated in Figure IV.20.

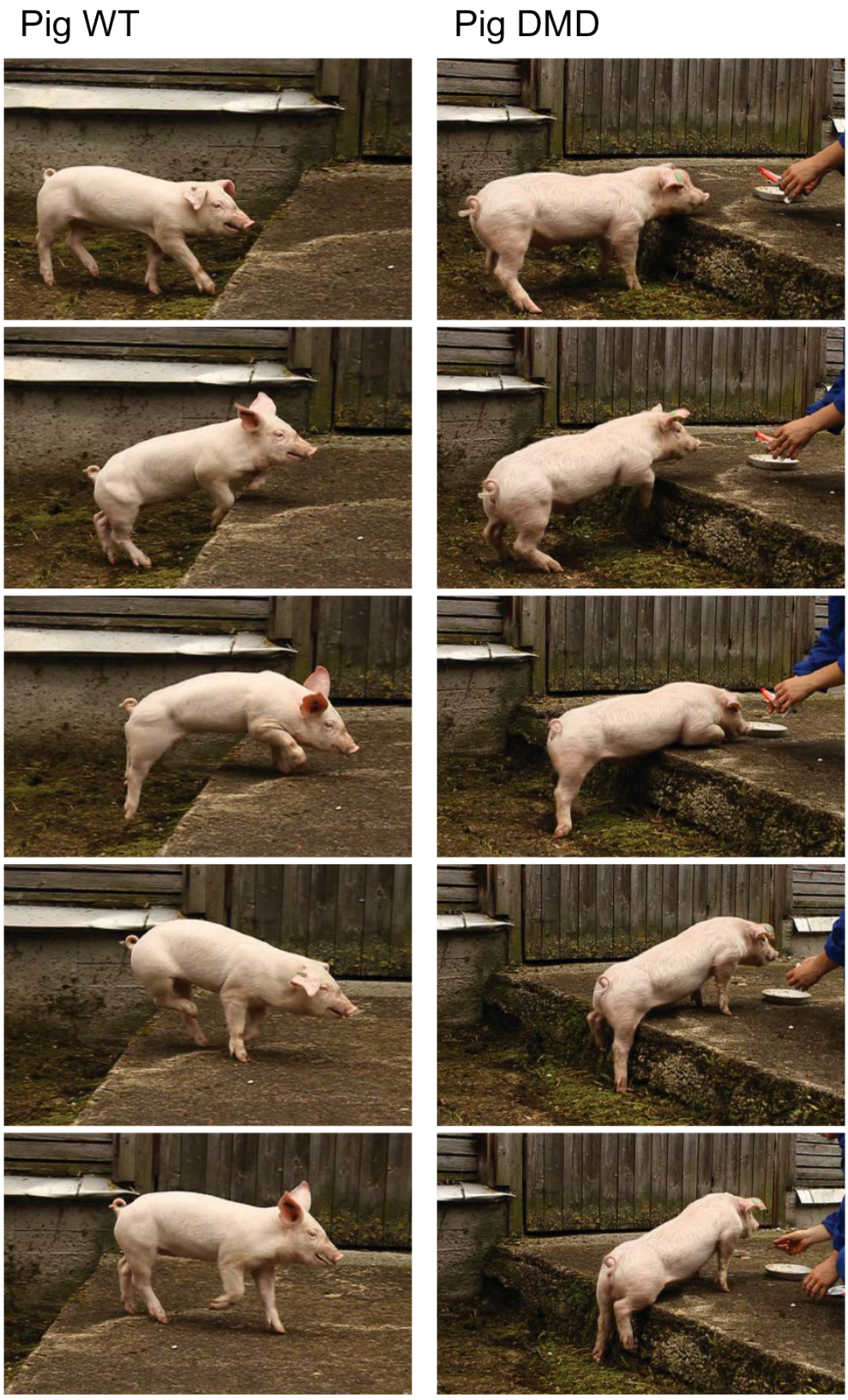

Figure IV.20 Comparison of the ability to climb a 25 cm

The ability of the *DMD* knockout pig to climb a 25 cm step was compared to a weight matched wild-type control animal; the wild-type control jumped the step repeatedly, whereas the *DMD* knockout pig failed to climb the step even once; WT: wild-type.

In conclusion led the replacement of exon 52 of the *DMD* gene with an antibiotic resistance cassette by homologous recombination to a frame-shift of the transcribed RNA and subsequently to a loss of function of the protein dystrophin. The delivered piglets had a histological phenotype, which corresponds to the human situation and showed signs of muscular weakness combined with a progressive enlargement of the skeletal, pharyngeal, laryngeal and tongue muscles.

V. DISCUSSION

DMD is a severe muscular wasting disease, resulting in the premature death of the affected persons (BLAKE et al., 2002). Beside management of symptoms and a treatment with glucocorticoids, which leads to a delay in the progression of the disease and a slight amelioration of the symptoms, there is no effective treatment available up to date (MANZUR et al., 2008). Animal models play a major role in the establishment of new treatments in clinical application (AIGNER et al., 2010), but as in the case of DMD, the existing animal models have different limitations in regard to the requirements set on an adequate animal model for DMD (WILLMANN et al., 2009). Pigs have been proven to be appropriate animal models for various applications in the field of biomedical research (AIGNER et al., 2010). Therefore, the aim of this work was to generate a tailored DMD pig model for advancement in therapeutical approaches and further investigation of the only partially understood pathomechanisms involved in the disease (DECONINCK & DAN, 2007).

For the establishment of a DMD pig model, it was decided to delete exon 52. Several aspects were to be considered while designing an appropriate genetic modification, as it was necessary to cause a loss of function of the protein dystrophin, corresponding to the human situation (WILLMANN et al., 2009). DMD is caused by a great variety of mutations in the *DMD* gene, therefore a mutation with a high frequency in affected persons was chosen. 60 - 72% of the mutations are deletions of one or more exons (MUNTONI et al., 2003; AARTSMA-RUS et al., 2006), located in two mutational hot spots, a minor hot spot between exons 2 and 20 and a major hot spot spanning from exons 47 to 53 (KOENIG et al., 1987; DEN DUNNEN et al., 1989). Exon 52 is one of the more frequently deleted exons, leading to a frame shift of the transcribed RNA and thus to a loss of function of dystrophin. The aim of the intended application of the pig model in therapeutical research had to be considered as well, when selecting an appropriate mutation. Generally, the severe DMD phenotype is caused by the complete loss of dystrophin's function, either due to a truncated non-functional protein or to a frame shift of the transcribed RNA, leading to a non-sense mediated decay of the RNA (KERR et al., 2001; MAQUAT, 2004). Whereas BMD patients have a mutation, which does not affect the reading frame and the produced dystrophin is shortened, but still more or less functional. One of the most promising therapeutical

approaches is the amelioration of the disease by transforming a DMD phenotype to a milder BMD phenotype through skipping a further exon (exon skipping) and thus restoring the reading frame (AARTSMA-RUS et al., 2009). It would therefore be advantageous if the DMD pig model would carry a mutation, which could be treated with exon skipping. Deletion of exon 52 would be treatable by skipping exon 51 and 53, which constitutes a possible treatment for a variety of mutations and from which approximately 25% of human DMD patients would benefit. Furthermore, the treatment by skipping exon 51 is already in clinical stages and proof of concept has been demonstrated (VAN DEUTEKOM et al., 2007; KINALI et al., 2009; CIRAK et al., 2011; GOEMANS et al., 2011). However, the efficiency of exon skipping has to be optimized and questions, like the optimal timing of the respective treatment, the appropriate administration and dosage in dependence of the stage of the disease, still have to be solved (WOOD, 2010). Besides the three full-length isoforms, the knockout of exon 52 affects the shorter isoforms Dp260 and Dp140. Isoforms Dp116 and Dp71 are still expressed, as their promoters are situated behind the deleted exon. Dp116 is expressed in the peripheral nervous tissue and Dp71 ubiquitously throughout the organism (BLAKE et al., 2002), except for the skeletal muscle (LEDERFEIN et al., 1992; AHN & KUNKEL, 1993). These isoforms however, lack the NH_2 terminus, which is essential for the role of dystrophin at the muscular membrane and will therefore not affect the muscular phenotype (ERVASTI, 2007).

The desired mutation of the *DMD* gene, the deletion of exon 52, required a defined site directed mutagenesis, which was to be introduced by homologous recombination using a bacterial artificial chromosome (BAC) as targeting vector. Alternatively to targeting by extended homologous arms, efficient strategies include the designer nucleases technologies and gene targeting by AAV vectors. The ZFN technology has already been successfully used in pigs to introduce targeted mutations (HAUSCHILD et al., 2011; WHYTE et al., 2011) and the combination of ZFN and homologous recombination, providing a further possibility for the introduction of a tailored mutation, has been successfully applied in human cells and in mouse cells (URNOV et al., 2005; CONNELLY et al., 2010). However, the design of appropriate ZNF pairs for the respective sequence and the off target effects of the ZFNs might still constitute possible drawbacks of this technology (PORTEUS & CARROLL, 2005). The recently established TALENs provide a further promising tool for targeted modifications of the genome (CHRISTIAN et al., 2010), as they are said to be easy to design and have a

high nuclease activity combined with a reduce cytotoxicity (MUSSOLINO et al., 2011). AAV vectors have already been used for a successful targeting in the pig (ROGERS et al., 2008). Though the precise process is still unknown, the homologous recombination pathway of double strand repair is said to play a role (FATTAH et al., 2008). The small packing size of 5 kb (HIRATA & RUSSELL, 2000; VASILEVA et al., 2006) and the special requirements on the lab in order to work with AAV vectors (Gentechnikgesetz and Gentechniksicherheitsverordung) made their use inappropriate for this study.

The targeting by homologous recombination requires a targeting vector carrying the designed modification, in this case the deletion of exon 52 by replacement with a resistance cassette, as well as sequences upstream and downstream of the modification cassette, which are homologous to the target locus. It is said, that an increased length of homology leads to a higher targeting efficiency (DENG & CAPECCHI, 1992; SCHEERER & ADAIR). Therefore, BACs were considered as adequate targeting vectors, as they can contain genomic DNA fragments of up to 200 kb and even larger (SHIZUYA et al., 1992). BAC vectors have already been used for targeted mutagenesis in various mouse models (TESTA et al., 2003; VALENZUELA et al., 2003; YANG & SEED, 2003) and human embryonic stem cells (SONG et al., 2010), achieving targeting efficiencies of up to 28%. Exon 52 of the porcine *DMD* gene was to be exchanged by homologous recombination with an antibiotic resistance cassette driven by a strong ubiquitously expressed promoter, in order to distinguish between cells with stably integrated transgene and negative cells. For the targeting, a neomycin/kanamycin resistance cassette, flanked by loxP sites, which was under the control of a mPGK and T7 promoter and had a bGH polyadenylation site, was used. The neomycin/kanamycin resistance cassette is frequently used for selection (VAN DER WEYDEN et al., 2002) and is well established in our lab as well as the ubiquitously expressed mPGK promoter (CHEAH & BEHRINGER, 2001). In the case of expression alterations caused by the selection cassette in or around the target locus, the resistance cassette flanking loxP sites provide the possibility to remove the disturbing fragment (FIERING et al., 1995; PHAM et al., 1996). The Cre recombinase is an efficient and reliable recombinase and also regularly used (SORRELL & KOLB, 2005). The positive selection strategy however, doesn't differentiate between random or site directed integration and a lot of clones have to be screened to find correctly targeted cell clone. Other selection strategies, like positive-negative selection (NAGY

et al., 2003) and gene trapping (SORRELL & KOLB, 2005), can be used to enrich correctly targeted cell clones. The frequently used positive-negative selection can generally achieve a 2-10 fold enrichment of correctly targeted cell clones. The overall efficiency of this method however, might be reduced due to damage of the negative selection cassette or the actual loss of it (SORRELL & KOLB, 2005). The application of this strategy in combination with BAC vectors is therefore unsuitable, as with an increasing length of the homologous arms the loss of the negative selection cassette becomes more likely. Equally, the quite efficient gene trapping approach by promoter trap (HANSON & SEDIVY, 1995) was considered unsuitable for the targeting of the *DMD* gene in primary kidney cells, as this method requires an active gene locus and it was not expected, that the *DMD* gene is generally expressed in kidney cells. Taking the expected high targeting efficiency, already achieved in other species' cells, and the aspects mentioned above into consideration, it was decided to solely use the positive selection strategy for the targeting of the porcine *DMD* gene with a BAC vector.

There are two different established phage based recombination protocols to introduce the desired modification into a BAC (ZHANG et al., 1998; COPELAND et al., 2001). BAC CH242-9G11 used for the targeting of the *DMD* gene was successfully modified by the protocol based on Copeland et al. 2001. The preassembled plasmid based modification vector, consisting of two homologous arms and the floxed resistance cassette, which was to be introduced by homologous recombination into the BAC vector, was examined by sequencing and several mutations, caused by PCR amplification, were found in the homologous arms. However, it seems that they did not inhibit the recombination process as 18.5% of the PCR screened colonies were correctly modified. During the recombination process in the SW106 cells unwanted rearrangements of the BAC vector might occur. Hence the modified BAC CH242-9G11 and the original CH242-9G11 were compared by restriction digest. Thereby the restriction pattern confirmed the integrity of the BACs, additionally expected minor changes of the restriction patterns proved the desired modifications of the BAC. These findings are in concordance with the statement, that BAC vectors are stable and convenient to handle (GIRALDO & MONTOLIU, 2001; LEE et al., 2001).

Sequence comparison of the overlapping 27 kb of two of the available BACs containing exon 52 (CH242-9G11 and CH242-27G20) revealed several major allelic differences. Besides a number of SNPs, a L1 Transposon and a microsatellite were found in closer proximity of the exon 52. The BACs represent only the genomic

characteristic of one individual, since they were generated from one Duroc sow. Examinations of the genotype with regard to the two features of several other pigs from different breeds confirmed a great distribution of the L1 Transposon and also a high variance of CA-repeats of the microsatellite throughout the breeds. It was shown that a high isogenicity of the sequences involved in the recombination process is beneficial in mouse ESCs (TE RIELE et al., 1992), although it may not be essential in all cell types (SEDIVY et al., 1999). Even so it has been shown that the BAC vectors generally overcome the need for isogenicity (VALENZUELA et al., 2003) the two major allelic differences were considered to impede the recombination process. Therefore, the genotype of the cell line used for the targeting experiments (Niere m) was examined for the L1 Transposon and the length of its microsatellite. Due to the concordance of BAC CH242-9G11 and Niere m in the two major allelic differences, CH242-9G11 was chosen as targeting vector, although it may still differ from Niere m in some SNPs, which have not been examined further. However, the targeting efficiency of 2.1% achieved in this study with a BAC differing in several SNPs from the targeting sequence confirms the assumption that BAC vectors reduce the need of isogenicity. It also mirrors the high targeting efficiencies of BACs already achieved in previous studies (VALENZUELA et al., 2003; YANG & SEED, 2003). In contrast to generally low number of targeting events, especially in somatic cells (DOETSCHMAN et al., 1987; SEDIVY & SHARP, 1989; HASTY et al., 1991; SEDIVY & DUTRIAUX, 1999) BACs provide a convenient tool for the targeted introduction of a defined mutation into the genome of porcine primary kidney cells, without additional enrichment strategies.

Five transfection experiments of the porcine primary kidney cell line Niere m with the linearized modified BAC vector were performed applying the nucleofection technology (HAMM et al., 2002), which is used routinely in our lab. All experiments were conducted with the same nucleofection program and the same nucleofection solution for primary mammalian fibroblasts. Reaction conditions however, varied in following parameters: cell confluence, DNA type, DNA volume, number of transfected cells, ratios of cells for co-seeding as well as time between nucleofection and selection start (see Table IV.1). A great variance of experimental conditions and a low number of experiments prohibited profound statistical analysis. However, the complete lack of any viable cell clone in experiment 100831B compared to the other four experiments may be ascribed to the DNA isolation method, as the endotoxins

were not removed from the DNA in this experiment. Overall 8 of 381 eventually evaluated cell clones were correctly targeted in the five nucleofection experiments: five cell clones in experiment 100203, two in experiment 100912 and one in experiment 100413. The diverging results obtained in these experiments for nucleofection can also be seen in several studies conducted to investigate the targeting efficiency and cell cytotoxicity by different transfection methods (JACOBSEN et al., 2006; SKRZYSZOWSKA et al., 2008; CAO et al., 2010; MAURISSE et al., 2010; MO et al., 2010). Resulting cell clones were screened by the qPCR based "loss-of-native-allele" assay (VALENZUELA et al., 2003; YANG & SEED, 2003), which provided a reliable tool to distinguish between clones undergone random integration of the targeting vector and correctly targeted cell clones. All copy number ratios of correctly targeted cell clones were far below the threshold set at 0.1 and the overall ratio values were quite stably at around 1 (see Table IV.2 and Table IV.3).

Three correctly targeted cell clones were used in SCNT and ET. Overall ten SCNTs and ETs were conducted, resulting in five pregnancies. Two pregnancies were lost in the first and the second half of the gestation period respectively. The pregnancy rate (50%) and delivery rate (70%) lie in the range observed in our lab (Dr. Mayuko Kurome, personal communication). Mirroring the general observed nuclear transfer efficiency (CAMPBELL et al., 2005; VAJTA et al., 2007). Ten piglets were delivered from the remaining three pregnancies. In addition with the other litters obtained from nuclear transfer of the cell line Niere m, with site directed modifications introduced by BAC vectors (unpublished data from our lab), this confirms the suitability of this targeting strategy for SCNT.

The knockout of exon 52 of the *DMD* gene in the delivered piglets was verified on the genomic level by the qPCR based "loss-of-native-allele" assay as well as by endpoint PCR. Furthermore, the transcriptome was analyzed for the resulting RNA transcripts. In wild-type controls all junctions between exons 50 to 54 respectively could be detected. In the *DMD* knockout piglets junctions between exons 50 and 51 as well as 53 and 54 were detected, but no sequence of exon 52. However, transcripts with an exon junction between 51 and 53 were identified. The knockout of exon 52 therefore leads to a transcript with a +1 frame shift and thus resulting in several stop codons in exon 53 and 54 positioned to render the transcript target for nonsense mediated RNA decay (MAQUAT, 2004) as observed in human DMD patients (KERR et al., 2001). In immunoblot analysis and immunofluorescence staining of muscle fiber cross sections

no dystrophin was detectable with the antibodies against the rod domain and the COOH terminal, except for isolated revertant fibers, confirming the general loss of the functional product of the DMD locus at the muscle membrane. The antibody against the rod domain should detect any truncated dystrophin. As no truncated dystrophin is seen, the transcript may be target of nonsense mediated RNA decay. The shorter isoforms Dp166 and Dp71 are generally not expressed in the skeletal muscle and were not detectable (BLAKE et al., 2002; LEDERFEIN et al., 1992; AHN & KUNKEL, 1993).

The histological analysis of *DMD* knockout piglets showed the typical hallmarks of the human dystrophic muscle, like fibers with centrally located nuclei, a rounded shape, basophilic fibers and varying fiber diameters with a high proportion of fibers with a small diameter. Necrotic fibers, as well as fibrosis, fatty replacement and infiltrations of cells of the immune system were also identified (BELL & CONEN, 1968; MCDOUALL et al., 1990; BLAKE et al., 2002). Additionally focal calcifications could be detected, which is also found in HFMD cats (GASCHEN & BURGUNDER, 2001). Initial measurements of the volume density of muscle fibers in the muscle of *DMD* knockout piglets compared to wild-type controls showed no significant difference. In combination with the increased proportion of smaller diameters of fiber cross sections determined by the measurement of the minimal Feret's diameter may indicate an increased number of muscle fibers. However, further histological examinations have to be conducted in order draw any validated conclusions.

Elevated serum CK values could be observed in all samples taken from *DMD* knockout piglets, compared to wild-type controls. Generally increased serum CK values are related with pathological processes of muscles in the pig (PLONAIT & BICKHARDT, 1988). They can also be mildly increased after exercise, yet the age matched control animals were treated and handled in the same way, thus suggesting a pathological origin. It has to be kept in mind, that the malign hyperthermia syndrome in the pig can cause elevated serum CK levels as well, but the piglets didn't show any sign of this disease (SWINDLE, 2007). Therefore, the elevated serum CK levels seem to be caused by the pathological processes in the muscles of the *DMD* knockout piglets, comparable to the generally highly increased levels (5000-150000 U/l) of human DMD patients (VERMA et al., 2010). Piglets #1249 and #1251 had grossly elevated levels, even compared to piglets #1263 and #1264. The great differences

between the individual piglets might correlate to the severe phenotype displayed by #1249 and #1251. For a profound analysis of the correlation of the serum CK levels and the phenotype, blood samples from DMD piglets as well as age matched wild-type controls should be obtained at regular intervals. It should also be considered to determine the DMD pigs' genotype concerning the malign hyperthermia syndrome, as one hypothesis for the pathophysiology of DMD is based on a disturbed calcium homeostasis by an increased influx through mechanosensitive voltage independent channels (DECONINCK & DAN, 2007) and the malign hyperthermia syndrome in pigs, caused by a mutation in the gene for the ryanodine receptor, is involved in calcium homeostasis in muscle cells as well (FUJII et al., 1991).

All life born DMD piglets showed impaired movement ability from birth onwards with differing severity. Piglets #1249 and #1251 from the first litter were not able to move and feed on their own. Their siblings (#1250 and #1252), on the other hand, moved and fed independently, although they were probably both crushed by the sow due to a decreased speed of movements. Piglets #1263 and #1264 from the second litter were highly affected for the first few days by the anesthesia applied to the sow for the caesarean. Therefore, they could only be evaluated after a week's time. They were then able to move and feed on their own, however, reduced movement ability, like an unsteady gait, was apparent. Piglet's #1301 phenotype equaled #1250 and #1252 from the first litter. It was not possible to evaluate #1300 as it had a spinal malformation, which may cause gait disturbances and movement's impairment. The malformation might be ascribed to the SCNT (PRATHER et al., 2004). Overall the DMD piglets showed a varying phenotype in young age. Only #1263 survived to an age of three months. Locomotion studies carried out with the nine-weeks-old DMD piglet showed an aberration of all gaits examined in comparison to weight matched controls. Characteristic for all gaits was a shortening of the strides and an irregularity of rhythm. The bunny hopping displayed by the DMD pig whilst galloping is also described in cats affected with HFMD (SHELTON & ENGVALL, 2005). In combination with the inability to climb a 25 cm step, the locomotion studies demonstrated a profound muscle weakness of the *DMD* knockout pig resembling the human situation (BLAKE et al., 2002), especially as the pig was not able to carry on after passing through the run several times. With increasing age #1263 showed an enlargement of all skeletal muscles. In order to distinguish between pseudo-hypertrophy, hypertrophy or hyperplasia of the muscles further histo-pathological

examinations have to be carried out, including quantitative stereological and morphometric analysis. However, an increase of fatty and fibrous tissue was notable in initial histological examinations. It has to be kept in mind that the enlarged tongue might be due to clonal procedure, as piglet #1261 had also an enlarged tongue and macroglossia is frequently described in clonal offspring (PRATHER et al., 2004). It is known that human DMD patients can develop a pseudo-hypertrophy of various skeletal muscles (EMERY, 1993), even cases exist with macroglossia (WEISS et al., 2007; MALHOTRA et al., 2011). Furthermore, is the phenotype of the cats affected with HFMD described with a characteristic enlargement of the muscles, particularly of the tongue muscles. The enlarged tongue has also been regularly seen in the GRMD dog (SHELTON & ENGVALL, 2005). Muscle hypertrophy is also apparent in the *mdx* mouse (DURBEEJ & CAMPBELL, 2002). However, as only one DMD pig reached the age of three months it is necessary to evaluate more pigs, in order to confirm these findings.

Additionally in piglet #1263 growth retardation was observed. This might have been caused by several reasons. First of all the piglets of the second (#1261-1264) and third (#1300-1301) litter were raised with an artificial feeding system, after piglets #1250 and #1252 of the first litter were presumably crushed by the sow. They were fed milk powder for piglets solved in warm water. It is unsure if the artificial feeding system represents an appropriate replacement for the sow as they completely lack the supply of stable specific maternal antibodies by the sow's milk, although piglets were fed with colostrum after birth. Diarrhea was often observed in the DMD piglets, which may have been caused by the milk powder or by impaired immune mechanisms. However, we did not raise any piglets in our lab in this manner at that time, therefore there were no wild-type piglets the DMD piglets could be compared to. It has to be kept in mind that the *DMD* knockout piglets can have an impaired movement and be therefore more prone to be crushed by the sow. In order to minimize the losses of piglets due to diarrhea and other diseases or due to the sow, the rearing system has to be evaluated and optimized.

The SCNT procedure has been described to give rise to epigenetic alterations involving changes in DNA methylation and histone modifications (ZHAO et al., 2010), which in this case might lead to altered gene expression levels between the single cell clones as well as individual cells and thus cause the different phenotypes observed in the newborn DMD piglets. Expression levels of genes involved in the

regenerating capacity and the up regulation of utrophin, functionally replacing dystrophin, are said to be responsible for the mild phenotype in the *mdx* mice (DURBEEJ & CAMPBELL, 2002). Furthermore, phenotype variations in several human DMD patients are ascribed to a different expression of genes influencing the alternative splicing process, causing the expression of a truncated dystrophin in some muscle fibers (revertant fibers) by the restoration of the reading frame (MUNTONI et al., 2003). Isolated revertant fibers were identified in the immunohistochemistry of the skeletal muscle of DMD piglets. In the long term the production of DMD pigs is to be achieved by establishing a breeding line. Phenotype variations in the cloned offspring might not be apparent in piglets obtained by breeding. The persistence of differences in the phenotype would constitute a limitation to the application of the DMD pig in the establishment of new treatment strategies, as the variable phenotypes impair the comparability of the experiments (WILLMANN et al., 2009). They could however, be advantageous for the investigation of mechanisms involved in the disease pathogenesis and for studying compensatory processes. A thorough characterization of the muscle pathology caused by DMD in the pig and the comparison of expression profiles between the individual DMD pigs, might lead to the new insights and improvement of the current knowledge of the muscular dystrophy.

The reduced life span however, caused by the obstruction of the airways by the enlarged muscles of tongue and larynx, observed in #1263, might constitute a hindrance for the generation of DMD pigs, as the production of DMD pigs from backup portions of correctly targeted cell clones is limited, and the recloning efficiency is reported to be very low (unpublished data from our lab). An increased life span to at least sexual maturity (> 6 months) would facilitate breeding of the DMD pigs, even if the muscle dystrophy would lead to infertility. The possibility of the collection of sperm for intratubal insemination provides an alternative method (VAZQUEZ et al., 2008). In the case that further DMD pigs also display a muscle enlargement and therefore do not reach sexual maturity, it can be taken under consideration to surgically remove the obstructions. Surgical procedures in the larynx are already established in the pig (MURISON et al., 2009). Furthermore, a female cell line could be used for targeting experiments to produce DMD sows for breeding, as females do very rarely display a severe DMD phenotype (EMERY, 1991).

Treatment strategies like gene replacement and exon skipping can be examined with the DMD piglets devoid of exon 52 (GOYENVALLE et al., 2011; PICHAVANT et

al., 2011). Especially the treatment by skipping of exon 51, which has already been tested with positive results in clinic trials (VAN DEUTEKOM et al., 2007; KINALI et al., 2009; CIRAK et al., 2011; GOEMANS et al., 2011), can be improved further. Certain aspects like the overall distribution and exon skipping efficiency have to be optimized (WOOD, 2010). The DMD pig offers the possibility to assess the efficiency of a certain treatment, the (side-) effects it causes throughout the organism, also in respect of long-term treatment. It could be utilize to solve questions like the optimal timing of the respective treatment, the appropriate administration and dosage in dependence of the stage of the disease.

Overall the DMD pigs display several aspects, which do comply with the requirements set for an ideal DMD animal model (WILLMANN et al., 2009). Their genetic modification is a mutation, frequently found in human DMD patients. It results in the complete loss of any functional protein dystrophin and thereby leads to a phenotype, which resembles the human situation. The establishment of a DMD breeding line and thorough characterization of the *DMD* knockout pigs, would render the porcine DMD animal model with the knockout of exon 52 an attractive possibility to evaluate, refine and advance therapeutical approaches for DMD treatment, as well as study pathological mechanisms

VI. SUMMARY

Generation of a tailored pig model of Duchenne muscular dystrophy

Duchenne muscular dystrophy (DMD), one of the most frequent heritable lethal muscular diseases, is characterized by a progressive muscle weakness leading to the premature death of affected persons. The disease is caused by a variety of mutations in the *DMD* gene, resulting in a loss of function of the protein dystrophin and subsequently in muscle degeneration. Up to date, no effective treatment is available, however, several promising therapeutical approaches are under investigation. Animal models are needed to develop, evaluate, refine and improve effective therapies for DMD. Existing animal models however, are of limited relevance. As the pig has proven to be an adequate animal model for various human diseases, it was decided to generate a tailored porcine DMD animal model.

Aim of this thesis was the production of a porcine DMD animal model, by introducing a defined mutation into the porcine *DMD* gene, which leads to a loss of function of the protein dystrophin. In order to provide an animal model with a mutation, which represents a great proportion of human DMD patients and is also target of several treatment approaches, exon 52 was to be deleted. Exon 52 was replaced by homologous recombination with an antibiotic resistance cassette using a bacterial artificial chromosome (BAC) as targeting vector. The desired mutation was introduced into the BAC by recombineering. DNA from the linearized modified BAC was transfected into primary porcine kidney cells by nucleofection. Obtained single cell clones were screened by the qPCR based “loss-of-homozygozity” assay, resulting in a targeting efficiency of 2.1%. Correctly targeted cell clones were used for nuclear transfer and subsequent transfer of cloned embryos into recipient gilts. Ten nuclear transfers were carried out resulting in three pregnancies delivered to term, each pregnancy originating from a different cell clone. Altogether ten piglets were born. Two were still born; seven were euthanized or died within two weeks, and one DMD piglet survived until the age of three months. With increasing age it developed a progressive enlargement of the skeletal muscles, also the tongue muscles and, as shown in the pathological examination, of the pharyngeal as well as laryngeal muscles. The knockout of exon 52 of the DMD piglets was verified on the genomic and transcriptomic level. Immunoblot and immunohistochemistry analysis showed the

loss of the dystrophin protein in the skeletal muscle, confirming the desired loss of function. Histological analysis of the skeletal muscles of the DMD piglets showed similar signs of degeneration and regeneration, as can be observed in human DMD patients. Furthermore, the measured serum creatine kinase values of DMD piglets were grossly increased compared to age matched controls. Locomotion studies were performed with the nine-weeks-old DMD piglet and weight matched controls. Alteration of gait patterns, impairment of movement capability and a striking muscle weakness could be observed. These findings render the tailored DMD pig a promising model to gain new insights in the DMD research.

VII. ZUSAMMENFASSUNG

Generierung eines Schweinemodells für die Duchenne Muskeldystrophie

Die Duchenne Muskeldystrophie (DMD) ist eine der häufigsten muskulären, letal verlaufenden Erbkrankheiten. Der Krankheitsverlauf ist geprägt durch eine progressive Muskelschwäche, die schließlich zum Tode des Patienten führt. Die Krankheit wird durch verschiedene Mutationen im *DMD* Gen verursacht, die letztendlich zu einem Funktionsverlust des Proteins Dystrophin führen, und nachfolgend den Untergang von Muskelfasern bedingen. Bis zum heutigen Tag gibt es keine effektiven Behandlungen; es existieren jedoch einige vielversprechende Therapieansätze.

Mittels der bereits existierenden Tiermodelle konnten Einblicke in die Pathophysiologie von DMD gewonnen werden, allerdings ist ihr Nutzen in der klinischen Forschung auf Grund von geno- bzw. phänotypischen Abweichungen zur Situation beim Menschen limitiert. Das Schwein hat sich in vielerlei Hinsicht als ein adäquates Tiermodell für eine Reihe von verschieden humanen Erkrankungen erwiesen.

Deshalb war es Ziel dieser Arbeit, ein Schweinemodell zu entwickeln, das, ähnlich wie beim Menschen, einen Funktionsverlust des Proteins Dystrophins, verursacht durch eine definierte Mutation im *DMD* Gen, aufweist. Um das Schweinemodell mit einer Mutation auszustatten, die einen großen Anteil der humanen DMD Patienten repräsentiert und zusätzlich noch Ziel mehrerer Therapieansätze ist, wurde beschlossen, eine Deletion des Exons 52 einzuführen. Das Exon 52 sollte durch homologe Rekombination mit einem bakteriellen artifiziellen Chromosom (BAC) als Targetingvektor durch eine Antibiotikaresistenzkassette ausgetauscht werden. Die gewünschte Mutation wurde mittels „Recombineering“ in den BAC eingefügt. DNA des linearisierten, modifizierten BACs wurde mittels Nukleofektion in primäre porcine Nierenzellen transfiziert. Gewonnen Einzelzellklone wurden anhand des „Verlust-des-nativen-Allels“ Assays basierend auf einer qPCR überprüft; die ermittelte Targetingeffizienz betrug 2.1%. Positive, geeignete Zellklone wurden anschließend im Kerntransfer eingesetzt und die gewonnen Embryonen auf Sauen übertragen, woraus insgesamt drei Würfe mit zusammen zehn Ferkeln resultierten. Jeder Wurf basiert auf einem andern Zellklon. Zwei der zehn Ferkel waren

Totgeburten, sieben wurden euthanasiert oder starben innerhalb der ersten zwei Wochen. Nur ein Schwein überlebte bis zu einem Alter von drei Monaten. Mit zunehmendem Alter konnte man bei diesem Schwein Umfangsvermehrungen der Skelettmuskulatur, der Zunge sowie der Pharynx-, als auch Larynxmuskulatur beobachten. Der Knockout des Exons 52 in den DMD Ferkeln wurde auf DNA- und RNA-Ebene durch verschiedene Methoden nachgewiesen. Im Immunoblot und in immunhistochemischen Untersuchungen konnte kein Dystrophin nachgewiesen werden. Die histologischen Untersuchungen von Skelettmuskeln der DMD Ferkel zeigten Symptome der Degeneration und Regenration, wie sie typischerweise im Muskel humaner DMD Patienten vorkommen. Klinisch konnten erhöhte Serum-Kreatinkinase-Werte gemessen werden. Vergleichende Bewegungsanalysen ergaben Unterschiede in den einzelnen Gangarten, wie auch eine Verminderung der Bewegungsfähigkeit und eine gravierende Muskelschwäche. Diese Resultate machen das DMD Schwein zu einem vielversprechenden Tiermodell um neue Einblicke in die DMD Forschung zu gewinnen.

VIII. REFERENCE LIST

Aartsma-Rus A, Van Deutekom JC, Fokkema IF, Van Ommen GJ, Den Dunnen JT. Entries in the Leiden Duchenne muscular dystrophy mutation database: an overview of mutation types and paradoxical cases that confirm the reading-frame rule. Muscle & nerve 2006; 34: 135-44.

Aartsma-Rus A, Fokkema I, Verschuuren J, Ginjaar I, van Deutekom J, van Ommen GJ, den Dunnen JT. Theoretic applicability of antisense-mediated exon skipping for Duchenne muscular dystrophy mutations. Human mutation 2009; 30: 293-9.

Ahn AH, Kunkel LM. The structural and functional diversity of dystrophin. Nature genetics 1993; 3: 283-91.

Aigner B, Renner S, Kessler B, Klymiuk N, Kurome M, Wunsch A, Wolf E. Transgenic pigs as models for translational biomedical research. Journal of molecular medicine 2010; 88: 653-64.

Amantana A, Moulton HM, Cate ML, Reddy MT, Whitehead T, Hassinger JN, Youngblood DS, Iversen PL. Pharmacokinetics, biodistribution, stability and toxicity of a cell-penetrating peptide-morpholino oligomer conjugate. Bioconjugate chemistry 2007; 18: 1325-31.

Ambrosio CE, Fadel L, Gaiad TP, Martins DS, Araujo KP, Zucconi E, Brolio MP, Giglio RF, Morini AC, Jazedje T, Froes TR, Feitosa ML, Valadares MC, Beltrao-Braga PC, Meirelles FV, Miglino MA. Identification of three distinguishable phenotypes in golden retriever muscular dystrophy. Genetics and molecular research : GMR 2009; 8: 389-96.

Aoki Y, Nakamura A, Yokota T, Saito T, Okazawa H, Nagata T, Takeda S. In-frame dystrophin following exon 51-skipping improves muscle pathology and function in the exon 52-deficient mdx mouse. Molecular therapy : the journal of the American Society of Gene Therapy 2010; 18: 1995-2005.

Araki E, Nakamura K, Nakao K, Kameya S, Kobayashi O, Nonaka I, Kobayashi T, Katsuki M. Targeted disruption of exon 52 in the mouse dystrophin gene induced muscle degeneration similar to that observed in Duchenne muscular dystrophy. Biochemical and biophysical research communications 1997; 238: 492-7.

Arikawa-Hirasawa E, Koga R, Tsukahara T, Nonaka I, Mitsudome A, Goto K, Beggs AH, Arahata K. A severe muscular dystrophy patient with an internally deleted very short (110 kD) dystrophin: presence of the binding site for dystrophin-associated glycoprotein (DAG) may not be enough for physiological function of dystrophin. Neuromuscular disorders : NMD 1995; 5: 429-38.

Austin RC, Howard PL, D'Souza VN, Klamut HJ, Ray PN. Cloning and characterization of alternatively spliced isoforms of Dp71. Human molecular genetics 1995; 4: 1475-83.

Bartlett RJ, Stockinger S, Denis MM, Bartlett WT, Inverardi L, Le TT, thi Man N, Morris GE, Bogan DJ, Metcalf-Bogan J, Kornegay JN. In vivo targeted repair of a point mutation in the canine dystrophin gene by a chimeric RNA/DNA oligonucleotide. Nature biotechnology 2000; 18: 615-22.

Beard BC, Keyser KA, Trobridge GD, Peterson LJ, Miller DG, Jacobs M, Kaul R, Kiem HP. Unique integration profiles in a canine model of long-term repopulating cells transduced with gammaretrovirus, lentivirus, or foamy virus. Human gene therapy 2007; 18: 423-34.

Beggs AH, Koenig M, Boyce FM, Kunkel LM. Detection of 98% of DMD/BMD gene deletions by polymerase chain reaction. Human genetics 1990; 86: 45-8.

Beggs AH, Hoffman EP, Snyder JR, Arahata K, Specht L, Shapiro F, Angelini C, Sugita H, Kunkel LM. Exploring the molecular basis for variability among patients with Becker muscular dystrophy: dystrophin gene and protein studies. American journal of human genetics 1991; 49: 54-67.

Bell CD, Conen PE. Histopathological changes in Duchenne muscular dystrophy. Journal of the neurological sciences 1968; 7: 529-44.

Besenfelder U, Modl J, Muller M, Brem G. Endoscopic embryo collection and embryo transfer into the oviduct and the uterus of pigs. Theriogenology 1997; 47: 1051-60.

Bessou C, Giugia JB, Franks CJ, Holden-Dye L, Segalat L. Mutations in the Caenorhabditis elegans dystrophin-like gene dys-1 lead to hyperactivity and suggest a link with cholinergic transmission. Neurogenetics 1998; 2: 61-72.

Betthauser J, Forsberg E, Augenstein M, Childs L, Eilertsen K, Enos J, Forsythe T, Golueke P, Jurgella G, Koppang R, Lesmeister T, Mallon K, Mell G, Misica P, Pace M, Pfister-Genskow M, Strelchenko N, Voelker G, Watt S, Thompson S, Bishop M. Production of cloned pigs from in vitro systems. Nature biotechnology 2000; 18: 1055-9.

Bies RD, Caskey CT, Fenwick R. An intact cysteine-rich domain is required for dystrophin function. The Journal of clinical investigation 1992; 90: 666-72.

Bish LT, Morine K, Sleeper MM, Sanmiguel J, Wu D, Gao G, Wilson JM, Sweeney HL. Adeno-associated virus (AAV) serotype 9 provides global cardiac gene transfer superior to AAV1, AAV6, AAV7, and AAV8 in the mouse and rat. Human gene therapy 2008; 19: 1359-68.

Blake DJ, Tinsley JM, Davies KE, Knight AE, Winder SJ, Kendrick-Jones J. Coiled-coil regions in the carboxy-terminal domains of dystrophin and related proteins: potentials for protein-protein interactions. Trends in biochemical sciences 1995; 20: 133-5.

Blake DJ, Weir A, Newey SE, Davies KE. Function and genetics of dystrophin and dystrophin-related proteins in muscle. Physiological reviews 2002; 82: 291-329.

Bork P, Sudol M. The WW domain: a signalling site in dystrophin? Trends in biochemical sciences 1994; 19: 531-3.

Bradley WG, Jones MZ, Mussini JM, Fawcett PR. Becker-type muscular dystrophy. Muscle & nerve 1978; 1: 111-32.

Briguet A, Courdier-Fruh I, Foster M, Meier T, Magyar JP. Histological parameters for the quantitative assessment of muscular dystrophy in the mdx-mouse. Neuromuscular disorders : NMD 2004; 14: 675-82.

Brunetti-Pierri N, Palmer DJ, Beaudet AL, Carey KD, Finegold M, Ng P. Acute toxicity after high-dose systemic injection of helper-dependent adenoviral vectors into nonhuman primates. Human gene therapy 2004; 15: 35-46.

Bulfield G, Siller WG, Wight PA, Moore KJ. X chromosome-linked muscular dystrophy (mdx) in the mouse. Proceedings of the National Academy of Sciences of the United States of America 1984; 81: 1189-92.

Byers TJ, Lidov HG, Kunkel LM. An alternative dystrophin transcript specific to peripheral nerve. Nature genetics 1993; 4: 77-81.

Campbell KH, Alberio R, Choi I, Fisher P, Kelly RD, Lee JH, Maalouf W. Cloning: eight years after Dolly. Reproduction in domestic animals = Zuchthygiene 2005; 40: 256-68.

Cao F, Xie X, Gollan T, Zhao L, Narsinh K, Lee RJ, Wu JC. Comparison of gene-transfer efficiency in human embryonic stem cells. Molecular imaging and biology : MIB : the official publication of the Academy of Molecular Imaging 2010; 12: 15-24.

Carpenter JL, Hoffman EP, Romanul FC, Kunkel LM, Rosales RK, Ma NS, Dasbach JJ, Rae JF, Moore FM, McAfee MB, et al. Feline muscular dystrophy with dystrophin deficiency. The American journal of pathology 1989; 135: 909-19.

Chandler KJ, Chandler RL, Broeckelmann EM, Hou Y, Southard-Smith EM, Mortlock DP. Relevance of BAC transgene copy number in mice: transgene copy number variation across multiple transgenic lines and correlations with transgene integrity and expression. Mammalian genome : official journal of the International Mammalian Genome Society 2007; 18: 693-708.

Chapman VM, Miller DR, Armstrong D, Caskey CT. Recovery of induced mutations for X chromosome-linked muscular dystrophy in mice. Proceedings of the National Academy of Sciences of the United States of America 1989; 86: 1292-6.

Cheah SS, Behringer RR. Contemporary gene targeting strategies for the novice. Molecular biotechnology 2001; 19: 297-304.

Chen K, Baxter T, Muir WM, Groenen MA, Schook LB. Genetic resources, genome mapping and evolutionary genomics of the pig (Sus scrofa). International journal of biological sciences 2007; 3: 153-65.

Choulika A, Perrin A, Dujon B, Nicolas JF. Induction of homologous recombination in mammalian chromosomes by using the I-SceI system of Saccharomyces cerevisiae. Molecular and cellular biology 1995; 15: 1968-73.

Christian M, Cermak T, Doyle EL, Schmidt C, Zhang F, Hummel A, Bogdanove AJ, Voytas DF. Targeting DNA double-strand breaks with TAL effector nucleases. Genetics 2010; 186: 757-61.

Cirak S, Arechavala-Gomeza V, Guglieri M, Feng L, Torelli S, Anthony K, Abbs S, Garralda ME, Bourke J, Wells DJ, Dickson G, Wood MJ, Wilton SD, Straub V, Kole R, Shrewsbury SB, Sewry C, Morgan JE, Bushby K, Muntoni F. Exon skipping and dystrophin restoration in patients with Duchenne muscular dystrophy after systemic phosphorodiamidate morpholino oligomer treatment: an open-label, phase 2, dose-escalation study. Lancet 2011; 378: 595-605.

Clarke MS, Khakee R, McNeil PL. Loss of cytoplasmic basic fibroblast growth factor

from physiologically wounded myofibers of normal and dystrophic muscle. Journal of cell science 1993; 106 (Pt 1): 121-33.

Collins CA, Morgan JE. Duchenne's muscular dystrophy: animal models used to investigate pathogenesis and develop therapeutic strategies. International journal of experimental pathology 2003; 84: 165-72.

Colosimo A, Goncz KK, Holmes AR, Kunzelmann K, Novelli G, Malone RW, Bennett MJ, Gruenert DC. Transfer and expression of foreign genes in mammalian cells. BioTechniques 2000; 29: 314-8, 20-2, 24 passim.

Connelly JP, Barker JC, Pruett-Miller S, Porteus MH. Gene correction by homologous recombination with zinc finger nucleases in primary cells from a mouse model of a generic recessive genetic disease. Molecular therapy : the journal of the American Society of Gene Therapy 2010; 18: 1103-10.

Cooper BJ, Winand NJ, Stedman H, Valentine BA, Hoffman EP, Kunkel LM, Scott MO, Fischbeck KH, Kornegay JN, Avery RJ, et al. The homologue of the Duchenne locus is defective in X-linked muscular dystrophy of dogs. Nature 1988; 334: 154-6.

Copeland NG, Jenkins NA, Court DL. Recombineering: a powerful new tool for mouse functional genomics. Nature reviews. Genetics 2001; 2: 769-79.

Cox GA, Phelps SF, Chapman VM, Chamberlain JS. New mdx mutation disrupts expression of muscle and nonmuscle isoforms of dystrophin. Nature genetics 1993; 4: 87-93.

D'Souza VN, Nguyen TM, Morris GE, Karges W, Pillers DA, Ray PN. A novel dystrophin isoform is required for normal retinal electrophysiology. Human molecular genetics 1995; 4: 837-42.

Deconinck N, Dan B. Pathophysiology of duchenne muscular dystrophy: current hypotheses. Pediatric neurology 2007; 36: 1-7.

Den Dunnen JT, Grootscholten PM, Bakker E, Blonden LA, Ginjaar HB, Wapenaar MC, van Paassen HM, van Broeckhoven C, Pearson PL, van Ommen GJ. Topography of the Duchenne muscular dystrophy (DMD) gene: FIGE and cDNA analysis of 194 cases reveals 115 deletions and 13 duplications. American journal of human genetics 1989; 45: 835-47.

Deng C, Capecchi MR. Reexamination of gene targeting frequency as a function of the extent of homology between the targeting vector and the target locus. Molecular and cellular biology 1992; 12: 3365-71.

Denning C, Burl S, Ainslie A, Bracken J, Dinnyes A, Fletcher J, King T, Ritchie M, Ritchie WA, Rollo M, de Sousa P, Travers A, Wilmut I, Clark AJ. Deletion of the alpha(1,3)galactosyl transferase (GGTA1) gene and the prion protein (PrP) gene in sheep. Nature biotechnology 2001; 19: 559-62.

Doetschman T, Gregg RG, Maeda N, Hooper ML, Melton DW, Thompson S, Smithies O. Targetted correction of a mutant HPRT gene in mouse embryonic stem cells. Nature 1987; 330: 576-8.

Donehower LA, Harvey M, Slagle BL, McArthur MJ, Montgomery CA, Jr., Butel JS, Bradley A. Mice deficient for p53 are developmentally normal but susceptible to spontaneous tumours. Nature 1992; 356: 215-21.

Duchenne G. Recherches sur la paralysie musculaire pseudohypertrophic ou paralysie myo-sclérosique. Archives Générales Médecine 1868; 11: 5-25, 179-209, 305-21, 421- 43, 552-88.

Durbeej M, Jung D, Hjalt T, Campbell KP, Ekblom P. Transient expression of Dp140, a product of the Duchenne muscular dystrophy locus, during kidney tubulogenesis. Developmental biology 1997; 181: 156-67.

Durbeej M, Campbell KP. Muscular dystrophies involving the dystrophin-glycoprotein complex: an overview of current mouse models. Current opinion in

genetics & development 2002; 12: 349-61.

Emery AE. Muscle histology and creatine kinase levels in the foetus in Duchenne muscular dystrophy. Nature 1977; 266: 472-3.

Emery AE, Burt D. Intracellular calcium and pathogenesis and antenatal diagnosis of Duchenne muscular dystrophy. British medical journal 1980; 280: 355-7.

Emery AE. Population frequencies of inherited neuromuscular diseases--a world survey. Neuromuscular disorders : NMD 1991; 1: 19-29.

Emery AE (1993) Duchenne Muscular Dystrophy 2nd edn. Oxford University Press Inc., New York

Ervasti JM. Dystrophin, its interactions with other proteins, and implications for muscular dystrophy. Biochimica et biophysica acta 2007; 1772: 108-17.

Fattah FJ, Lichter NF, Fattah KR, Oh S, Hendrickson EA. Ku70, an essential gene, modulates the frequency of rAAV-mediated gene targeting in human somatic cells. Proceedings of the National Academy of Sciences of the United States of America 2008; 105: 8703-8.

Feener CA, Koenig M, Kunkel LM. Alternative splicing of human dystrophin mRNA generates isoforms at the carboxy terminus. Nature 1989; 338: 509-11.

Felgner PL, Gadek TR, Holm M, Roman R, Chan HW, Wenz M, Northrop JP, Ringold GM, Danielsen M. Lipofection: a highly efficient, lipid-mediated DNA-transfection procedure. Proceedings of the National Academy of Sciences of the United States of America 1987; 84: 7413-7.

Ferlini A, Sewry C, Melis MA, Mateddu A, Muntoni F. X-linked dilated cardiomyopathy and the dystrophin gene. Neuromuscular disorders : NMD 1999; 9: 339-46.

Fiering S, Epner E, Robinson K, Zhuang Y, Telling A, Hu M, Martin DI, Enver T, Ley TJ, Groudine M. Targeted deletion of 5'HS2 of the murine beta-globin LCR reveals that it is not essential for proper regulation of the beta-globin locus. Genes & development 1995; 9: 2203-13.

Fletcher S, Honeyman K, Fall AM, Harding PL, Johnsen RD, Wilton SD. Dystrophin expression in the mdx mouse after localised and systemic administration of a morpholino antisense oligonucleotide. The journal of gene medicine 2006; 8: 207-16.

Follenzi A, Ailles LE, Bakovic S, Geuna M, Naldini L. Gene transfer by lentiviral vectors is limited by nuclear translocation and rescued by HIV-1 pol sequences. Nature genetics 2000; 25: 217-22.

Fujii J, Otsu K, Zorzato F, de Leon S, Khanna VK, Weiler JE, O'Brien PJ, MacLennan DH. Identification of a mutation in porcine ryanodine receptor associated with malignant hyperthermia. Science 1991; 253: 448-51.

Gaschen F, Burgunder JM. Changes of skeletal muscle in young dystrophin-deficient cats: a morphological and morphometric study. Acta neuropathologica 2001; 101: 591-600.

Gaschen FP, Hoffman EP, Gorospe JR, Uhl EW, Senior DF, Cardinet GH, 3rd, Pearce LK. Dystrophin deficiency causes lethal muscle hypertrophy in cats. Journal of the neurological sciences 1992; 110: 149-59.

Gaschen L, Lang J, Lin S, Ade-Damilano M, Busato A, Lombard CW, Gaschen FP. Cardiomyopathy in dystrophin-deficient hypertrophic feline muscular dystrophy. Journal of veterinary internal medicine / American College of Veterinary Internal Medicine 1999; 13: 346-56.

Giraldo P, Montoliu L. Size matters: use of YACs, BACs and PACs in transgenic animals. Transgenic research 2001; 10: 83-103.

Goemans NM, Tulinius M, van den Akker JT, Burm BE, Ekhart PF, Heuvelmans N, Holling T, Janson AA, Platenburg GJ, Sipkens JA, Sitsen JM, Aartsma-Rus A, van Ommen GJ, Buyse G, Darin N, Verschuuren JJ, Campion GV, de Kimpe SJ, van Deutekom JC. Systemic administration of PRO051 in Duchenne's muscular dystrophy. The New England journal of medicine 2011; 364: 1513-22.

Gomez-Rodriguez J, Washington V, Cheng J, Dutra A, Pak E, Liu P, McVicar DW, Schwartzberg PL. Advantages of q-PCR as a method of screening for gene targeting in mammalian cells using conventional and whole BAC-based constructs. Nucleic acids research 2008; 36: e117.

Gowers W. Clinical Lecture on pseudo-hypetrophic muscular paralysis The Lancet 1879a; 114: 113-6.

Gowers W. Clinical Lecture ON PSEUDO-HYPERTROPHIC MUSCULAR PARALYSIS. The Lancet 1879b; 114: 73-5.

Gowers W. Clinical lecture on pseudo-hypertrophic muscular pralysis. The Lancet 1879c; 114: 37-9.

Gowers W. Clinical Lecture ON PSEUDO - HYPERTROPHIC MUSCULAR PARALYSIS. The Lancet 1879d; 114: 1-2.

Goyenvalle A, Vulin A, Fougerousse F, Leturcq F, Kaplan JC, Garcia L, Danos O. Rescue of dystrophic muscle through U7 snRNA-mediated exon skipping. Science 2004; 306: 1796-9.

Goyenvalle A, Seto JT, Davies KE, Chamberlain J. Therapeutic approaches to muscular dystrophy. Human molecular genetics 2011;

Gregorevic P, Blankinship MJ, Allen JM, Crawford RW, Meuse L, Miller DG, Russell DW, Chamberlain JS. Systemic delivery of genes to striated muscles using adeno-associated viral vectors. Nature medicine 2004; 10: 828-34.

Grounds MD, Radley HG, Lynch GS, Nagaraju K, De Luca A. Towards developing standard operating procedures for pre-clinical testing in the mdx mouse model of Duchenne muscular dystrophy. Neurobiology of disease 2008; 31: 1-19.

Gualandi F, Trabanelli C, Rimessi P, Calzolari E, Toffolatti L, Patarnello T, Kunz G, Muntoni F, Ferlini A. Multiple exon skipping and RNA circularisation contribute to the severe phenotypic expression of exon 5 dystrophin deletion. Journal of medical genetics 2003; 40: e100.

Gundersen. Notes on the estimation of the numerical density of arbitrary profiles: the edge effect. Journal of Microscopy 1977; 111: 219-23.

Guyon JR, Mosley AN, Zhou Y, O'Brien KF, Sheng X, Chiang K, Davidson AJ, Volinski JM, Zon LI, Kunkel LM. The dystrophin associated protein complex in zebrafish. Human molecular genetics 2003; 12: 601-15.

Haber JE. Partners and pathwaysrepairing a double-strand break. Trends in genetics : TIG 2000; 16: 259-64.

Haldane JB. The rate of spontaneous mutation of a human gene. 1935. Journal of genetics 2004; 83: 235-44.

Hamm A, Krott N, Breibach I, Blindt R, Bosserhoff AK. Efficient transfection method for primary cells. Tissue engineering 2002; 8: 235-45.

Hanson KD, Sedivy JM. Analysis of biological selections for high-efficiency gene targeting. Molecular and cellular biology 1995; 15: 45-51.

Harper SQ, Hauser MA, DelloRusso C, Duan D, Crawford RW, Phelps SF, Harper HA, Robinson AS, Engelhardt JF, Brooks SV, Chamberlain JS. Modular flexibility of dystrophin: implications for gene therapy of Duchenne muscular dystrophy. Nature medicine 2002; 8: 253-61.

Hasty P, Rivera-Perez J, Chang C, Bradley A. Target frequency and integration pattern for insertion and replacement vectors in embryonic stem cells. Molecular and cellular biology 1991; 11: 4509-17.

Hauschild J, Petersen B, Santiago Y, Queisser AL, Carnwath JW, Lucas-Hahn A, Zhang L, Meng X, Gregory PD, Schwinzer R, Cost GJ, Niemann H. Efficient generation of a biallelic knockout in pigs using zinc-finger nucleases. Proceedings of the National Academy of Sciences of the United States of America 2011; 108: 12013-7.

Hendrie PC, Russell DW. Gene targeting with viral vectors. Molecular therapy : the journal of the American Society of Gene Therapy 2005; 12: 9-17.

Hinton VJ, De Vivo DC, Nereo NE, Goldstein E, Stern Y. Poor verbal working memory across intellectual level in boys with Duchenne dystrophy. Neurology 2000; 54: 2127-32.

Hirata RK, Russell DW. Design and packaging of adeno-associated virus gene targeting vectors. Journal of virology 2000; 74: 4612-20.

Hoffman EP, Brown RH, Jr., Kunkel LM. Dystrophin: the protein product of the Duchenne muscular dystrophy locus. Cell 1987; 51: 919-28.

Hofmann A, Kessler B, Ewerling S, Weppert M, Vogg B, Ludwig H, Stojkovic M, Boelhauve M, Brem G, Wolf E, Pfeifer A. Efficient transgenesis in farm animals by lentiviral vectors. EMBO reports 2003; 4: 1054-60.

Hofmann A, Kessler B, Ewerling S, Kabermann A, Brem G, Wolf E, Pfeifer A. Epigenetic regulation of lentiviral transgene vectors in a large animal model. Molecular therapy : the journal of the American Society of Gene Therapy 2006; 13: 59-66.

Hosoda F, Nishimura S, Uchida H, Ohki M. An F factor based cloning system for

large DNA fragments. Nucleic acids research 1990; 18: 3863-9.

Howell JM, Fletcher S, Kakulas BA, O'Hara M, Lochmuller H, Karpati G. Use of the dog model for Duchenne muscular dystrophy in gene therapy trials. Neuromuscular disorders : NMD 1997; 7: 325-8.

Howell JM, Lochmuller H, O'Hara A, Fletcher S, Kakulas BA, Massie B, Nalbantoglu J, Karpati G. High-level dystrophin expression after adenovirus-mediated dystrophin minigene transfer to skeletal muscle of dystrophic dogs: prolongation of expression with immunosuppression. Human gene therapy 1998; 9: 629-34.

Humphray SJ, Scott CE, Clark R, Marron B, Bender C, Camm N, Davis J, Jenks A, Noon A, Patel M, Sehra H, Yang F, Rogatcheva MB, Milan D, Chardon P, Rohrer G, Nonneman D, de Jong P, Meyers SN, Archibald A, Beever JE, Schook LB, Rogers J. A high utility integrated map of the pig genome. Genome biology 2007; 8: R139.

Im WB, Phelps SF, Copen EH, Adams EG, Slightom JL, Chamberlain JS. Differential expression of dystrophin isoforms in strains of mdx mice with different mutations. Human molecular genetics 1996; 5: 1149-53.

Jacobsen F, Mertens-Rill J, Beller J, Hirsch T, Daigeler A, Langer S, Lehnhardt M, Steinau HU, Steinstraesser L. Nucleofection: a new method for cutaneous gene transfer? Journal of biomedicine & biotechnology 2006; 2006: 26060.

Jasin M, Berg P. Homologous integration in mammalian cells without target gene selection. Genes & development 1988; 2: 1353-63.

Jearawiriyapaisarn N, Moulton HM, Buckley B, Roberts J, Sazani P, Fucharoen S, Iversen PL, Kole R. Sustained dystrophin expression induced by peptide-conjugated morpholino oligomers in the muscles of mdx mice. Molecular therapy : the journal of the American Society of Gene Therapy 2008; 16: 1624-9.

Jennekens FG, ten Kate LP, de Visser M, Wintzen AR. Diagnostic criteria for

Duchenne and Becker muscular dystrophy and myotonic dystrophy. Neuromuscular disorders : NMD 1991; 1: 389-91.

Jorgensen FG, Hobolth A, Hornshoj H, Bendixen C, Fredholm M, Schierup MH. Comparative analysis of protein coding sequences from human, mouse and the domesticated pig. BMC biology 2005; 3: 2.

Kameya S, Araki E, Katsuki M, Mizota A, Adachi E, Nakahara K, Nonaka I, Sakuragi S, Takeda S, Nabeshima Y. Dp260 disrupted mice revealed prolonged implicit time of the b-wave in ERG and loss of accumulation of beta-dystroglycan in the outer plexiform layer of the retina. Human molecular genetics 1997; 6: 2195-203.

Kamphus J, Coenen M, Kienzle E, Pallauf J, Simon O, Zentek J (2004) Supplemente zu Vorlesung und Übungen in der Tierernährung, 10 edn. M. & H. Schaper Alfeld-Hannover

Kerr TP, Sewry CA, Robb SA, Roberts RG. Long mutant dystrophins and variable phenotypes: evasion of nonsense-mediated decay? Human genetics 2001; 109: 402-7.

Khurana TS, Watkins SC, Chafey P, Chelly J, Tome FM, Fardeau M, Kaplan JC, Kunkel LM. Immunolocalization and developmental expression of dystrophin related protein in skeletal muscle. Neuromuscular disorders : NMD 1991; 1: 185-94.

Kinali M, Arechavala-Gomeza V, Feng L, Cirak S, Hunt D, Adkin C, Guglieri M, Ashton E, Abbs S, Nihoyannopoulos P, Garralda ME, Rutherford M, McCulley C, Popplewell L, Graham IR, Dickson G, Wood MJ, Wells DJ, Wilton SD, Kole R, Straub V, Bushby K, Sewry C, Morgan JE, Muntoni F. Local restoration of dystrophin expression with the morpholino oligomer AVI-4658 in Duchenne muscular dystrophy: a single-blind, placebo-controlled, dose-escalation, proof-of-concept study. Lancet neurology 2009; 8: 918-28.

Kingston HM, Harper PS, Pearson PL, Davies KE, Williamson R, Page D. Localisation of gene for Becker muscular dystrophy. Lancet 1983a; 2: 1200.

Kingston HM, Thomas NS, Pearson PL, Sarfarazi M, Harper PS. Genetic linkage between Becker muscular dystrophy and a polymorphic DNA sequence on the short arm of the X chromosome. Journal of medical genetics 1983b; 20: 255-8.

Klymiuk N, Aigner B, Brem G, Wolf E. Genetic modification of pigs as organ donors for xenotransplantation. Molecular reproduction and development 2010; 77: 209-21.

Koenig M, Hoffman EP, Bertelson CJ, Monaco AP, Feener C, Kunkel LM. Complete cloning of the Duchenne muscular dystrophy (DMD) cDNA and preliminary genomic organization of the DMD gene in normal and affected individuals. Cell 1987; 50: 509-17.

Koenig M, Monaco AP, Kunkel LM. The complete sequence of dystrophin predicts a rod-shaped cytoskeletal protein. Cell 1988; 53: 219-28.

Koenig M, Beggs AH, Moyer M, Scherpf S, Heindrich K, Bettecken T, Meng G, Muller CR, Lindlof M, Kaariainen H, et al. The molecular basis for Duchenne versus Becker muscular dystrophy: correlation of severity with type of deletion. American journal of human genetics 1989; 45: 498-506.

Koenig M, Kunkel LM. Detailed analysis of the repeat domain of dystrophin reveals four potential hinge segments that may confer flexibility. The Journal of biological chemistry 1990; 265: 4560-6.

Kornegay JN, Li J, Bogan JR, Bogan DJ, Chen C, Zheng H, Wang B, Qiao C, Howard JF, Jr., Xiao X. Widespread muscle expression of an AAV9 human mini-dystrophin vector after intravenous injection in neonatal dystrophin-deficient dogs. Molecular therapy : the journal of the American Society of Gene Therapy 2010; 18: 1501-8.

Kudoh H, Ikeda H, Kakitani M, Ueda A, Hayasaka M, Tomizuka K, Hanaoka K. A new model mouse for Duchenne muscular dystrophy produced by 2.4 Mb deletion of dystrophin gene using Cre-loxP recombination system. Biochemical and biophysical research communications 2005; 328: 507-16.

Kunkel LM, Monaco AP, Middlesworth W, Ochs HD, Latt SA. Specific cloning of DNA fragments absent from the DNA of a male patient with an X chromosome deletion. Proceedings of the National Academy of Sciences of the United States of America 1985; 82: 4778-82.

Kuroiwa Y, Kasinathan P, Matsushita H, Sathiyaselan J, Sullivan EJ, Kakitani M, Tomizuka K, Ishida I, Robl JM. Sequential targeting of the genes encoding immunoglobulin-mu and prion protein in cattle. Nature genetics 2004; 36: 775-80.

Kuroiwa Y, Kasinathan P, Sathiyaseelan T, Jiao JA, Matsushita H, Sathiyaseelan J, Wu H, Mellquist J, Hammitt M, Koster J, Kamoda S, Tachibana K, Ishida I, Robl JM. Antigen-specific human polyclonal antibodies from hyperimmunized cattle. Nature biotechnology 2009; 27: 173-81.

Kurome M, Ueda H, Tomii R, Naruse K, Nagashima H. Production of transgenic-clone pigs by the combination of ICSI-mediated gene transfer with somatic cell nuclear transfer. Transgenic research 2006; 15: 229-40.

Lai L, Kolber-Simonds D, Park KW, Cheong HT, Greenstein JL, Im GS, Samuel M, Bonk A, Rieke A, Day BN, Murphy CN, Carter DB, Hawley RJ, Prather RS. Production of alpha-1,3-galactosyltransferase knockout pigs by nuclear transfer cloning. Science 2002; 295: 1089-92.

Lederfein D, Levy Z, Augier N, Mornet D, Morris G, Fuchs O, Yaffe D, Nudel U. A 71-kilodalton protein is a major product of the Duchenne muscular dystrophy gene in brain and other nonmuscle tissues. Proceedings of the National Academy of Sciences of the United States of America 1992; 89: 5346-50.

Lee EC, Yu D, Martinez de Velasco J, Tessarollo L, Swing DA, Court DL, Jenkins NA, Copeland NG. A highly efficient Escherichia coli-based chromosome engineering system adapted for recombinogenic targeting and subcloning of BAC DNA. Genomics 2001; 73: 56-65.

Lefaucheur JP, Pastoret C, Sebille A. Phenotype of dystrophinopathy in old mdx mice. The Anatomical record 1995; 242: 70-6.

Li S, Kimura E, Fall BM, Reyes M, Angello JC, Welikson R, Hauschka SD, Chamberlain JS. Stable transduction of myogenic cells with lentiviral vectors expressing a minidystrophin. Gene therapy 2005; 12: 1099-108.

Lidov HG, Selig S, Kunkel LM. Dp140: a novel 140 kDa CNS transcript from the dystrophin locus. Human molecular genetics 1995; 4: 329-35.

Liechti-Gallati S, Koenig M, Kunkel LM, Frey D, Boltshauser E, Schneider V, Braga S, Moser H. Molecular deletion patterns in Duchenne and Becker type muscular dystrophy. Human genetics 1989; 81: 343-8.

Liu P, Jenkins NA, Copeland NG. A highly efficient recombineering-based method for generating conditional knockout mutations. Genome research 2003; 13: 476-84.

Lu QL, Mann CJ, Lou F, Bou-Gharios G, Morris GE, Xue SA, Fletcher S, Partridge TA, Wilton SD. Functional amounts of dystrophin produced by skipping the mutated exon in the mdx dystrophic mouse. Nature medicine 2003; 9: 1009-14.

Lunney JK. Advances in swine biomedical model genomics. International journal of biological sciences 2007; 3: 179-84.

MacKenzie TC, Kobinger GP, Louboutin JP, Radu A, Javazon EH, Sena-Esteves M, Wilson JM, Flake AW. Transduction of satellite cells after prenatal intramuscular administration of lentiviral vectors. The journal of gene medicine 2005; 7: 50-8.

Malhotra HS, Juyal R, Malhotra KP, Shukla R. Macroglossia associated with 271 bp deletion in exon 50 of dystrophin gene. Annals of Indian Academy of Neurology 2011; 14: 47-9.

Manzur AY, Kuntzer T, Pike M, Swan A. Glucocorticoid corticosteroids for

Duchenne muscular dystrophy. Cochrane database of systematic reviews 2008: CD003725.

Maquat LE. Nonsense-mediated mRNA decay: splicing, translation and mRNP dynamics. Nature reviews. Molecular cell biology 2004; 5: 89-99.

Maurisse R, De Semir D, Emamekhoo H, Bedayat B, Abdolmohammadi A, Parsi H, Gruenert DC. Comparative transfection of DNA into primary and transformed mammalian cells from different lineages. BMC biotechnology 2010; 10: 9.

McClorey G, Moulton HM, Iversen PL, Fletcher S, Wilton SD. Antisense oligonucleotide-induced exon skipping restores dystrophin expression in vitro in a canine model of DMD. Gene therapy 2006; 13: 1373-81.

McCreath KJ, Howcroft J, Campbell KH, Colman A, Schnieke AE, Kind AJ. Production of gene-targeted sheep by nuclear transfer from cultured somatic cells. Nature 2000; 405: 1066-9.

McDouall RM, Dunn MJ, Dubowitz V. Nature of the mononuclear infiltrate and the mechanism of muscle damage in juvenile dermatomyositis and Duchenne muscular dystrophy. Journal of the neurological sciences 1990; 99: 199-217.

McGeachie JK, Grounds MD, Partridge TA, Morgan JE. Age-related changes in replication of myogenic cells in mdx mice: quantitative autoradiographic studies. Journal of the neurological sciences 1993; 119: 169-79.

Mehler MF. Brain dystrophin, neurogenetics and mental retardation. Brain research. Brain research reviews 2000; 32: 277-307.

Mendell JR, Campbell K, Rodino-Klapac L, Sahenk Z, Shilling C, Lewis S, Bowles D, Gray S, Li C, Galloway G, Malik V, Coley B, Clark KR, Li J, Xiao X, Samulski J, McPhee SW, Samulski RJ, Walker CM. Dystrophin immunity in Duchenne's muscular dystrophy. The New England journal of medicine 2010; 363: 1429-37.

Mendicino M, Ramsoondar J, Phelps C, Vaught T, Ball S, Leroith T, Monahan J, Chen S, Dandro A, Boone J, Jobst P, Vance A, Wertz N, Bergman Z, Sun XZ, Polejaeva I, Butler J, Dai Y, Ayares D, Wells K. Generation of antibody- and B cell-deficient pigs by targeted disruption of the J-region gene segment of the heavy chain locus. Transgenic research 2011; 20: 625-41.

Meryon E. On fatty degeneration of the voluntary muscles: report of the Royal Medical and Chirurgical Society. The Lancet 1851; 58: 588-9.

Meryon E. On Granular and Fatty Degeneration of the Voluntary Muscles. Medico-chirurgical transactions 1852; 35: 73-84 1.

Mo D, Potter BA, Bertrand CA, Hildebrand JD, Bruns JR, Weisz OA. Nucleofection disrupts tight junction fence function to alter membrane polarity of renal epithelial cells. American journal of physiology. Renal physiology 2010; 299: F1178-84.

Mokri B, Engel AG. Duchenne dystrophy: electron microscopic findings pointing to a basic or early abnormality in the plasma membrane of the muscle fiber. Neurology 1975; 25: 1111-20.

Monaco AP, Neve RL, Colletti-Feener C, Bertelson CJ, Kurnit DM, Kunkel LM. Isolation of candidate cDNAs for portions of the Duchenne muscular dystrophy gene. Nature 1986; 323: 646-50.

Monaco AP, Bertelson CJ, Liechti-Gallati S, Moser H, Kunkel LM. An explanation for the phenotypic differences between patients bearing partial deletions of the DMD locus. Genomics 1988; 2: 90-5.

Moore MJ, Flotte TR. Autoimmunity in a genetic disease-a cautionary tale. The New England journal of medicine 2010; 363: 1473-5.

Moser H. Duchenne muscular dystrophy: pathogenetic aspects and genetic prevention. Human genetics 1984; 66: 17-40.

Moulton HM, Moulton JD. Morpholinos and their peptide conjugates: therapeutic promise and challenge for Duchenne muscular dystrophy. Biochimica et biophysica acta 2010; 1798: 2296-303.

Muller J, Vayssiere N, Royuela M, Leger ME, Muller A, Bacou F, Pons F, Hugon G, Mornet D. Comparative evolution of muscular dystrophy in diaphragm, gastrocnemius and masseter muscles from old male mdx mice. Journal of muscle research and cell motility 2001; 22: 133-9.

Muntoni F, Torelli S, Ferlini A. Dystrophin and mutations: one gene, several proteins, multiple phenotypes. The Lancet Neurology 2003; 2: 731-40.

Murison PJ, Jones A, Mitchard L, Burt R, Birchall MA. Development of perioperative care for pigs undergoing laryngeal transplantation: a case series. Laboratory animals 2009; 43: 338-43.

Mussolino C, Morbitzer R, Lutge F, Dannemann N, Lahaye T, Cathomen T. A novel TALE nuclease scaffold enables high genome editing activity in combination with low toxicity. Nucleic acids research 2011;

Nagy A, Gertsenstein M, Vintersten K, Behringer RR (2003) Manipulating the Mouse Embryo: A Laboratory Manual 3rd ed. . Cold Spring Harbor Laboratory Press, Cold Spring Harbor, New York. 399-429

Nakamura A, Takeda S. Exon-skipping therapy for Duchenne muscular dystrophy. Neuropathology : official journal of the Japanese Society of Neuropathology 2009; 29: 494-501.

Nakamura A, Takeda S. Mammalian models of duchenne muscular dystrophy: pathological characteristics and therapeutic applications. Journal of biomedicine & biotechnology 2011; 2011: 184393.

Neumann E, Schaefer-Ridder M, Wang Y, Hofschneider PH. Gene transfer into

mouse lyoma cells by electroporation in high electric fields. The EMBO journal 1982; 1: 841-5.

Nowak KJ, Davies KE. Duchenne muscular dystrophy and dystrophin: pathogenesis and opportunities for treatment. EMBO reports 2004; 5: 872-6.

Ohshima S, Shin JH, Yuasa K, Nishiyama A, Kira J, Okada T, Takeda S. Transduction efficiency and immune response associated with the administration of AAV8 vector into dog skeletal muscle. Molecular therapy : the journal of the American Society of Gene Therapy 2009; 17: 73-80.

Onishi A, Iwamoto M, Akita T, Mikawa S, Takeda K, Awata T, Hanada H, Perry AC. Pig cloning by microinjection of fetal fibroblast nuclei. Science 2000; 289: 1188-90.

Oudet C, Hanauer A, Clemens P, Caskey T, Mandel JL. Two hot spots of recombination in the DMD gene correlate with the deletion prone regions. Human molecular genetics 1992; 1: 599-603.

Pardo B, Gomez-Gonzalez B, Aguilera A. DNA repair in mammalian cells: DNA double-strand break repair: how to fix a broken relationship. Cellular and molecular life sciences : CMLS 2009; 66: 1039-56.

Perkins KJ, Davies KE. The role of utrophin in the potential therapy of Duchenne muscular dystrophy. Neuromuscular disorders : NMD 2002; 12 Suppl 1: S78-89.

Pfeifer A. Lentiviral transgenesis. Transgenic research 2004; 13: 513-22.

Pham CT, MacIvor DM, Hug BA, Heusel JW, Ley TJ. Long-range disruption of gene expression by a selectable marker cassette. Proceedings of the National Academy of Sciences of the United States of America 1996; 93: 13090-5.

Pichavant C, Aartsma-Rus A, Clemens PR, Davies KE, Dickson G, Takeda S, Wilton SD, Wolff JA, Wooddell CI, Xiao X, Tremblay JP. Current Status of Pharmaceutical

and Genetic Therapeutic Approaches to Treat DMD. Molecular therapy : the journal of the American Society of Gene Therapy 2011;

Pillers DA, Bulman DE, Weleber RG, Sigesmund DA, Musarella MA, Powell BR, Murphey WH, Westall C, Panton C, Becker LE, et al. Dystrophin expression in the human retina is required for normal function as defined by electroretinography. Nature genetics 1993; 4: 82-6.

Plonait H, Bickhardt K (1988) Lehrbuch der Schweinekrankheiten. Verlag Paul Parey

Polejaeva IA, Chen SH, Vaught TD, Page RL, Mullins J, Ball S, Dai Y, Boone J, Walker S, Ayares DL, Colman A, Campbell KH. Cloned pigs produced by nuclear transfer from adult somatic cells. Nature 2000; 407: 86-90.

Ponting CP, Blake DJ, Davies KE, Kendrick-Jones J, Winder SJ. ZZ and TAZ: new putative zinc fingers in dystrophin and other proteins. Trends in biochemical sciences 1996; 21: 11-3.

Porteus MH, Carroll D. Gene targeting using zinc finger nucleases. Nature biotechnology 2005; 23: 967-73.

Prather RS, Sutovsky P, Green JA. Nuclear remodeling and reprogramming in transgenic pig production. Experimental biology and medicine 2004; 229: 1120-6.

Quinlan JG, Hahn HS, Wong BL, Lorenz JN, Wenisch AS, Levin LS. Evolution of the mdx mouse cardiomyopathy: physiological and morphological findings. Neuromuscular disorders : NMD 2004; 14: 491-6.

Ramsoondar J, Mendicino M, Phelps C, Vaught T, Ball S, Monahan J, Chen S, Dandro A, Boone J, Jobst P, Vance A, Wertz N, Polejaeva I, Butler J, Dai Y, Ayares D, Wells K. Targeted disruption of the porcine immunoglobulin kappa light chain locus. Transgenic research 2011; 20: 643-53.

Rando TA. The dystrophin-glycoprotein complex, cellular signaling, and the regulation of cell survival in the muscular dystrophies. Muscle & nerve 2001; 24: 1575-94.

Raper SE, Chirmule N, Lee FS, Wivel NA, Bagg A, Gao GP, Wilson JM, Batshaw ML. Fatal systemic inflammatory response syndrome in a ornithine transcarbamylase deficient patient following adenoviral gene transfer. Molecular genetics and metabolism 2003; 80: 148-58.

Ray PN, Belfall B, Duff C, Logan C, Kean V, Thompson MW, Sylvester JE, Gorski JL, Schmickel RD, Worton RG. Cloning of the breakpoint of an X;21 translocation associated with Duchenne muscular dystrophy. Nature 1985; 318: 672-5.

Recillas-Targa F. Multiple strategies for gene transfer, expression, knockdown, and chromatin influence in mammalian cell lines and transgenic animals. Molecular biotechnology 2006; 34: 337-54.

Rehbinder C, Baneux P, Forbes D, van Herck H, Nicklas W, Rugaya Z, Winkler G. FELASA recommendations for the health monitoring of breeding colonies and experimental units of cats, dogs and pigs. Report of the Federation of European Laboratory Animal Science Associations (FELASA) Working Group on Animal Health. Laboratory animals 1998; 32: 1-17.

Renner S, Fehlings C, Herbach N, Hofmann A, von Waldthausen DC, Kessler B, Ulrichs K, Chodnevskaja I, Moskalenko V, Amselgruber W, Goke B, Pfeifer A, Wanke R, Wolf E. Glucose intolerance and reduced proliferation of pancreatic beta-cells in transgenic pigs with impaired glucose-dependent insulinotropic polypeptide function. Diabetes 2010; 59: 1228-38.

Richt JA, Kasinathan P, Hamir AN, Castilla J, Sathiyaseelan T, Vargas F, Sathiyaseelan J, Wu H, Matsushita H, Koster J, Kato S, Ishida I, Soto C, Robl JM, Kuroiwa Y. Production of cattle lacking prion protein. Nature biotechnology 2007; 25: 132-8.

Roberts RG, Coffey AJ, Bobrow M, Bentley DR. Exon structure of the human dystrophin gene. Genomics 1993; 16: 536-8.

Roberts RG, Gardner RJ, Bobrow M. Searching for the 1 in 2,400,000: a review of dystrophin gene point mutations. Human mutation 1994; 4: 1-11.

Robl JM, Wang Z, Kasinathan P, Kuroiwa Y. Transgenic animal production and animal biotechnology. Theriogenology 2007; 67: 127-33.

Rogers CS, Hao Y, Rokhlina T, Samuel M, Stoltz DA, Li Y, Petroff E, Vermeer DW, Kabel AC, Yan Z, Spate L, Wax D, Murphy CN, Rieke A, Whitworth K, Linville ML, Korte SW, Engelhardt JF, Welsh MJ, Prather RS. Production of CFTR-null and CFTR-DeltaF508 heterozygous pigs by adeno-associated virus-mediated gene targeting and somatic cell nuclear transfer. The Journal of clinical investigation 2008; 118: 1571-7.

Rouet P, Smih F, Jasin M. Expression of a site-specific endonuclease stimulates homologous recombination in mammalian cells. Proceedings of the National Academy of Sciences of the United States of America 1994; 91: 6064-8.

Russell DW, Hirata RK. Human gene targeting by viral vectors. Nature genetics 1998; 18: 325-30.

Rybakova IN, Amann KJ, Ervasti JM. A new model for the interaction of dystrophin with F-actin. The Journal of cell biology 1996; 135: 661-72.

Schatzberg SJ, Olby NJ, Breen M, Anderson LV, Langford CF, Dickens HF, Wilton SD, Zeiss CJ, Binns MM, Kornegay JN, Morris GE, Sharp NJ. Molecular analysis of a spontaneous dystrophin 'knockout' dog. Neuromuscular disorders : NMD 1999; 9: 289-95.

Scheerer JB, Adair GM. Homology dependence of targeted recombination at the Chinese hamster APRT locus. Molecular and cellular biology 1994; 14: 6663-73.

Schultz BR, Chamberlain JS. Recombinant adeno-associated virus transduction and integration. Molecular therapy : the journal of the American Society of Gene Therapy 2008; 16: 1189-99.

Sedivy JM, Sharp PA. Positive genetic selection for gene disruption in mammalian cells by homologous recombination. Proceedings of the National Academy of Sciences of the United States of America 1989; 86: 227-31.

Sedivy JM, Vogelstein B, Liber HL, Hendrickson EA, Rosmarin A. Gene Targeting in Human Cells Without Isogenic DNA. Science 1999; 283: 9.

Sedivy JM, Dutriaux A. Gene targeting and somatic cell genetics--a rebirth or a coming of age? Trends in genetics : TIG 1999; 15: 88-90.

Seidman MM, Glazer PM. The potential for gene repair via triple helix formation. The Journal of clinical investigation 2003; 112: 487-94.

Sendai Y, Sawada T, Urakawa M, Shinkai Y, Kubota K, Hoshi H, Aoyagi Y. alpha1,3-Galactosyltransferase-gene knockout in cattle using a single targeting vector with loxP sequences and cre-expressing adenovirus. Transplantation 2006; 81: 760-6.

Sharp NJ, Kornegay JN, Van Camp SD, Herbstreith MH, Secore SL, Kettle S, Hung WY, Constantinou CD, Dykstra MJ, Roses AD, et al. An error in dystrophin mRNA processing in golden retriever muscular dystrophy, an animal homologue of Duchenne muscular dystrophy. Genomics 1992; 13: 115-21.

Shelton GD, Engvall E. Canine and feline models of human inherited muscle diseases. Neuromuscular disorders : NMD 2005; 15: 127-38.

Shi W, Zakhartchenko V, Wolf E. Epigenetic reprogramming in mammalian nuclear transfer. Differentiation; research in biological diversity 2003; 71: 91-113.

Shimatsu Y, Katagiri K, Furuta T, Nakura M, Tanioka Y, Yuasa K, Tomohiro M,

Kornegay JN, Nonaka I, Takeda S. Canine X-linked muscular dystrophy in Japan (CXMDJ). Experimental animals / Japanese Association for Laboratory Animal Science 2003; 52: 93-7.

Shizuya H, Birren B, Kim UJ, Mancino V, Slepak T, Tachiiri Y, Simon M. Cloning and stable maintenance of 300-kilobase-pair fragments of human DNA in Escherichia coli using an F-factor-based vector. Proceedings of the National Academy of Sciences of the United States of America 1992; 89: 8794-7.

Sironi M, Pozzoli U, Cagliani R, Giorda R, Comi GP, Bardoni A, Menozzi G, Bresolin N. Relevance of sequence and structure elements for deletion events in the dystrophin gene major hot-spot. Human genetics 2003; 112: 272-88.

Skrzyszowska M, Samiec M, Slomski R, Lipinski D, Maly E. Development of porcine transgenic nuclear-transferred embryos derived from fibroblast cells transfected by the novel technique of nucleofection or standard lipofection. Theriogenology 2008; 70: 248-59.

Smithies O, Gregg RG, Boggs SS, Koralewski MA, Kucherlapati RS. Insertion of DNA sequences into the human chromosomal beta-globin locus by homologous recombination. Nature 1985; 317: 230-4.

Song H, Chung SK, Xu Y. Modeling disease in human ESCs using an efficient BAC-based homologous recombination system. Cell stem cell 2010; 6: 80-9.

Sorrell DA, Kolb AF. Targeted modification of mammalian genomes. Biotechnology advances 2005; 23: 431-69.

Straub V, Rafael JA, Chamberlain JS, Campbell KP. Animal models for muscular dystrophy show different patterns of sarcolemmal disruption. The Journal of cell biology 1997; 139: 375-85.

Swindle M (2007) Swine in the Laboratory: Surgery, Anesthesia, Imaging, and

Experimental Techniques

te Riele H, Maandag ER, Berns A. Highly efficient gene targeting in embryonic stem cells through homologous recombination with isogenic DNA constructs. Proceedings of the National Academy of Sciences of the United States of America 1992; 89: 5128-32.

Testa G, Zhang Y, Vintersten K, Benes V, Pijnappel WW, Chambers I, Smith AJ, Smith AG, Stewart AF. Engineering the mouse genome with bacterial artificial chromosomes to create multipurpose alleles. Nature biotechnology 2003; 21: 443-7.

Thomas KR, Capecchi MR. Site-directed mutagenesis by gene targeting in mouse embryo-derived stem cells. Cell 1987; 51: 503-12.

Tinsley JM, Blake DJ, Roche A, Fairbrother U, Riss J, Byth BC, Knight AE, Kendrick-Jones J, Suthers GK, Love DR, et al. Primary structure of dystrophin-related protein. Nature 1992; 360: 591-3.

Tuffery-Giraud S, Beroud C, Leturcq F, Yaou RB, Hamroun D, Michel-Calemard L, Moizard MP, Bernard R, Cossee M, Boisseau P, Blayau M, Creveaux I, Guiochon-Mantel A, de Martinville B, Philippe C, Monnier N, Bieth E, Khau Van Kien P, Desmet FO, Humbertclaude V, Kaplan JC, Chelly J, Claustres M. Genotype-phenotype analysis in 2,405 patients with a dystrophinopathy using the UMD-DMD database: a model of nationwide knowledgebase. Human mutation 2009; 30: 934-45.

Urnov FD, Miller JC, Lee YL, Beausejour CM, Rock JM, Augustus S, Jamieson AC, Porteus MH, Gregory PD, Holmes MC. Highly efficient endogenous human gene correction using designed zinc-finger nucleases. Nature 2005; 435: 646-51.

Vainzof M, Passos-Bueno MR, Takata RI, Pavanello Rde C, Zatz M. Intrafamilial variability in dystrophin abundance correlated with difference in the severity of the phenotype. Journal of the neurological sciences 1993; 119: 38-42.

Vajta G, Zhang Y, Machaty Z. Somatic cell nuclear transfer in pigs: recent achievements and future possibilities. Reproduction, fertility, and development 2007; 19: 403-23.

Valentine BA, Cooper BJ, de Lahunta A, O'Quinn R, Blue JT. Canine X-linked muscular dystrophy. An animal model of Duchenne muscular dystrophy: clinical studies. Journal of the neurological sciences 1988; 88: 69-81.

Valenzuela DM, Murphy AJ, Frendewey D, Gale NW, Economides AN, Auerbach W, Poueymirou WT, Adams NC, Rojas J, Yasenchak J, Chernomorsky R, Boucher M, Elsasser AL, Esau L, Zheng J, Griffiths JA, Wang X, Su H, Xue Y, Dominguez MG, Noguera I, Torres R, Macdonald LE, Stewart AF, DeChiara TM, Yancopoulos GD. High-throughput engineering of the mouse genome coupled with high-resolution expression analysis. Nature biotechnology 2003; 21: 652-9.

van der Weyden L, Adams DJ, Bradley A. Tools for targeted manipulation of the mouse genome. Physiological genomics 2002; 11: 133-64.

van Deutekom JC, van Ommen GJ. Advances in Duchenne muscular dystrophy gene therapy. Nature reviews. Genetics 2003; 4: 774-83.

van Deutekom JC, Janson AA, Ginjaar IB, Frankhuizen WS, Aartsma-Rus A, Bremmer-Bout M, den Dunnen JT, Koop K, van der Kooi AJ, Goemans NM, de Kimpe SJ, Ekhart PF, Venneker EH, Platenburg GJ, Verschuuren JJ, van Ommen GJ. Local dystrophin restoration with antisense oligonucleotide PRO051. The New England journal of medicine 2007; 357: 2677-86.

Vandebrouck C, Martin D, Colson-Van Schoor M, Debaix H, Gailly P. Involvement of TRPC in the abnormal calcium influx observed in dystrophic (mdx) mouse skeletal muscle fibers. The Journal of cell biology 2002; 158: 1089-96.

Vasileva A, Linden RM, Jessberger R. Homologous recombination is required for AAV-mediated gene targeting. Nucleic acids research 2006; 34: 3345-60.

Vasquez KM, Marburger K, Intody Z, Wilson JH. Manipulating the mammalian genome by homologous recombination. Proceedings of the National Academy of Sciences of the United States of America 2001; 98: 8403-10.

Vazquez JM, Roca J, Gil MA, Cuello C, Parrilla I, Vazquez JL, Martinez EA. New developments in low-dose insemination technology. Theriogenology 2008; 70: 1216-24.

Verma S, Anziska Y, Cracco J. Review of Duchenne muscular dystrophy (DMD) for the pediatricians in the community. Clinical pediatrics 2010; 49: 1011-7.

Vos JH, van der Linde-Sipman JS, Goedegebuure SA. Dystrophy-like myopathy in the cat. Journal of comparative pathology 1986; 96: 335-41.

Walmsley GL, Arechavala-Gomeza V, Fernandez-Fuente M, Burke MM, Nagel N, Holder A, Stanley R, Chandler K, Marks SL, Muntoni F, Shelton GD, Piercy RJ. A duchenne muscular dystrophy gene hot spot mutation in dystrophin-deficient cavalier king charles spaniels is amenable to exon 51 skipping. PloS one 2010; 5: e8647.

Wang Z, Zhu T, Qiao C, Zhou L, Wang B, Zhang J, Chen C, Li J, Xiao X. Adeno-associated virus serotype 8 efficiently delivers genes to muscle and heart. Nature biotechnology 2005; 23: 321-8.

Weiss C, Jakubiczka S, Huebner A, Klopocki E, Kress W, Voit T, Hubner C, Schuelke M. Tandem duplication of DMD exon 18 associated with epilepsy, macroglossia, and endocrinologic abnormalities. Muscle & nerve 2007; 35: 396-401.

Wells DJ. Therapeutic restoration of dystrophin expression in Duchenne muscular dystrophy. Journal of muscle research and cell motility 2006; 27: 387-98.

Wernersson R, Schierup MH, Jorgensen FG, Gorodkin J, Panitz F, Staerfeldt HH, Christensen OF, Mailund T, Hornshoj H, Klein A, Wang J, Liu B, Hu S, Dong W, Li W, Wong GK, Yu J, Bendixen C, Fredholm M, Brunak S, Yang H, Bolund L. Pigs in

sequence space: a 0.66X coverage pig genome survey based on shotgun sequencing. BMC genomics 2005; 6: 70.

Whyte JJ, Zhao J, Wells KD, Samuel MS, Whitworth KM, Walters EM, Laughlin MH, Prather RS. Gene targeting with zinc finger nucleases to produce cloned eGFP knockout pigs. Molecular reproduction and development 2011; 78: 2.

Willmann R, Possekel S, Dubach-Powell J, Meier T, Ruegg MA. Mammalian animal models for Duchenne muscular dystrophy. Neuromuscular disorders : NMD 2009; 19: 241-9.

Wilmut I, Schnieke AE, McWhir J, Kind AJ, Campbell KH. Viable offspring derived from fetal and adult mammalian cells. Nature 1997; 385: 810-3.

Winand NJ, Edwards M, Pradhan D, Berian CA, Cooper BJ. Deletion of the dystrophin muscle promoter in feline muscular dystrophy. Neuromuscular disorders : NMD 1994; 4: 433-45.

Wolf E, Zakhartchenko V, Brem G. Nuclear transfer in mammals: recent developments and future perspectives. Journal of biotechnology 1998; 65: 99-110.

Wood MJ. Toward an oligonucleotide therapy for Duchenne muscular dystrophy: a complex development challenge. Science translational medicine 2010; 2: 25ps15.

Yanez RJ, Porter AC. Influence of DNA delivery method on gene targeting frequencies in human cells. Somatic cell and molecular genetics 1999; 25: 27-31.

Yang Y, Seed B. Site-specific gene targeting in mouse embryonic stem cells with intact bacterial artificial chromosomes. Nature biotechnology 2003; 21: 447-51.

Yokota T, Lu QL, Partridge T, Kobayashi M, Nakamura A, Takeda S, Hoffman E. Efficacy of systemic morpholino exon-skipping in Duchenne dystrophy dogs. Annals of neurology 2009; 65: 667-76.

Yu G, Chen J, Yu H, Liu S, Xu X, Sha H, Zhang X, Wu G, Xu S, Cheng G. Functional disruption of the prion protein gene in cloned goats. The Journal of general virology 2006; 87: 1019-27.

Yuasa K, Yoshimura M, Urasawa N, Ohshima S, Howell JM, Nakamura A, Hijikata T, Miyagoe-Suzuki Y, Takeda S. Injection of a recombinant AAV serotype 2 into canine skeletal muscles evokes strong immune responses against transgene products. Gene therapy 2007; 14: 1249-60.

Zhang Y, Buchholz F, Muyrers JP, Stewart AF. A new logic for DNA engineering using recombination in Escherichia coli. Nature genetics 1998; 20: 123-8.

Zhao J, Whyte J, Prather RS. Effect of epigenetic regulation during swine embryogenesis and on cloning by nuclear transfer. Cell and tissue research 2010; 341: 13-21.

Zhu C, Li B, Yu G, Chen J, Yu H, Xu X, Wu Y, Zhang A, Cheng G. Production of Prnp -/- goats by gene targeting in adult fibroblasts. Transgenic research 2009; 18: 163-71.

IX. INDEX OF FIGURES

X. INDEX OF TABLES

XI. ACKNOWLEDGEMENTS

First of all I would like to thank Prof. Dr. Eckhard Wolf for providing me the opportunity to work on this project at the Chair for Molecular Animal Breeding and Biotechnology, Moorversuchsgut, Ludwig-Maximilians-Universität Munich, for his support, for reviewing this manuscript and especially for the things I have learned from him.

I am particularly thankful to my mentors at the Moorversuchsgut Dr. Nikolai Klymiuk, Dr. Annegret Wünsch and Katrin Krähe for their support, scientific suggestions and guidance and to Prof. Dr. Bernhard Aigner for his scientific advice.

I also would like to acknowledge Prof. Dr. Maggie Walter and the entire team of the Friedrich Baur Institute, especially Maria Schmuck for great collaboration.

Special thanks to the members of the Chair for Veterinary Pathology, especially Prof. Dr. Rüdiger Wanke for his scientific support, Dr. Nadja Herbach and Dr. Andreas Blutke for his immense help at my weekend in the institute.

I show my gratitude to the LAFUGA team Munich for their transcriptome analysis and the Pig Clinic Munich for measuring the serum creatine kinase levels.

I am particularly grateful to all my colleagues at the Moorveruchsgut for sharing a memorable time. Many thanks to Dr. Barbara Keßler for her great support. Another acknowledgement goes to Siegfried Elsner, Christian Erdle and Peter Rieblinger for their excellent animal care.

I would like to acknowledge the Bayerische Forschungsstiftung to support my work financially and Prof. Dr. Micheal Roaf to review parts of this work.

Finally I would like to express my deepest gratitude to Reinhard for his constant support, patience and for every single day. I would like to thank my parents for believing in me and for everything.